Structural Insights into Apoptotic Regulation by BCL-2 Family

Qian Liu

Department of Biochemistry
McGill University
Montreal, Quebec, Canada

June 2010

A thesis submitted to the Faculty of Graduate Studies and Research at McGill University in partial fulfillment of the requirements for the degree of Doctor of Philosophy in Biochemistry

McGill

Abstract

Myeloid cell leukemia 1 (MCL-1), an anti-apoptotic BCL-2 member, is active in the preservation of mitochondrial integrity during apoptosis. By collective data from nuclear magnetic resonance (NMR) spectroscopy and titration calorimetry, we revealed the selectivity of MCL-1 in binding BH3 ligands of interest to mammalian biology, and proved that the core domain of MCL-1 (cMCL-1) is necessary and sufficient for BH3 ligand binding. We characterized the *in vitro* protein-protein interaction between cMCL-1 and activated BID, which occurs in a very slow manner in solution but is otherwise similar to the interaction between cMCL-1 and BID-BH3 peptide. We also present the solution structure of complex cMCL-1:BID-BH3, which may greatly facilitate drug discovery studies of human tumor malignancies.

BAK, a multi-region pro-apoptotic protein, directly mediates the mitochondrial outer membrane permeablization (MOMP). We completed a structural investigation of BAK by X-ray crystallography. We report two structures of BAK's homo-dimers, one zinc-mediated (cBAK) and one disulphide-bond-linked (cBAK-o). Their dimerizing sites locate closely at D160 and H164 in cBAK and C166 in cBAK-o, which allow them to compose a unique regulatory element to switch BAK's activity as suggested in mitochondria activity-testing assays.

BAK is tightly regulated through protein-protein interactions by MCL-1. We characterize the conformational changes in BAK and MCL-1 using detergents to mimic the membrane environment, and studied their interaction *in vitro*. The non-ionic detergent IGEPAL and the zwitterionic detergent CHAPS have different effects on these two proteins, but both initiate the heterodimerization. The complex of MCL-1 and BAK can be disrupted by either a BID-BH3 peptide, which acts through binding to MCL-1, or a mutation in BH3 region of BAK (L78A), demonstrating the essential role of BAK's BH3 in its regulation by MCL-1.

This thesis concludes with a hybrid model for BAK activation: BAK can be self-regulated through the red-ox element, and get initiated for conformational changes by BH3-only activators or other dynamic-boosting factors. The inhibition of MCL-1 is performed by interacting with both BH3-only proteins and BH3-accessible BAK.

Résumé

La protéine MCL-1 (Myeloid cell leukemia 1), qui appartient à la classe de protéines anti-apoptotiques BCL-2, joue un rôle dans le maintien de l'intégrité mitochondriale durant l'apoptose. Les résultats obtenus par résonance magnétique nucléaire (RMN) et par titrage calorimétrique, nous ont permis de mettre en évidence la sélectivité de la protéine MCL-1 pour les ligands mammifères d'interêt biologiques qui contiennent le motif BH3 et nous avons ainsi démontré que le domaine central du facteur MCL-1 (cMCL-1) est nécessaire et suffisant pour cette interaction. Nous avons caractérisé *in vitro* l'interaction entre le domaine cMCL-1 et le facteur activé BID; cette interaction se produit lentement en solution mais est similaire à celle observée entre le domaine cMCL-1 et le peptide BID-BH3. De plus nous avons résolu la structure du complexe cMCL-1:BID-BH3, qui est une cible potentielle qui pourrait être à la base d'un criblage d'une banque de petites molécules dans le cas de tumeurs humaines malignes.

BAK, une protéine pro-apoptotic modulaire, permet la perméabilité de la membrane externe de la mitochondrie: ce mécanisme est dénommé "MOMP" pour "*the mitochondrial outer membrane permeablization*". Nous avons accompli l'étude structurale de la protéine BAK par cristallographie et diffraction de rayons X. Nous présentons deux complexes de la protéine BAK: un homodimère lié par une molécule de zinc (cBAK) et une qui contient un pont disulfure (cBAK-o). Le site de dimérisation se situe proche des résidu D160 et H164 pour cBAK et C166 pour cBAK-o, ce qui leur confère un élément de régulation unique pour moduler l'activité de BAK comme suggéré dans des essais d'activité mitochondriale.

La protéine BAK est finement régulée grâce à son interaction protéine-protéine avec MCL-1. Nous avons caractérisé les changements conformations des facteurs BAK et MCL-1 à l'aide de détergents pour modéliser un environnement membranaire et étudier leur interaction *in vitro*. Les détergents IGEPAL (non-ionic), et CHAPS (de type zwitterion) ont des effets différents sur ces deux

protéines mais initient leur hétérodimérisation. Le complexe formé par MCL-1 et BAK peut être dissocié soit par le peptide BID-BH3 en interagissant avec MCL-1, soit par une mutation du motif BH3 de la protéine BAK (L78A), ce qui montre le rôle essentiel du peptide BH3 dans la régulation du facteur BAK par MCL-1.

En conclusion, nous avons établi un modèle hybride d'activation de la protéine BAK : elle peut s'auto-réguler grâce à un élément redox associé à des changements de conformation qui sont initiés par des activateurs qui contiennent seulement le motif BH3 ou bien par d'autres activateurs dynamiques. L'inhibition de la protéine MCL-1 se produit en interagissant avec des facteurs qui contiennent seulement BH3 ou lorsque le motif BH3 de BAK devient accessible.

Acknowledgements

My utmost gratitude goes to my supervisor, Dr. Kalle Gehring, who offered me the opportunity to do research in his laboratory, to work on exciting projects and to learn many skills. This thesis would not have been possible without his encouragement, knowledge, guidance, patience and support from the initial to the final level.

I would like to acknowledge the following people, who have made available their supports and encouragement in a number of ways during the course of my thesis. Dr. Tudor Moldoveanu, a post-doc fellow, showed me all the important skills from protein purification to molecular cloning, provided me fruitful discussions, and shared the amazing BAK project. Dr. Tara Sprules, the NMR manager, kindly offered me invaluable assistance in acquiring and processing the NMR data and the use of NMRViewJ software. Dr. Guennadi Kozlov and Dr. Alexey Denisov, were great resources of technical support in solving protein structures. Dr. Jean-Francois Trempe was always ready to answer my questions whenever I need his help.

I would also like to express my appreciations to Dr. Gordon Shore and Dr. Albert Berghuis, who are my RAC members, for their helpful comments and discussions. Dr. Mark Watson from GeminX generously helped in protein constructs, cell growth, and mitochondria assays. Thanks to Edna Matta-Camacho for her help in protein purification during my pregnancy, and Marie Menade for translating my thesis abstract into French.

I am heartily thankful to Angelika, Edna, Ekaterina, Marie, Nura, Tara, and Yan for their friendship and all the good times, which made the study memorable. Thanks to all the members of the lab, past and present, for their contribution to my graduate school experience.

Finally, I would like to dedicate this publication to my husband Larry Yang, my daughter Gracelyn Yang, and my parents Guiquan Liu and Zhanqun Liu. Their unreserved love, understanding and support are very important for all my achievements.

Contribution of Authors

As permitted under the guidelines of the Faculty of Graduate Studies and Research, previously published materials are included in this dissertation.

Chapter 2:

Qian Liu, Tudor Moldoveanu, Tara Sprules, Edna Matta-Camacho, Nura Mansur-Azzam and Kalle Gehring. (2010*) J. Biol. Chem.* 285, 19615-19624.

The work presented in this chapter was carried out by myself. I did the construct subcloning, protein and peptide purification, ITC, NMR titration, size exclusion chromatography, structure calculation, and wrote the paper. Dr. T. Moldoveanu showed me all the necessary experimental techniques and generously shared the construct of μ-calpain. Dr. Tara Sprules acquired all the three-dimentional experiments on the Varian Unity Inova 800MHz or 500MHz spectrometer. E. Matta-Camacho, a Ph.D. student in Dr. K. Gehring's lab, helped me with a few preps of cMCL-1 in my pregnancy. Dr. Nura Mansur-Azzam shared her protocol to purify BID-BH3 peptide, and purified a few preps.

Chapter 3:

1. T. Moldoveanu, Q. Liu, A. Tocilj, M. Watson, G. Shore, and K. Gehring, The X-ray structure of a BAK homodimer reveals an inhibitory zinc-binding site. Mol Cell 24 (2006) 677-688.

2. T. Moldoveanu, Q. Liu, M. Watson, D. R. Green and K. Gehring, Disulphide-Bonded BAK Homodimers Escape Inhibition by Zinc. (Manuscript in preparation).

This project was carried out in cooperation with Dr. Tudor Moldoveanu. In the 1st paper, my contribution includes the cloning of protein constructs (including FLAG-BAK-ΔTM-His_6, MEAS-BAK-ΔTM-His_6, GST-FLAG-BAK-ΔTM, and GST-MEAS-BAK-ΔTM), limited proteolysis on FLAG-BAK-HMK-ΔTM-His_6, all of the site-directed mutagenesis (C14S, D160A, H164A, D160A/H164A, C166S), some of the protein purification, some of the *in vitro* cytochrome *c* (cyt *c*) release assays, and the western blots. In the 2nd paper, I performed the protein purification of cBAK-o, screened and optimized the condition for the crystal in $C222_1$ space group, and solved the structure together with Dr. Tudor Moldoveanu. In this chapter, I combined the results that I was involved in obtaining, rewrote the text and made further discussions.

Chapter 4:

Qian Liu and Kalle Gehring. Hetero-dimerization of BAK and MCL-1 activated by detergent micelles. (manuscript submitted to *J. Biol. Chem.* MS ID#: JBC/2010/144857).

The work presented in this chapter was done by myself, except that the co-fraction of BAK and MCL-1 in analytical gel-filtration was conducted together with Dr. Tudor Moldoveanu. I carried out all the rest experiments, analyzed the results and wrote the manuscript.

Table of Contents

List of Tables and Figures

Chapter 1

Chapter 2

Chapter 3

Chapter 4

Chapter 5

Abbreviations

APAF-1	apoptotic protease activating factor-1
ARE	adenine-rich element
BCL-2	B-cell CLL/lymphoma 2
BH	BCL-2 homology
CAM	competitively activating model
cBAK	calpain cut Bak in the reduced form
cBAK-o	calpain cut Bak in the oxidized form
CNS	crystallography and NMR system
COSY	correlation spectroscopy
CSA	chemical shift anisotropy
cBID	calpain cut BID
cMCL-1	core domain of MCL-1
CRE	cyclic AMP-response element
CSFs	colony stimulating factors
CYANA	combined assignment and dynamics algorithm for NMR applications
cyt c	cytochrome c
DAM	directly activating model
DD	death domain
DISC	death-inducing signaling complex
DKO	double knockout
DLC	dynein light chain
ER	endoplasmic reticulum
FADD	Fas-associated adaptor protein with death domain
FCS	fluorescence correlation spectroscopy
FIDA	fluorescence distribution analysis
GFs	growth factors
GST	glutathione S-transferase

HMK	heavy-chain myosin kinase
HSQC	heteronuclear single quantum coherence
IAPs	inhibitor of apoptosis proteins
IF	interferon
ILs	interleukins
IP	immunoprecipitation
IR	ionizing radiation
ITC	isothermal titration calorimetry
LUVs	large unilamellar vesicles
MAC	mitochondrial apoptosis-induced channel
MCL-1	myeloid cell leukemia -1
MOM	mitochondrial outer membrane
MOMP	mitochondrial outer membrane permeablization
NOE	nuclear overhauser effect
NOESY	nuclear overhauser enhancement sepectroscopy
NMR	nuclear magnetic resonance
NPC	neural precursor cell
NSCLC	non-small cell lung cancers
RDC	residual dipolar coupling
RMSD	root mean square deviation
SAR	structure-activity relationship
tBID	truncated BID
tBID-C	C-terminal portion of tBID
tBID-N	N-terminal portion of tBID
TOCSY	total correlation spectroscopy
TM	transmembrane
TNF-alpha	tumor necrosis factor-alpha
ULR	unstructured loop regions

Chapter 1: Apoptosis and the regulating BCL-2 family of proteins

1.1 Apoptosis and its pathways

Apoptosis, also called programmed cell death, is a normal process in living organisms in which cells die. It is the most common mechanism by which the body eliminates damaged or unneeded cells without causing local inflammation (Norbury and Hickson, 2001). It is widely spread in metazoans (Tittel and Steller, 2000) such as mammals, insects (Richardson and Kumar, 2002), nematodes (Liu and Hengartner, 1999) and cnidaria (Cikala et al., 1999), and also possibly in plants (Solomon et al., 1999) and yeast (Frohlich and Madeo, 2000; Skulachev, 2002). Cells undergoing apoptosis have a morphologically distinct pattern (Figure 1.1A) including cell condensation, fragmentation of the nucleus, bubbling of the plasma membrane, chromatin condensation and nucleosomal fragmentation. This was first observed by light microscopy many years ago (Kerr, 1965; Kerr et al., 1972) and further characterized by transmission electron-microscopy (Hacker, 2000; Ziegler and Groscurth, 2004).

Apoptosis plays a vital role in embryonic development (Vaux and Korsmeyer, 1999), in immune cell differentiation and maturation (Opferman and Korsmeyer, 2003), and in adult tissue homeostasis (Fulda and Debatin, 2004). It can tightly control cells' viability and its abnormal regulation is frequently seen in many human diseases (Reed, 2000). Excessive apoptosis contributes to neurodegenerative diseases such as AIDS, Alzheimer's, Parkinson's and Huntington's diseases (Fesik, 2000), while insufficient apoptosis allows cells to grow faster and live longer, and results in cancer and autoimmune disorders (Fesik, 2000).

The apoptotic regulation is normally through two signaling pathways: an extrinsic pathway and an intrinsic pathway. They both merge at the activation of a series of

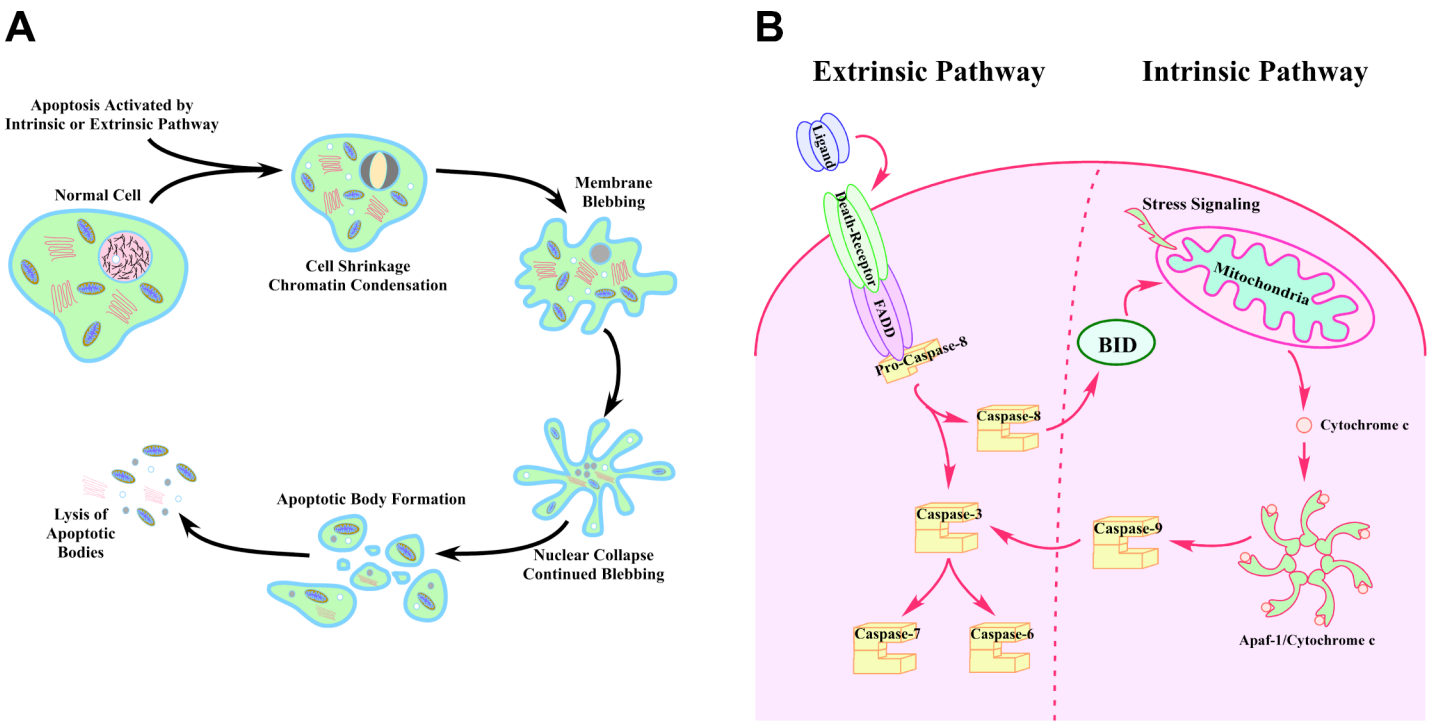

Figure 1.1: Apoptosis and its pathways. (A) Hallmarks of apoptosis including cell condensation, fragmentation of the nucleus, bubbling of the plasma membrane, chromatin condensation and nucleosomal fragmentation. This figure was modified from (Kerr, 1995). (B) Schematic representation of apoptotic pathways. Extrinsic apoptotic pathway is initiated by death ligands from outside of the cells, while the intrinsic pathway is stimulated by intracellular stress signalings. Both of these two pathways converge on the activation of caspases, which leads to the caspase cascade and final apoptosis.

caspases, which leads to the apoptotic cascade resulting in DNA and protein cleavage and cell disassembly (Figure 1.1B).

The extrinsic apoptotic pathway, also known as the death receptor pathway or caspase 8/10 dependent pathway, is initiated by stimuli from outside the cells. On the target cell surface, there are many transmembrane death receptors, such as DR4, DR5, CD95/Fas, and the tumor necrosis factor-alpha (TNF-alpha) receptor 1 (Ashkenazi, 2002). They are activated by specific pro-apoptotic signal ligands including Apo2L/TRAIL and CD95L/FasL to trigger the extrinsic apoptosis; their conserved cytoplasmic death domain (DD) can bind the Fas-associated adaptor protein with death domain (FADD), forming the death-inducing signaling complex (DISC) (Sartorius et al., 2001). The complex will next stimulate the autoproteolysis of procaspases-8 to release the active caspase-8 dimer into the cytosol, which can in turn activate a series of caspases 3, 6 and 7 and converge on the intrinsic apoptotic pathway (Denault and Salvesen, 2002).

The intrinsic apoptotic pathway, also referred to as the mitochondrial pathway, functions in response to intracellular stresses including growth factor withdrawal (O'Connor et al., 2000), DNA damage (Schuler and Green, 2001), unfolded protein stress (Breckenridge et al., 2003), detachment from the extracellular matrix (Martin and Vuori, 2004), and other types of severe cell stresses. This pathway is mainly regulated by the BCL-2 (B-cell CLL/lymphoma 2) family of proteins, which leads to the disruption of the mitochondrial membrane and the release of pro-apoptotic proteins, such as cytochrome c (Salvesen and Renatus, 2002). The released cytochrome c, through binding with the adaptor apoptotic protease activating factor-1 (APAF-1) and procaspase-9, forms a large size complex called the apoptosome that has the ability to activate caspase-9 (Denault and Salvesen, 2002). Subsequently, the caspases-3, 6, and 7, which are normally kept inactive by inhibitor of apoptosis proteins (IAPs), are activated by caspase-9, resulting in the apoptotic caspase cascade (Earnshaw et al., 1999).

1.2 Introduction to BCL-2 family

The BCL-2 family of proteins plays a central role in regulating intrinsic apoptosis. They are located in mitochondrial, smooth endoplasmic reticulum, and perinuclear membranes (Green and Reed, 1998). The first gene identified in this family is *bcl-2*, which resides in the long arm of chromosome 18 (Tsujimoto and Croce, 1986). Its genetic deregulation and expression is caused by the translocation to the long arm of chromosome 14 [t(14:18)] that occurs in most cases of follicular lymphoma (Chen-Levy et al., 1989; Hockenbery, 1992). The realization that it has a special role in cancer started this exciting field of research. To date, a large and still growing number of BCL-2 members have been discovered by biochemical, genetic, and molecular techniques. They are not limited mammalian cells, for example, ced-9 is from nematode (Hengartner et al., 1992), BHRF1 is from Epstein-Barr virus (Pearson et al., 1987), and LMW5 is from African swine fever virus (Neilan et al., 1993).

The BCL-2 members are very conserved, and are related to each other by regions known as BCL-2 Homology (BH) regions (Chittenden et al., 1995; Yin et al., 1994). According to their functions and sequence similarity, they are classified into three groups (Figure 1.2). The anti-apoptotic proteins (BCL-2, BCL-w, BCL-X_L, MCL-1 and A1) share up to four BH regions named BH1-4, and prevent cells from entering apoptosis. BAX and BAK, contain three regions, BH1-3, and can promote cell death by oligomerization that permeablizes the mitochondria outer membrane. They are called multi-region pro-apoptotic proteins. The last group is also pro-apoptotic. These proteins including BID, BIM, BAD, BMF, BIK, PUMA, NOXA, HRK/DPS (Harakiri), BLK, NIP3, bNIP3, MULE and so on, only share one region, BH3, which is a 16-25 residues long, and are called BH3-only proteins. These three family members form a large and delicate network that regulates the intrinsic apoptosis pathway and the cell's fate.

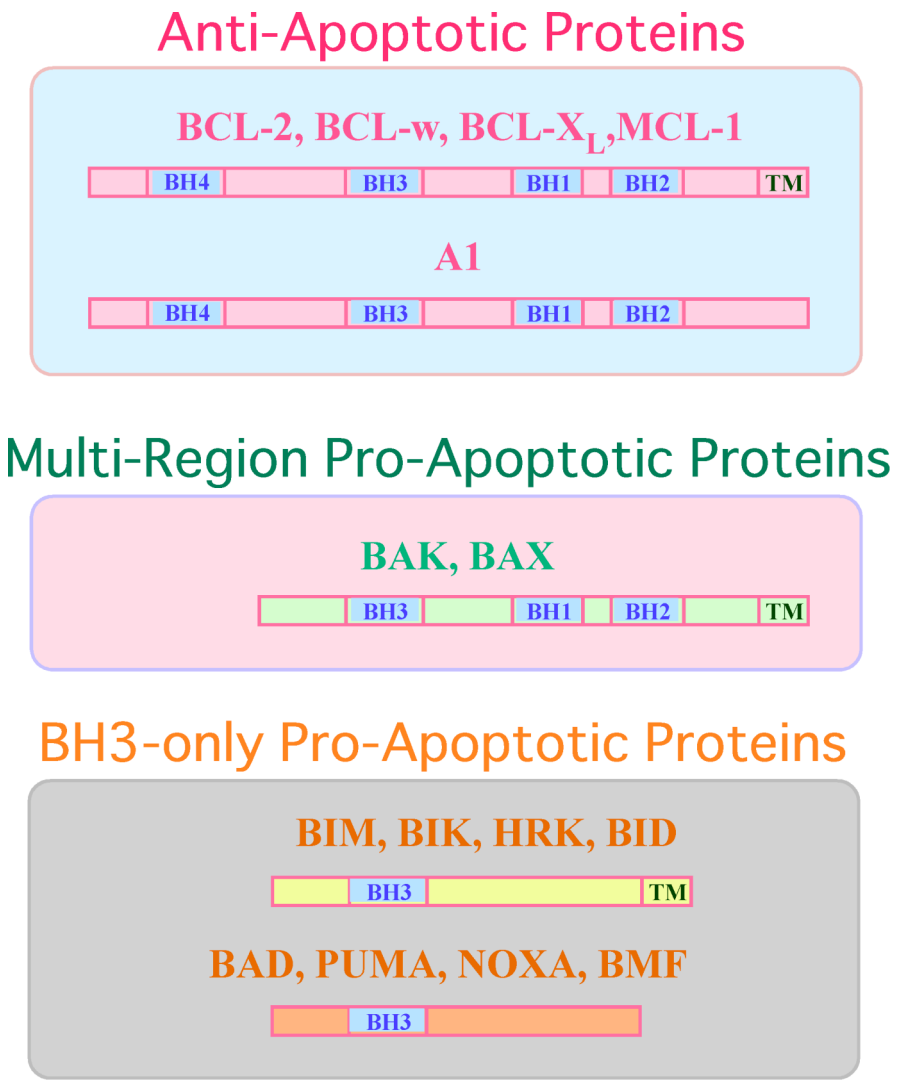

Figure 1.2: Schematic representations of the BCL-2 family of proteins. The anti-apoptotic proteins in the blue box contain four BH regions (BH1-BH4) and, except for A1, a C-terminal transmembrane (TM) helix. The multi-region pro-apoptotic proteins in the pink box share three BH regions (BH1-BH3) and a C-terminal TM helix. The BH3-only apoptotic proteins in the grey box have only one BH3 region; some have a TM helix and others don't.

1.3 Structural characteristics of BCL-2 members

Structural analysis is an important tool for exploring the functions of proteins. Since 1996 when the solution and crystal structures of BCL-X_L were first published (Muchmore et al., 1996), many three-dimensional structures of proteins in the BCL-2 family have been solved by NMR spectroscopy or X-ray crystallography (Chuang et al., 2002; Kawasaki et al., 2007; Opferman et al., 2005; Opferman et al., 2003; Zhu et al., 2004). As shown in Figure 1.3, no matter whether the activities are anti- or pro- apoptotic, the structure of each protein shares a very similar "signature" fold: an alpha helical bundle formed by 7 or 8 helices surrounding a central helix. However, the differences among these structures offer interesting insights into the regulation of their activities.

The most apparent difference is the hydrophobic groove formed by helix α2 to α5, α7 and α8. In BCL-X_L (Figure1.3A) (Muchmore et al., 1996), MCL-1 (Figure 1.3B) (Day et al., 2005) and BCL-2 (Figure 1.3C) (Petros et al., 2001) the grooves are open and act as "ligand receptors" when performing their anti-apoptotic activities. In BCL-w (Figure 1.3D) (Denisov et al., 2003; Hinds et al., 2003) and BAX (Figure 1.3E) (Suzuki et al., 2000), the groove is blocked by an extra C-terminal helix, which needs to be displaced for activation. For the BH3-only protein BID (Figure 1.3F) (Chou et al., 1999; McDonnell et al., 1999), the groove is much shallower and narrower compared to other BCL-2 members and allows no ligand binding. This variety in the size of the hydrophobic groove, together with differences in its electrostatic character, partially explains the relationship between structure and function of BCL-2 proteins. The groove contributes to the selectivity of protein-protein interactions and carries out a specific role in apoptotic regulation.

In the crystal structure of BCL-X_L, electron density was not detectable for residues from 28 to 80, which lie between the first and second helix. In addition, the medium- and long- range NOEs for these residues were also absent in NMR

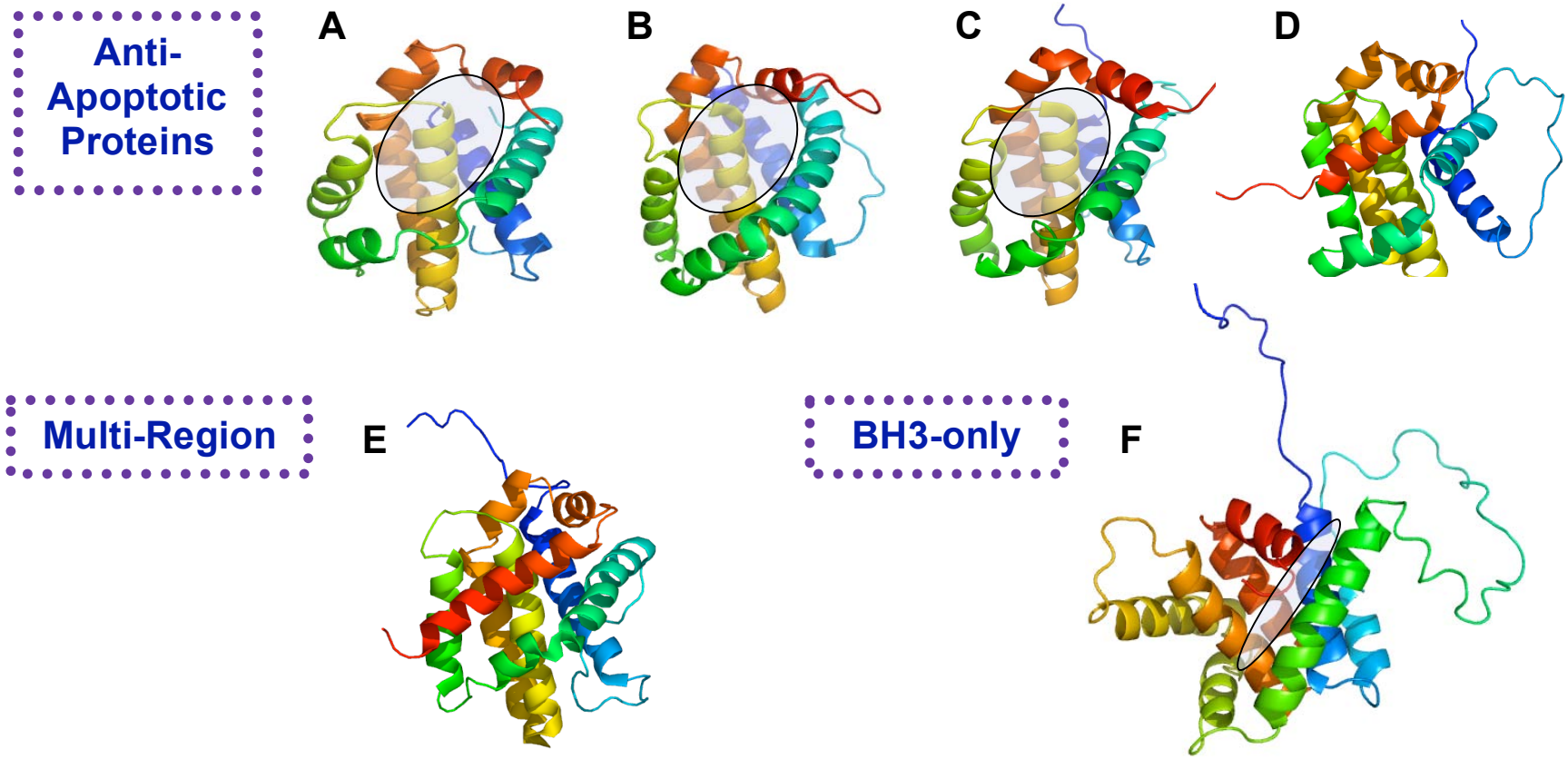

Figure 1.3: The structures of BCL-2 family. The cartoon structures were shown for (A) 1MAZ, human BCL-X_L (Muchmore et al., 1996), (B) 1WSX, mouse MCL-1 (Day et al., 2005), (C) 1G5M, human BCL-2 (Petros et al., 2001), (D) 1MK3, human BCL-w (Denisov et al., 2003), (E) 1F16, mouse BAX (Suzuki et al., 2000), and (F) 2BID, human BID (Chou et al., 1999).

studies, indicating that they adopt an unstructured conformation (Muchmore et al., 1996). By aligning the primary sequences and comparing the three-dimensional structures, it is clearly shown that the unstructured loop regions (ULRs) appear in most of BCL-2 members but vary in length, for example the ULRs in BCL-X_L, BCL-2, and BID are very long, while the ones in BCL-w and MCL-1 are much shorter. Although in the beginning it was believed that the ULR doesn't play much role in regulating BCL-X_L's anti-apoptotic ability (Muchmore et al., 1996), later reports revealed that long ULRs in a few BCL-2 members are involved in post-translational modifications and protein-protein interactions to act as switches for the proteins' activities.

For most of the BCL-2 members, another important component is the transmembrane (TM) region. Since they target membranes and it is hard to study membrane proteins, the solved structures of BCL-2 family proteins were mostly derived from constructs with TM deletions. One exception is BAX, which has a soluble conformation in which its C-terminal TM region (residue 170 to 188) folds back into the hydrophobic groove. The solution structure of BAX (Figure 1.3E) is the only structure of a full-length BCL-2 protein (Suzuki et al., 2000). Its C-terminal α-helix is not exposed to the membrane environment, which guarantees the cytosolic localization and inactivation of BAX in the absence of death stimuli.

All together, the structural studies on BCL-2 members have identified a few regions that are critical for the proteins to perform their anti- or pro-apoptotic activities. These characteristic structures not only determine the function(s) of the proteins, but also act as indispensable targets for regulation.

1.4 Regulation for BCL-2 family at multi-levels

The BCL-2 family of proteins is regulated at multiple-levels, including transcriptional, post-transcriptional, and post-translational regulation (Figure 1.4).

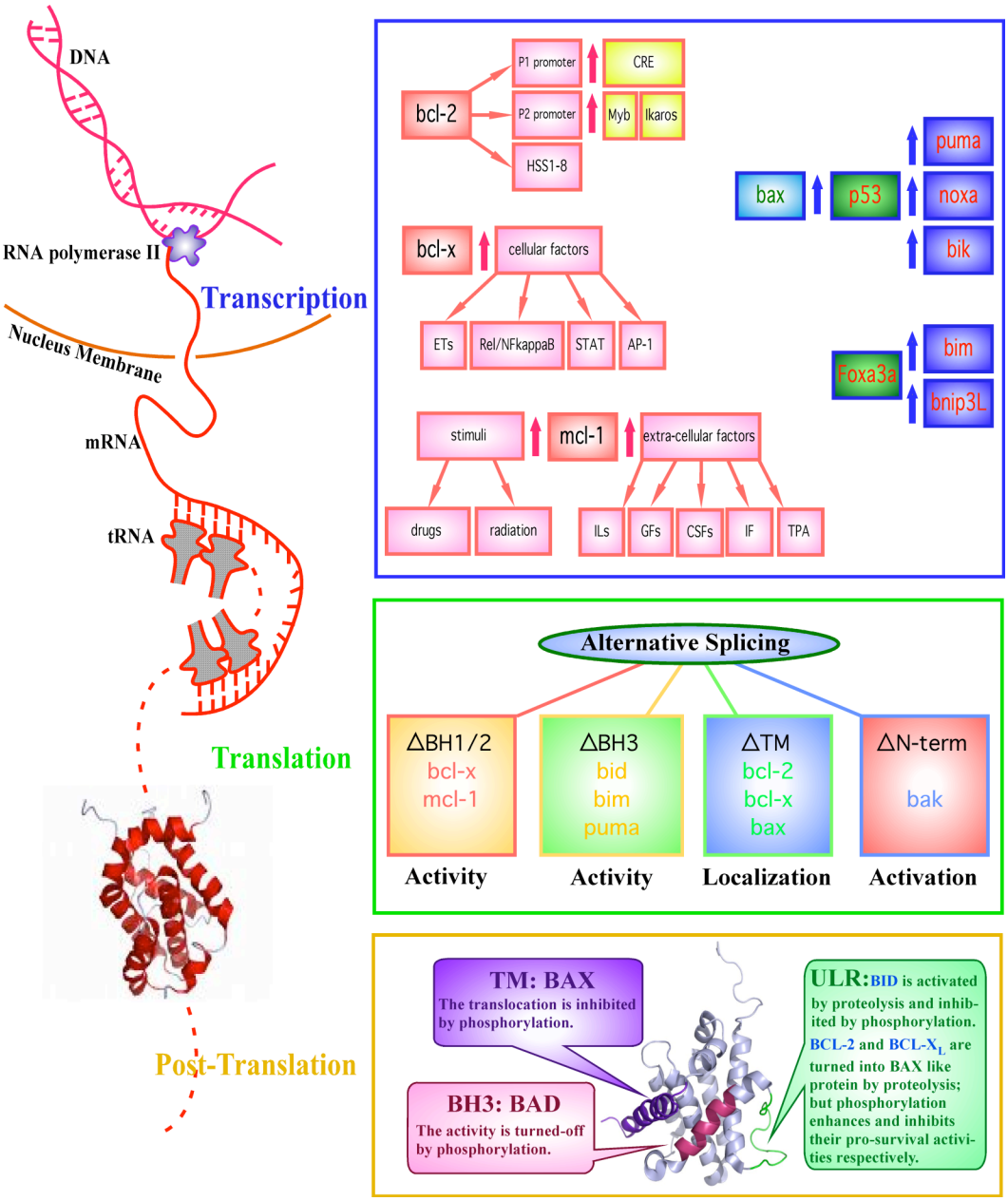

Figure 1.4: Multiple levels of regulation of BCL-2 proteins. Regulation occurs at three levels: transcriptional (blue box), translational (green box), and post-translational (yellow). BCL-2 family proteins regulated at each level are shown.

Their combination and integration provide the possibility of either large or minor modulations on protein levels at all the stages a cell may encounter.

1.4.1 Transcriptional regulation

Firstly, the mRNA levels of the BCL-2 proteins are regulated. For anti-apoptotic proteins, one of the best-understood examples is the *bcl-2* gene in human, which is around 200kb and comprises of three exons (Lang et al., 2005). This gene is under the initiation of P1 and P2 promoters (Seto et al., 1988). The P1 promoter is positively induced by cyclic AMP-response element (CRE) (Wilson et al., 1996), which together with Sp1 binding site of P1 can also mediate the previously mentioned t(14;18) translocation expressed from *Eμ* enhancer (Dong et al., 1999). On the other hand, it is repressed by an element located upstream of the P2 promoter (Young and Korsmeyer, 1993). Myb family of transcription factors (in chicken T cells) and Ikaros family member Alios are the activators for the transcription of the P2 promoter (Seto et al., 1988). *bcl-2* transcription is also regulated through DNAse I hypersensitive sites (HSS1-8) (Seto et al., 1988) and p53 tumor suppressor (Miyashita et al., 1994). Further, the stability of mRNAs modulated through an adenine- and uracil-rich element (ARE) contributes in the down-regulation of bcl-2 expression (Schiavone et al., 2000). As for the *bcl-x* gene, it is regulated by many different cellular factors including Ets, Rel/NFkappaB, STAT and AP-1 transcription factor families (Sevilla et al., 2001). The modulation of *mcl-1* gene is cell-type dependent. It is up-regulated by anti-apoptotic extra-cellular stimuli, such as interleukins (ILs), growth factors (GFs), colony stimulating factors (CSFs), interferon (IF), and TPA (Craig, 2002), but can also be induced by pro-apoptotic stimuli such as drugs or radiation to antagonize early DNA damage (Zhan et al., 1997).

The regulation of pro-apoptotic proteins at the transcriptional level involves many different factors and the tumor suppressor p53 has proved to be one of the major factors. In response to DNA damage, the cellular level of p53 increases, which in

turn transcriptionally up-regulates the pro-apoptotic genes including *puma* (Nakano and Vousden, 2001), *noxa* (Oda et al., 2000), *bik* (Mathai et al., 2002) and *bax* (Miyashita and Reed, 1995). Remarkably PUMA, the gene product of *puma*, plays a vital role in p53-mediated apoptosis by coupling the nuclear and cytoplasmic function of p53 (Chipuk et al., 2005). Another important transcriptional factor is Foxo3a. After the removal of the survival signals like P13K/Akt that can phosphorylate and inactivate it, Foxo3a can induce *bim* (Dijkers et al., 2000) and *bnip3L* (Real et al., 2005) expression in different cell types.

1.4.2 Post-transcriptional regulation

Alternative splicing of a primary transcript is a vital mechanism for enhancing proteomic diversity (Black, 2000; Modrek et al., 2001). It is very commonly involved in the post-transcriptional regulation of almost every BCL-2 member known. Taking the *bcl-2* gene as an example, two overlapping open reading frames lead to the translation of two spliced forms, BCL-2α (239 amino acids and 26KD) and BCL-2β (205 amino acids, 22KD) (Batistatou et al., 1993; Nunez et al., 1990; Tsujimoto and Croce, 1986), which differ only in their C-termini. Splicing can generate another short open reading frame upstream of the *bcl-2* gene that down-regulates *bcl-2* by competition for initiating ribosomes (Savill et al., 1996). The *bcl-x* gene generates three products by alternative splicing: BCL-X_L which contains BH1-4 and the TM region and is anti-apoptotic; BCL-X_S which lacks the BH1 and BH2 regions and behaves as a BH3-only pro-apoptotic protein; and BCL-X_β whose function is not yet clear and doesn't have the TM region (Boise et al., 1993). For *mcl-1*, there are also a pair of antagonistic splicing isoforms: MCL-1 and MCL-1S. The BH3-only MCL-1S specifically dimerizes with the anti-apoptotic MCL-1 and the ratio between these two proteins determines the fate of the MCL-1 expressing cells (Bae et al., 2000).

Pro-apoptotic BCL-2 members also have alternative splicing variants. For the genes *bid*, *bim* and *puma*, many variants have been reported differing from each other in structural properties and cellular localization (Nakano and Vousden, 2001; O'Connor et al., 1998; Renshaw et al., 2004). The variants with BH3 region are pro-apoptotic, while the others are neither anti- nor pro-apoptotic. The *bax* gene produces eight pro-apoptotic variants, four of which contain the TM region that targets mitochondria when activated (Apte et al., 1995; Cartron et al., 2002; Oltvai et al., 1993; Shi et al., 1999; Wolter et al., 1997; Zhou et al., 1998). For *bak*, one variant N-BAK was found in neuron cells and is conserved in human, mouse and rat species (Sun et al., 2001).

Taken together, alternative splicing of BCL-2 members is very important in regulating their anti- or pro- apoptotic activities and their cellular localizations in their specific cell types. A minor shift of the relative ratio between their splicing variants can result in some forms of cancer.

1.4.3 Post-translational regulation

At the post-translational level, the BCL-2 family of proteins is regulated through a variety of mechanisms, such as proteolytic cleavage, phosphorylation, ubiquitin-dependent degradation, and translocation. They mainly target in the ULR, BH3 region, and some member-specific regions.

As mentioned in Section 1.3, long ULRs provide opportunities to regulate BCL-2 members. For example, the BID protein performs its pro-apoptotic activity mainly through truncated forms (tBID); its activation is dependent on proteolytic cleavage in its ULR (residue 41 to 79) between the second and third helix. This cleavage can be affected by many different proteases: caspases (Gross et al., 1999; Li et al., 1998; Luo et al., 1998), calpain (Chen et al., 2001; Mandic et al., 2002), Granzyme B (Barry et al., 2000; Sutton et al., 2000; Wang et al., 2001), lysosomal enzymes (Reiners et al., 2002; Stoka et al., 2001) and other unknown

proteases (Deng et al., 2003; Werner et al., 2004). In response to a set of death stimuli, including death receptor engagement, ischemia/reperfusion, cytotoxic T cell attack, lysosome photo-damage, and DNA damaging agents, these proteases are activated and specifically cleave the ULR of full-length BID. After the cleavage, the N-terminal portion of the molecule (tBID-N) remains bound to tBID-C (Zha et al., 2000) until further interaction with cardiolipin (Liu et al., 2005) or unconventional ubiquitination and proteasome-dependent degradation (Tait et al., 2007) that lead to the exposure of the BH3 region of tBID-C. This is the final step allowing tBID to act as a potent initiator of mitochondrial apoptosis. The activation of BID through caspase-8 can be effectively inhibited by the phosphorylation at Ser61, Ser64 and Thr59, all of which locate in the ULR (Degli Esposti et al., 2003; Desagher et al., 2001). A mutant in Ser61 that almost completely abolished the phosphorylation was found to be more toxic than wild-type BID. In addition, the long ULRs in BCL-2 (residue 25 to 91) and BCL-X_L (residue 21 to 84) are subjected to proteolytic cleavage and their deletions significantly reduced apoptosis compared to the wild-type proteins (Chang et al., 1997; Uhlmann et al., 1996). Caspase-3 cleaves BCL-2 after Asp34, and cleaves BCL-X_L after Asp61 and Asp76. Calpain can cleave BCL-X_L after Asp60. All of these cleavages generate N-terminal truncated constructs, which surprisingly perform as BAX/BAK-like pro-apoptotic proteins (Cheng et al., 1997; Jonas et al., 2004). For BCL-X_L, the phosphorylation at Ser62 induced by vinblastine partially disables its ability to antagonize BAX, resulting in defective anti-apoptotic activity (Upreti et al., 2008). Contrarily, the phosphorylation of BCL-2 promotes its pro-survival activity. The single phosphorylation at Ser70 induced by IL-3, PKC or erythropoietin is vital for its full activity (Ito et al., 1997), and the hyper-phosphorylation of BCL-2 at Ser70, Ser87 and Thr69 in response to paclitaxel confers enhanced anti-apoptotic activity (Scatena et al., 1998).

The BH3 region, is the most striking region of homology among BCL-2 proteins. This region not only mediates protein-protein interactions among BCL-2 family, but also takes part in post-translational regulation. Taking BAD as an example,

phosphorylation of the BH3 region at either Ser112 or Ser136 allows it to bind 14-3-3 chaperones to turn off its pro-apoptotic activity. BAD can be reactivated through dephosphorylation of both sites (Datta et al., 1997; She et al., 2005).

Some BCL-2 members contain other, special regions of member-specific regulation. MCL-1 has a long N-terminal sequence (residue 1 to 170), in which the first 79 amino acids regulate the protein's localization (Germain and Duronio, 2007) and the following 91 residues, comprising two PEST regions, control the protein's half-life. The Lys136 in PESTs, together with Lys194 and Lys197 in the ULR, is sensitive to poly-ubiquitination by MULE (LASU1), which can lead to ubiquitin-dependent proteasome degradation and are responsible for MCL-1's very short half-life (Warr et al., 2005; Zhong et al., 2005). In the PEST regions, there are also sites for limited proteolysis, such as Asp127 and Asp 157 for caspase-3 cleavage (Weng et al., 2005), Asp117, Asp127 and Asp157 for Granzyme B and so on (Han et al., 2005). After these cuts, the C-terminal fragments, containing intact BH1-3 and TM regions, were reported to have increased stability but perform different activities, from anti-apoptotic, neutral, to pro-apoptotic (Clohessy et al., 2004; Herrant et al., 2004; Michels et al., 2004). Additionally, full-length MCL-1 is subject to phosphorylation induced by Erk-/GSK3 at Thr92 and Thr163 in PESTs. This results in its association with Pin1, a recently identified peptidyl-prolyl cis/trans isomerase, and the increased stability (Ding et al., 2008). Another example is the specific regulation of BIM and BMF. These two proteins share a conserved dynein light chain (DLC)-binding region, which mediates their interactions with DLC1 or DLC2, respectively. This binding leads to their association with the dynein motor complex and their cytoplasmic localization. In response to distinct apoptotic stimuli, BIM and BMF can be released by the dynein motor complex, and migrate to mitochondria to perform their pro-apoptotic activities of antagonizing anti-apoptotic proteins (Puthalakath et al., 1999; Puthalakath et al., 2001).

Through a wide variety of mechanisms, the levels of active BCL-2 members are tightly controlled, which serves to guarantee that these proteins perform their physiological activities properly.

1.5 Physiological roles of BCL-2 members

Knockout studies have demonstrated that BCL-2 members have specific physiological roles *in vivo* as summarized in Table 1.1. BCL-X_L regulates the survival of erythroid progenitors and neuronal cells. Its deficiency in mice leads to embryonic lethality and excessive cell death of immature lymphocytes and neurons (Motoyama et al., 1995), while its over-expression correlates with resistance to anti-cancer chemotherapeutic agents (Amundson et al., 2000). BCL-2 is necessary for the survival of mature T and B lymphocytes. Its loss results in growth retardation, renal failure and apoptosis of lymphocytes (Veis et al., 1993), and its high-expression always correlates with poor survivals of tumor (Fesik, 2005). MCL-1, a very special anti-apoptotic protein, not only plays an interesting role in the implantation of the developing embryo (Rinkenberger et al., 2000), but also is essential for both the development and maintenance of lymphocytes (Opferman et al., 2003) and the hematopoietic system (Opferman et al., 2005); its over-expression is always seen in haematopoietic and lymphoid cancers, such as multiple myeloma and chronic lymphocytic leukaemia (Alvi et al., 2005; Derenne et al., 2002). BCL-w exhibits the ability to regulate spermatogenesis, and its ablation leads to male infertility (Print et al., 1998). It was also reported that BCL-w may play an important protective role in neurons in the diseased brain (Zhu et al., 2004) and that its over-expression promotes the growth of non-small cell lung cancers (NSCLC) (Kawasaki et al., 2007). A1 is involved in inhibition of certain types of neutrophil apoptosis (Hamasaki et al., 1998) and its high level expression in mice perturbs the late stage B-cell function (Chuang et al., 2002).

The multi-region pro-apoptotic proteins also display critical functions. BAX was reported to be responsible for immature neuronal cell death (White et al., 1998),

Table 1.1: Physiological Roles of BCL-2 Members

Group	Member	Responsible Physiological Roles
Anti-apoptotic Proteins	BCL-X_L	• The survival of erythroid progenitors and neuronal cells
	BCL-2	• The survival of mature T and B lymphocytes
	MCL-1	• The implantation of a developing embryo • The development and maintenance of lymphocytes and hematopoietic system
	BCL-w	• The regulation of spermatogenesis • The survival of neurons in the diseased brain
	A1	• The inhibition of certain types of neutrophil apoptosis
Multi-region Pro-apoptotic Proteins	BAX	• Immature neuronal cell death • Homeostasis of lymphoid and reproductive organs • Tumor suppression
	BAK	• Not clear yet, but similar to the roles of BAX
BH3-only Pro-apoptotic Proteins	BID	• Lipid transfer between mitochondria membranes • Myeloid homeostasis and tumor suppression • Caspase-2 induced apoptosis • The demise of neurons from cerebral ischemia
	BIM	• Embryogenesis • The control of hematopoietic cell death • The fate of anergic B cells • The inhibition of autoimmunity
	PUMA	• Hematopoietic cell death triggered by IR, deregulated c-Myc expression, and cytokine withdrawal • Apoptosis of mast cells induced by cytokine deprivation • Neuronal apoptosis induced by DNA damage in sympathetic neurons
	NOXA	• Mediator of p53-dependent apoptosis
	BMF	• B cell homeostasis • The prevention of thymic lymphoma development induced by gamma irradiation

homeostasis of lymphoid and reproductive organs (Knudson et al., 1995), and tumor suppression (Eischen et al., 2002; Knudson et al., 2001; Shibata et al., 1999). It also responds to stresses, including DNA damage and ischemia-reperfusion injury (Hochhauser et al., 2003). The phenotypic abnormalities caused by BAK's depletion is not known yet, since *bak*$^{-/-}$ mice were found to develop normally without any age-related disorders. However, *bax*$^{-/-}$*bak*$^{-/-}$ animals displayed multiple developmental defects in several tissues and showed the resistance to a few apoptotic stimuli including staurosporine, ultraviolet radiation, growth factor deprivation and etoposide (Lindsten et al., 2000; Wei et al., 2001), suggesting that these two proteins might be functionally redundant.

As for BH3-only proteins, the studies on their physiological roles have mainly focused on a few better known members. BID, serving as the bridge between the intrinsic and extrinsic apoptotic pathways, shows lipid transfer activity between mitochondria membranes (Esposti et al., 2001). In addition, it was reported that it is required for myeloid homeostasis and tumor suppression (Zinkel et al., 2003), necessary for caspase-2 induced apoptosis (Bonzon et al., 2006) and possibly contributes to the demise of nerve cells in cerebral ischemia (Plesnila et al., 2002). BIM plays an essential role in embryogenesis, the control of hematopoietic cell death, and the fate of anergic B cells, and also acts as a barrier against autoimmunity (Bouillet et al., 2000; Oliver et al., 2006). Its ablation in mice results in increased numbers of lymphocytes, plasma cells, and myeloid cells, and facilitates the development of fatal autoimmune glomerulonephritis (Strasser et al., 2000). PUMA is likely a tumor suppressor, required for hematopoietic cell death triggered by ionizing radiation (IR), deregulated c-Myc expression, and cytokine withdrawal (Ekoff et al., 2007; Jeffers et al., 2003). It is also critical in cytokine deprivation induced apoptosis of mast cells (Ekoff et al., 2007), and necessary and sufficient for neuronal apoptosis induced by DNA damage in sympathetic neurons (Wyttenbach and Tolkovsky, 2006). Together with another essential mediator of p53-dependent apoptosis NOXA (Kiryu-Seo et al., 2005; Shibue et al., 2003), it further displays a key regulatory ability in neural precursor

cell (NPC) death. Recently, Villunger and co-workers addressed the function of the BH3-only protein BMF. Its depletion impairs B cell homeostasis and accelerates gamma irradiation-induced thymic lymphoma development (Labi et al., 2008). Taken together these studies suggest that the various BCL-2 family proteins are each assigned specific responsibilities in cells and animals. How they fulfill these duties is an inevitable question. The answer will be of great value for the treatment of BCL-2 family-related diseases.

1.6 Cellular localizations of BCL-2 members

The cellular localizations of BCL-2 members, which mainly focus on the cytoplasmic face of mitochondria, ER, and/or nucleus, are obviously crucial for their function in apoptotic regulation. As shown in Figure 1.2, some of the members contain a hydrophobic TM sequence at the COOH terminus and belong to a large group of tail-anchored membrane proteins (Wattenberg and Lithgow, 2001). The TM region not only helps the protein to anchor into either MOM or ER membrane by spanning the membrane in a α-helical conformation (Antonsson, 2001), but also plays a major role in directing the protein into its cellular destination.

Generally speaking for all the tail-anchored proteins, higher hydrophobicity of the TM region indicates an ER-targeting protein, while lower hydrophobicity is seen in MOM-targeting proteins (Horie et al., 2002). The mean hydrophobicity of the TM regions in BCL-2 tailed-anchored proteins doesn't show obvious differences, but there are some tendencies in the shape of their hydropathy plots. Increased hydrophobicity in the C-terminal half of the TM region is implicated in MOM-targeted proteins, yet the ER- and nuclear-targeted proteins display more hydrophobicity in the N-terminal half of their TM regions (Schinzel et al., 2004). Another determinant for the protein's localization is the flanking residues around the TM regions. Higher positive charges can increase the specificity to MOM, whereas fewer basic residues result in more protein accumulation on ER or

nuclear outer membrane (Horie et al., 2002). In the anti-apoptotic proteins, the TM region of BCL-2 shows decreasing hydrophobicity in its C-terminal sequence and contains fewer basic residues. This agrees with the finding that the majority of endogenous BCL-2 lies on the membrane of ER and nucleus, and only about one-third of it targets to MOM (Lithgow et al., 1994; Nguyen et al., 1993). In contrast, the TM regions of BCL-X_L, BCL-B, and BCL-w display less hydrophobicity in their N-terminal sequences, which leads to their higher specificity in targeting on MOM (Kaufmann et al., 2003; Ke et al., 2001).

As for the multi-region pro-apoptotic group, BAK is expressed as a completely tail-anchored protein inserted in MOM and, to a small extent, the ER membrane, whilst BAX mainly stays in the cytosol as a soluble protein (Figure 1.3E) and only translocates to mitochondria or the ER when its TM region becomes accessible to membranes during apoptosis (Wolter et al., 1997). This relocation can be inhibited by phosphorylation at Ser184, which is activated by PI3K/Akt and mediated by Akt (Gardai et al., 2004). For BH3-only proteins, although some members including BID, BIM, and HRK were reported to contain TM regions at their C-termini, which might help them with membrane targeting, they are sequestered elsewhere in healthy cells and require transcriptional or post-translational regulation to translocate to the MOM. Two examples are the over-expression of BIM (O'Connor et al., 1998) and the proteolytic activation of BID (tBID) (Grinberg et al., 2002).

1.7 Cellular behaviors of BCL-2 members ---- Protein-protein interactions

To date, much research has been carried out to explore how the BCL-2 family regulates intrinsic apoptosis. Although we are still far from full understanding, agreement has been reached on a few points. Anti-apoptotic proteins execute their pro-survival activities through sequestering pro-apoptotic proteins. The BH3-only group proteins are the real death-initiators. Whether directly or indirectly or both, their over-expression can activate the multi-region BAX/BAK (death-effectors) to

oligomerize and permeablize the MOM, which is a critical step for the release of the pro-apoptotic factor cytochrome c and the following caspase cascade. The protein-protein interactions between BCL-2 members are the major mechanism that is involved in regulating these steps. Here, the literature on hetero-dimerization, homo-dimerization and oligomerization of BCL-2 proteins will be reviewed.

1.7.1 Hetero-dimerization (Figure 1.5)

Hetero-dimerization usually happens between members bearing opposite bioactivities, and the interactions between anti-apoptotic proteins and BH3-only members are very stable and easy to detect by either immunoprecipitation (IP) or other *in vitro* means. The binding has been characterized in detail by structural studies and quantified by titration studies, using BH3 peptides to mimic the BH3-only proteins. The 3D crystal structure of BCL-X_L:BIM-BH3 complex (Figure 1.6A) reveals that the anti-apoptotic BCL-X_L uses its hydrophobic groove as a "ligand receptor" to hold the BIM BH3 peptide, which forms an amphipathic α-helix (Liu et al., 2003). By affinity tests, it was shown that the binding affinities for different pairs of BCL-2 proteins vary from nanomolar affinity to undetectable, demonstrating these protein-protein interactions are member-specific. BIM and PUMA potently engage all the anti-apoptotic members; BAD only binds BCL-2, BCL-X_L, and BCL-w, but not A1 and MCL-1; and NOXA is the specific antagonist to MCL-1 and A1 (Chen et al., 2005). This information acquired with BH3 peptides has deepened our understanding on the selectivity of interactions, but it is not known yet whether the full-length BH3-only proteins will perform similarly to the peptides.

The interactions between anti-apoptotic members and multi-region BAX/BAK are less clear. BAX was identified as a BCL-2 binding protein in yeast two-hybrid experiments (Oltvai et al., 1993), but this was observed in immunoprecipitations (IP) only in the presence of detergents (Hsu and Youle, 1997; Suzuki et al., 2000).

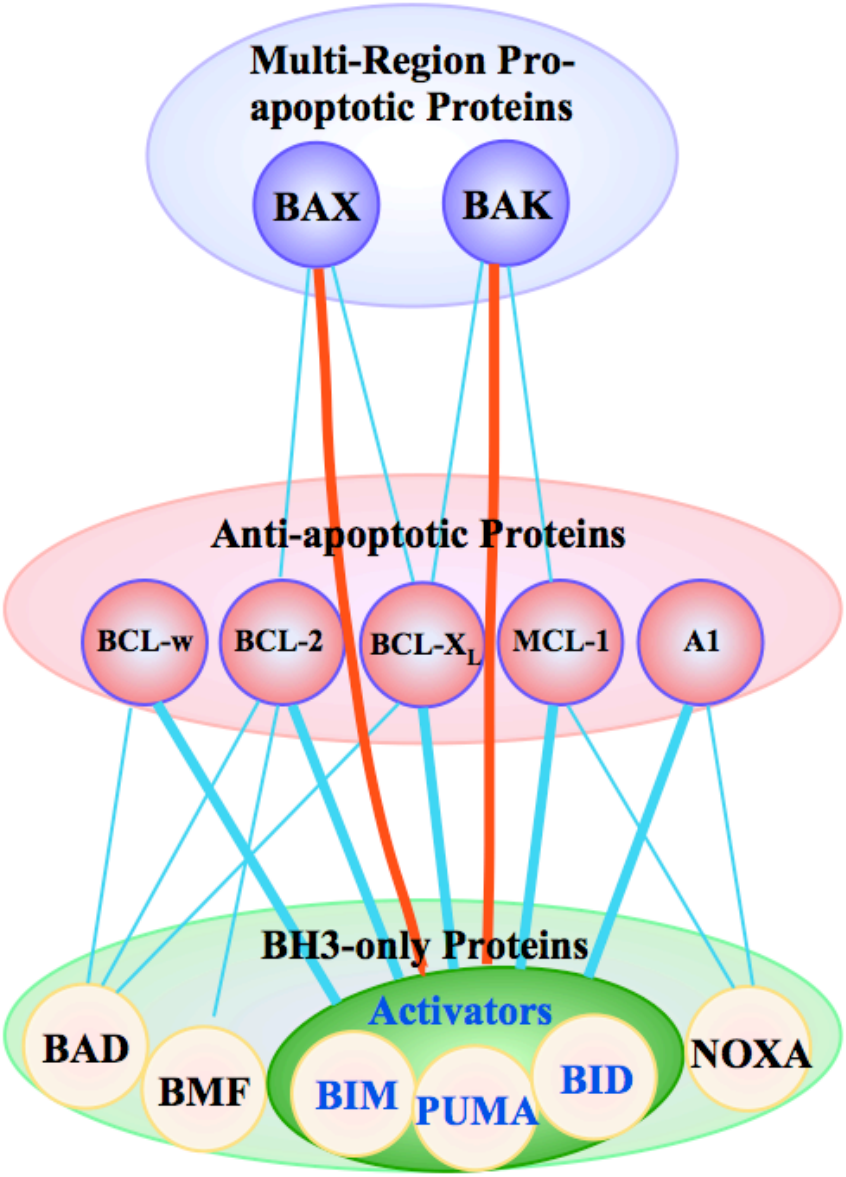

Figure 1.5: Hetero-dimerization among BCL-2 family of proteins. Every pair of proteins connected by a line will interact with each other, blue lines represent inhibition, and red lines represent activation. Since each of the activator proteins, BIM, PUMA and BID, interact with identical partners, those interactions are grouped and represented by bold lines.

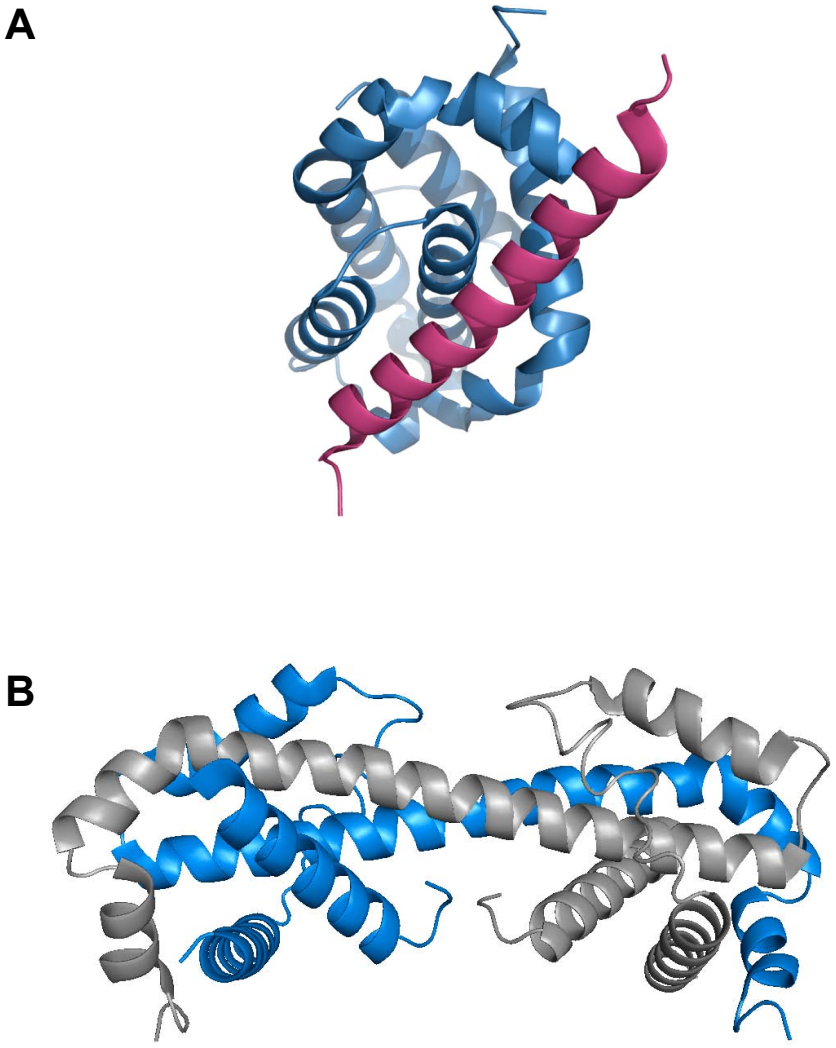

Figure 1.6: Three-dimensional models showing the mechanisms of dimerization between BCL-2 proteins. (A) Hetero-dimerization represented by crystal structure of BCL-X_L:BIM-BH3 complex (1PQ1). BCL-X_L is in blue and the BIM-BH3 peptide is in pink. (B) Homo-dimerization represented by the crystal structure of the swapped helix dimer of BCL-X_L (2B48). One molecule is in blue and the other is in grey.

Similarly in IP experiments with detergents, BAK was found sequestered by BCL-X_L and MCL-1, but not by BCL-2 (Leu et al., 2004; Willis et al., 2005). Also, these specific interactions are not constitutive in cells, and only a small fraction of BAX/BAK can be co-immunoprecipated with anti-apoptotic proteins (Hsu and Youle, 1997; Sedlak et al., 1995). All of these findings suggest that these interactions necessarily require further stimulation and/or conformational changes that might be provided by membrane targeting of the proteins or detergent mimicking *in vitro*. The requirement for detergents also makes the interactions harder to examine structurally.

The most controversial hetero-dimerization is between BAX/BAK and BH3-only proteins, which are both pro-apoptotic. Experiments with BAK-deficient mitochondria and blocking antibodies first demonstrated that tBID could bind BAK to induce the release of cytochrome c (Wei et al., 2000). Further using large unilamellar vesicles (LUVs) and a panel of BH3 peptides, it was proven that only BID and BIM could directly induce the conformational change of BAX and BAK, indicating a division of BH3-only proteins into those that work via BAX/BAK and those that work by inhibiting anti-apoptotic BLC-2 proteins (Kuwana et al., 2005; Kuwana et al., 2002; Letai et al., 2002; Lovell et al., 2008). Although there was much functional evidence, there was little evidence for a direct interaction by structural or binding analysis until recently when a stapled BID/BIM peptide was reported to directly bind BAX through a novel site composing helix α1, α6, and the loop between α1 and α2 (Gavathiotis et al., 2008; Walensky et al., 2006). This binding site is different from the classical canonical groove formed by BH1-3 regions of anti-apoptotic proteins, and might indicate a special mechanism for BAX's activation. As for BAK, so far, there is no obvious evidence for its direct binding with BH3-only proteins or BH3 peptides, which may suggest that BAK uses different mechanisms for its activation.

1.7.2 Homo-dimerization

Homo-dimerization is much less understood except for the protein BCL-X_L. Many factors can induce BCL-X_L to form homo-dimers through two different pathways. It was first reported that basic pH could promote the formation of a non-covalently linked homo-dimer and its structure was solved by crystallography showing two BCL-X_L monomers swap their carboxy-terminal regions leaving those two hydrophobic grooves available for ligand-binding (O'Neill et al., 2006). Our laboratory also observed this swapping by NMR data (Figure 1.6B), and found that heat could also induce dimerization (Denisov et al., 2007). In another recent article, the authors, using PAGE, chemical cross-linking, Raman spectroscopy and Ellman reaction, proved that in the presence of non-ionic detergents both acidic and basic pH could contribute to the homo-dimerization of BCL-X_L, but through different pathways (Feng et al., 2008). In an acidic environment, the homo-dimer is linked by non-ionic bonds and retains the ability to bind ligands; however, at neutral and basic pHs, the homo-dimer is linked by disulphide bond, and does not bind BH3 peptides. These two distinct pathways raise the questions whether other BCL-2 members will homo-dimerize in similar ways and what physiological role the homo-dimerization would play in apoptotic regulation.

1.7.3 Oligomerization and activation of BAX/BAK

BAX and BAK, the multi-region pro-ain poptotic proteins, are believed to have more than one stable conformation in cells and perform their pro-apoptotic activities upon remarkable conformational changes. When located in the cytosol, BAX is held as a soluble inactive monomer. Its activation requires BAX's translocation to MOM and its homo-oligomerization. Recombinant BAX expressed in bacteria usually exists as a monomer in solution, which is around 22kDa; while in the presence of detergent to mimic the membrane, it has been reported to form oligomers of 96kDa, 160kDa, 200kDa, and 260kDa dependent

on the size of the detergent micelles (Antonsson et al., 2000; Antonsson et al., 2001; Valentijn et al., 2008). Oligomeric BAX is an important component of the mitochondrial apoptosis-induced channel (MAC), which is critical for the release of cytochrome c and activation of pro-apoptotic caspases (Dejean et al., 2005). It forms as an oligomeric unit comprising helix 2 (BH3 region), helix 4 and helix 5 (George et al., 2007). Although in the literature the oligomerization of BAX is always considered as part of its activation, recently there have been some novel opinions. By fluorescence correlation spectroscopy (FCS) and fluorescence-intensity distribution analysis (FIDA), detergent activated BAX was observed to be a monomer (Ivashyna et al., 2009), and by blue-native PAGE it was shown that the BAX oligomer was not in an active conformation (Valentijn et al., 2008). These new experiments suggest that oligomerization of BAX doesn't necessarily correlate with its activation, and BAX might have at least two monomeric conformations and two oligomeric conformations: an active one and an inactive one.

Although BAX and BAK may function similarly, they could be activated through different mechanisms. The oligomerization of BAK is less well understood. A reported homo-dimer formed by the BH3 region of one molecule engaging the hydrophobic groove of the other molecule was shown to be essential to nucleate the oligomerization of BAK (Dewson et al., 2008). In addition, p53 can directly initiate the oligomerization of BAK and facilitate the transcription-independent apoptosis through the p53 DNA binding domain (Pietsch et al., 2008).

1.8 Possible models for BCL-2 regulated intrinsic apoptosis

Several models have been developed to explain the physiological roles and cellular behavior of BCL-2 proteins in regulating apoptosis. The observation that BCL-2 blocks the activation of caspases by interacting with BAX and BAD lead to the original "Rheostat" model of BCL-2 function. In this model, anti- and pro-apoptotic proteins interact with each other to neutralize their activities, and their

relative ratio determines the cell's fate, either to live or to die (Oltvai et al., 1993; Yang et al., 1995). This model is the foundation of our current understanding of apoptotic regulation. However, with the collection of more and more complicated data, it started to show its weakness and it fails to explain the specificity of each BCL-2 member. This has led to the development of two other popular models: the competitively activating model (CAM) and the directly activating model (DAM) (Figure 1.7).

CAM describes an indirect activation process in which BH3-only proteins are proposed to activate BAX/BAK by releasing them from their specific anti-apoptotic partners. This occurs through the BH3-only proteins competitively binding to the pocket of the anti-apoptotic proteins and without direct interactions between the BH3-only proteins and BAX/BAK. Once sufficient BAX/BAK are released, apoptosis will occur (Chen et al., 2005; Willis et al., 2005; Willis et al., 2007). This model is based on the observation that BH3 peptides derived from BH3-only proteins have different binding affinities for anti-apoptotic members. But its weakness is that it is based on results with BH3 peptides. The anti-apoptotic members and activated BH3-only proteins have rarely been shown to interact with each other in solution, although they functionally interact in a lipid environment (Kluck et al., 1997). This indicates that the interactions are not only affinity-dependent but depend on cellular localization. It remains unclear whether the binding affinities tested *in vitro* using BH3 peptides accurately reflect the activities of BH3-only proteins *in vivo*.

DAM takes the assumption that BH3-only proteins can directly bind and activate BAX/BAK, and that the roles of anti-apoptotic proteins are to sequester the BH3-only members to prevent apoptosis. Since only BIM, tBID and PUMA have been reported to hold the ability to directly activate BAX/BAK (Cartron et al., 2004; Kuwana et al., 2005; Letai et al., 2002; Wei et al., 2000), they are called "direct activators", whereas the rest of BH3-only members are classified as "sensitizers". Sensitizers can compete with "direct activators" for the binding to

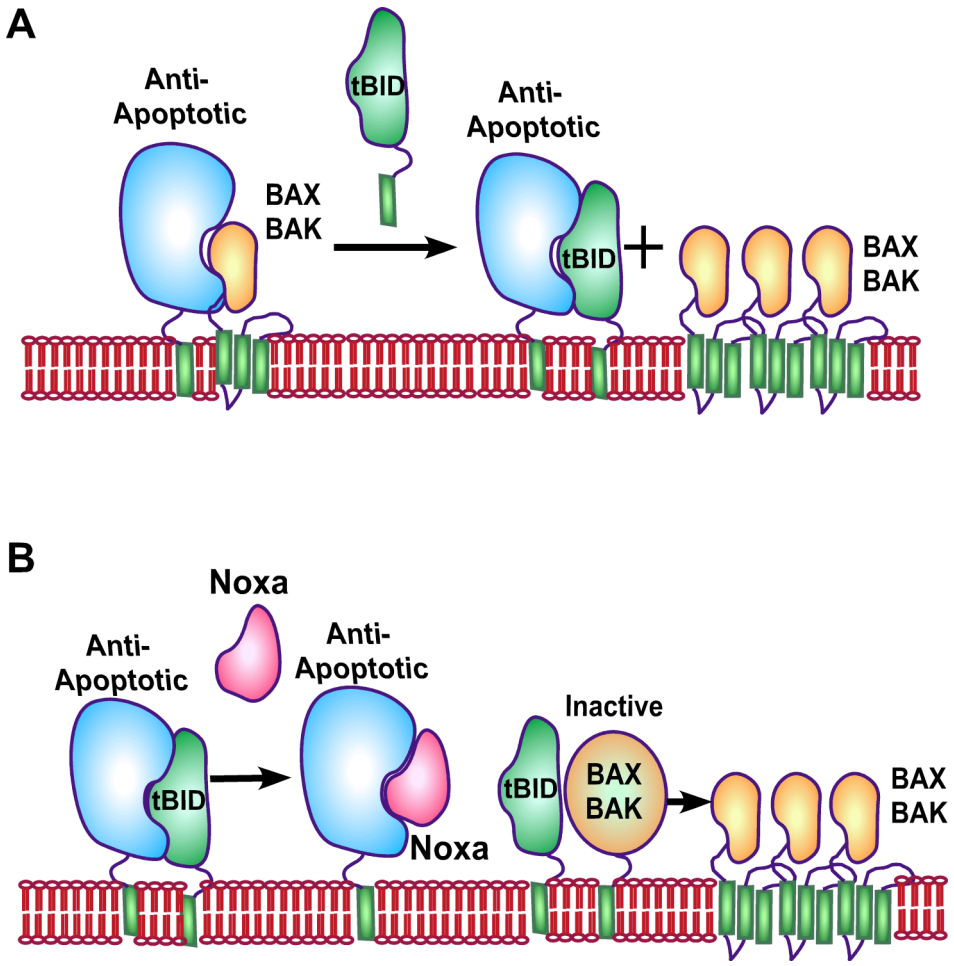

Figure 1.7: Models of BAK/BAX activation. (A) Competitive-activating model (CAM), which suggests the action of BH3-only proteins is to release BAK/BAX from anti-apoptotic proteins. (B) Direct-activating model (DAM), which implies the direct activation of BAK/BAX by activators such as BID, BIM, PUMA.

anti-apoptotic proteins. This releases the direct activators and allows them to activate BAX/BAK and induce apoptosis (Certo et al., 2006). This model is a breakthrough compared to the conventional concept of "neutralization"; however, it has to be noted that the basis for this model, which is the direct interaction between BAX/BAK and "activators", is still subject to debate. As discussed in Section 1.8.1, there has been very little *in vitro* evidence for these interactions except when a stapled BID/BIM BH3 peptide was used. This raises questions about whether other components would participate during activation and what are the determinants for these interactions.

There are a few basic assumptions in these two models. (1) The CAM assumes that the initiation of binding between BAX/BAK and anti-apoptotic proteins triggered by other signals or stimuli is upstream of BH3-only protein-induced BAX/BAK activation; while in DAM, BAX/BAK are free until the activation. (2) The CAM keeps the classical definition of BH3-only proteins, whereas the DAM involves a new classification that divides BH3-only proteins into two subsets "activators" and "sensitizers": the activators can bind both anti-apoptotic proteins and BAX/BAK, and the sensitizers can only bind anti-apoptotic protein. (3) In CAM, there is only one type of competition, that is for anti-apoptotic proteins between BAX/BAK and BH3-only proteins; however, the DAM, though not called "competitive", proposes two different types of competitions. One is the competition for "activators" between anti-apoptotic proteins and BAX/BAK, and the other is between "activators" and "sensitizers" who are competing for anti-apoptotic proteins.

In some cases, one model fits the data better, while in other cases, the other model is more suitable. This has lead to a split in the field between scholars holding different opinions (Certo et al., 2006; Chipuk and Green, 2008; Hacker and Weber, 2007; Willis et al., 2007). We are still uncertain which model could be more correct or whether both situations would occur in different conditions (including cell types, cell stages, stimuli, signaling, and so on). Nevertheless,

what is clear is that both models agree on the special roles of BH3-only proteins in initiating apoptosis and the effective roles of BAX/BAK in executing apoptosis, both of which embodied the development of the classical "Rheostat" model.

1.9 BCL-2 members as drug-targets for cancer therapy

As mentioned in Section 1.5, BCL-2 family proteins are commonly associated with cancer but they are distinct from other oncogene proteins that promote proliferation rather than cell death (Vaux et al., 1988). As anti-apoptotic proteins promote the survival of cancer cells, they have been considered as therapeutic targets, and their inhibitors are expected to induce apoptosis in cancer cells (Lauria et al., 1997; Reed, 1999). The two regulatory models of BCL-2 family, reviewed in Section 1.8, both support the role of BH3-only proteins as inhibitors of anti-apoptotic proteins *in vivo* through their BH3 regions. Therefore, the BH3-peptide mimetics have been pursued as the most promising candidates for small-molecule compounds for cancer therapy.

Based on the binding affinities of BH3 peptides to anti-apoptotic proteins and their complex structures, modified peptides (Sadowsky et al., 2007; Walensky et al., 2004) and peptidomimetics (Kutzki et al., 2002; Saraogi and Hamilton, 2008) have been designed and tested for their ability to induce apotosis. More recently small-molecule inhibitors, such as gossypol, ABT-737, ABT-263, HA14-1, GX15-070 (obatoclax) and so on, have been developed that interact with anti-apoptotic proteins directly (Lessene et al., 2008). The most famous two GX15-070 and ABT-737 will be briefly reviewed.

GX15-070 is the first specifically designed BCL-2 small-molecule inhibitor, and it binds to BCL-2, BCL-X_L, BCL-w and MCL-1 with low micromolar affinities (Zhai et al., 2006). In cell studies, it was observed that GX15-070 could disrupt the BAK:MCL-1 complex by antagonizing MCL-1 (Nguyen et al., 2007),

suggesting its capacity to overcome MCL-1-mediated resistance to apoptosis. It is currently in phase I/II trials either as a single agent or combined with other agents. Recent reports showed that it has *in vitro* activity in a range of tumor types and *in vivo* activity in hematological malignancies (Konopleva et al., 2008; Li et al., 2008; Perez-Galan et al., 2007).

ABT-737 is a product of a structure-activity relationship (SAR) fragment screen (Shuker et al., 1996). It binds BCL-2, BCL-X_L and BCL-w with nanomolar affinities, but fails to interact with MCL-1, A1 and BCL-B (Oltersdorf et al., 2005). It was reported to be effective in repressing the growth of tumors in which BCL-2 was over-expressed, but in tumors over-expressing MCL-1, its efficiency was largely reduced (van Delft et al., 2006) and could be increased when MCL-1 was down regulated (Chen et al., 2007). ABT-737 is highly active in several cell-line models, but has not moved into clinical trials.

Other small-molecule inhibitors showed varying results in different tumor cell-lines, which might be due to their different binding profiles to anti-apoptotic proteins (Zeitlin et al., 2008). Since each type of tumor has its own over-expression profile of anti-apoptotic proteins, the sensitivity to a specific inhibitor or a combination of a few inhibitors will vary. Aiming for more effective and less toxic cancer therapy, the development for more specific inhibitors is highly expected.

1.10 Rationale, objectives, and scope of this thesis

As reviewed from Section 1.1 to 1.9, studies on the BCL-2 family have deepened and widened in the last two decades. Many facts have been discovered; however, there are still quite a few intriguing questions that remain.

Firstly, what is the origin of specificity in the BCL-2 family? So far, progress has been made in dividing BH3-only proteins into "sensitizers" and "activators". However, our knowledge of this specificity is far from sufficient, and we are still collecting data. The more information we gather under different conditions and by different methods, the closer we are to understanding BCL-2 protein specificity.

Another intensely researched issue is about BAX/BAK oligomerization and permeablization. How this process is initiated is not clear yet. It is not known whether it follows the "competitive" activating model or the "direct" activating model, or a combinion of these two. It would be very useful to know how the BAX/BAK oligomers are structured and how they permeablize MOM.

The real motivation that drives researchers in the BCL-2 field is to uncover the mechanisms by which cancers avoid apoptosis and to find possible treatments. It is not surprising that the field has shown very high enthusiasm for the search for small-molecule inhibitors targeting BCL-2 members. Although a few candidates have already displayed great potential, new drugs are expected to improve future cancer therapy with higher binding affinity and more specific targeting.

In the following chapters, I will describe the work that I have carried out to answer these questions using representative proteins from each BCL-2 sub-group: MCL-1 (anti-apoptotic protein), BAK (multi-region pro-apoptotic protein), and BID (BH3-only protein). The major results cover (a) the selectivity of human MCL-1 for binding BH3 peptides (Chapter 2), (b) the solution NMR structure of MCL-1 in complex with a high affinity ligand (Chapter 2), (c) the structure of

BAK, which provided insights into the mechanism of BAK activation (Chapter 3), and (d) a study of the interactions between MCL-1 and BAK (Chapter 4). The relationships among the chapters in this thesis were illustrated in Figure 1.8.

These studies took advantage of access to a wide variety of BCL-2 family proteins and state-of-the-art instruments and expertise in structural studies using NMR spectroscopy, X-ray crystallography, and isothermal titration calorimetry. It is my hope that these studies will not only help to answer the question about the origin of the specificity of BCL-2 proteins, but also to facilitate the structure-based human MCL-1-targeted drug-designing and drug-screening.

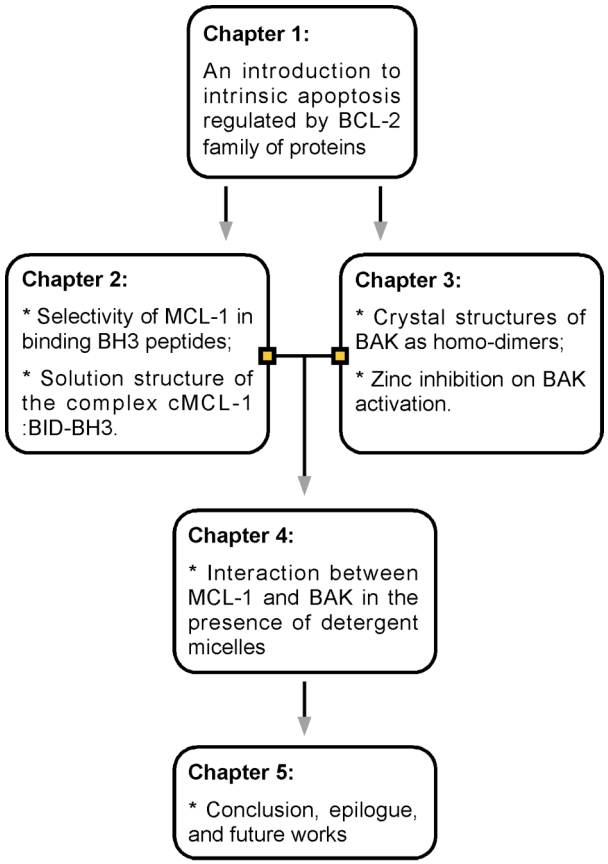

Figure 1.8: Chart illustration of the relationships among the chapters in this thesis. In chapter 2 and chapter 3, MCL-1 and BAK were structurally studied respectively, while in chapter 4 their interaction in between was examined.

Chapter 2

Apoptotic Regulation by MCL-1 Through Hetero-Dimerization

Qian Liu, Tudor Moldoveanu, Tara Sprules, Edna Matta-Camacho, Nura Mansur-Azzam and Kalle Gehring. (2010*) J. Biol. Chem.* 285, 19615-19624.

MCL-1 is a unique anti-apoptotic member in BCL-2 family, and its deregulation is tightly related to different diseases, especially cancer. To investigate its regulatory mechanism, its interactions with BH3-only proteins were tested and presented in this chapter with affinity studies and a structure of a complex.

2.1 Abstract

MCL-1, an anti-apoptotic BCL-2 family member active in the preservation of mitochondrial integrity during apoptosis, has fundamental roles in development and haematopoiesis and is dysregulated in human cancers. It bears a unique, intrinsically unstructured, N-terminal sequence, which leads to its instability in cells and hinders protein production and structural characterization. Here, we present collective data from NMR spectroscopy and titration calorimetry to reveal the selectivity of MCL-1 in binding BH3 ligands of interest for mammalian biology. The N-terminal sequence weakens the BH3 interactions but doesn't affect selectivity. Its removal by calpain-mediated limited proteolysis results in a stable BCL-2-like core domain of MCL-1 (cMCL-1). This core is necessary and sufficient for BH3 ligand binding. Significantly, we also characterized the in vitro protein-protein interaction between cMCL-1 and activated BID by size exclusion chromatography and NMR titrations. This interaction occurs in a very slow manner in solution but is otherwise similar to the interaction between cMCL-1 and BID-BH3 peptide. We also present the solution structure of complex cMCL-1:hBID-BH3, which completes the family portrait of MCL-1 complexes and may facilitate drug discovery against human tumors.

2.2 Preface

MCL-1 belongs to the anti-apoptotic family but is unique due to its short half-life, the presence of an extra N-terminal sequence, and its particular selectivity in binding BH3 peptides. Its concentration in vivo is tightly regulated at multiple levels, and its N-terminal sequence presents many sites for post-translational modifications, including poly-ubiquitination (Warr et al., 2005; Zhong et al., 2005) at K136, limited proteolysis (Han et al., 2005; Weng et al., 2005) at D117, D127, D157, and phosphorylation (Ding et al., 2008; Kobayashi et al., 2007) of T64, T92, T163, T159. These modifications are involved in regulating its activity in binding pro-apoptotic proteins, or in regulating its concentration by either promoting or blocking its degradation. A deregulated, high level of MCL-1 has been correlated with various haematopoietic and lymphoid cancers (Alvi et al., 2005; Cavarretta et al., 2007; Derenne et al., 2002). It plays a major pro-survival role and is therefore an ideal therapeutic target (Sieghart et al., 2006). One way to develop specific human MCL-1 targeting drugs is to explore its interactions with other partners, specifically BH3-only proteins (Fesik, 2005). In that aim, we optimized the expression and purification of various human MCL-1 constructs, and characterized their binding affinities to a panel of human BH3 peptides using a combination of structural and thermodynamic approaches.

BID, a BH3-only protein, performs its pro-apoptotic activity after it is proteolytically activated to a truncated form that is known as tBID (Li et al., 1998; Luo et al., 1998). It was reported that tBID could initiate BAX/BAK-dependent mitochondrial apoptosis (Wei et al., 2000), and this process could be inhibited by MCL-1 through its direct interaction with tBID (Clohessy et al., 2006). Here, we addressed the in vitro hetero-dimerization between a calpain-digested construct of each protein (cMCL-1 and cBID) by size exclusion chromatography and NMR titrations. In addition, we present the structure of cMCL-1:hBID-BH3 complex solved by NMR spectroscopy. The work reveals the structural basis of peptide recognition and insights for the rational design of drugs to specifically target MCL-1.

2.3 Results

2.3.1 The optimization of human MCL-1 constructs

Previous structural studies have been carried out on MCL-1 from Mus musculus (mouse) with N- and C-terminal deletions (ΔN151 and ΔC23) and on a mouse/human chimeric variant (Czabotar et al., 2007; Day et al., 2005; Day et al., 2008). However, the comparable construct (ΔN170 and ΔC23 from Homo sapiens (human) MCL-1 failed to express as a soluble recombinant protein (Czabotar et al., 2007). The sequence alignment (Figure 2.1) showed the change of E182 in the mouse to the corresponding R202 in the human MCL-1, which possibly results in a change in the electrostatic charge and could be responsible for the differences in expression.

To obtain better expression, we screened different constructs of human MCL-1 as shown in Figure 2.2A. A soluble fragment containing the complete N-terminal sequence, which we term ΔC23, showed degradation during purification despite the presence of protease inhibitors (Figure 2.2B). Two N-terminal deletions, ΔN119-ΔC23 and ΔN151-ΔC7, could be well purified; however, they didn't yield interpretable NMR spectra or diffracting crystals. We then turned to limited proteolysis of MCL-1 ΔN119-ΔC23 using trypsin, chymotrypsin, and calpain. These generated smaller protease resistant constructs with sizes of 17kDa, 17kDa and 20kDa, respectively (Figure 2.2C). We used N-terminal sequencing to determine the sites of cleavage. The first two α-helices and the loop between α2 and α3 are before sites of cleavage by both trypsin (after residue 199) and chymotrypsin (after residue 201) (Figure 2.1). In contrast, calpain cuts MCL-1 before the first α-helix (after residue 162) and retains the intact eight helical bundle (Figure 2.1 and 2.2A). This fragment, which we call cMCL-1 (ΔN162-ΔC24), produced high-resolution spectra, and could inhibit cBAK-induced cytochrome (cyt) c release from purified mitochondria from KB tumor cells (Figure 2.2D (Moldoveanu et al., 2006)). However, the fragment failed to express

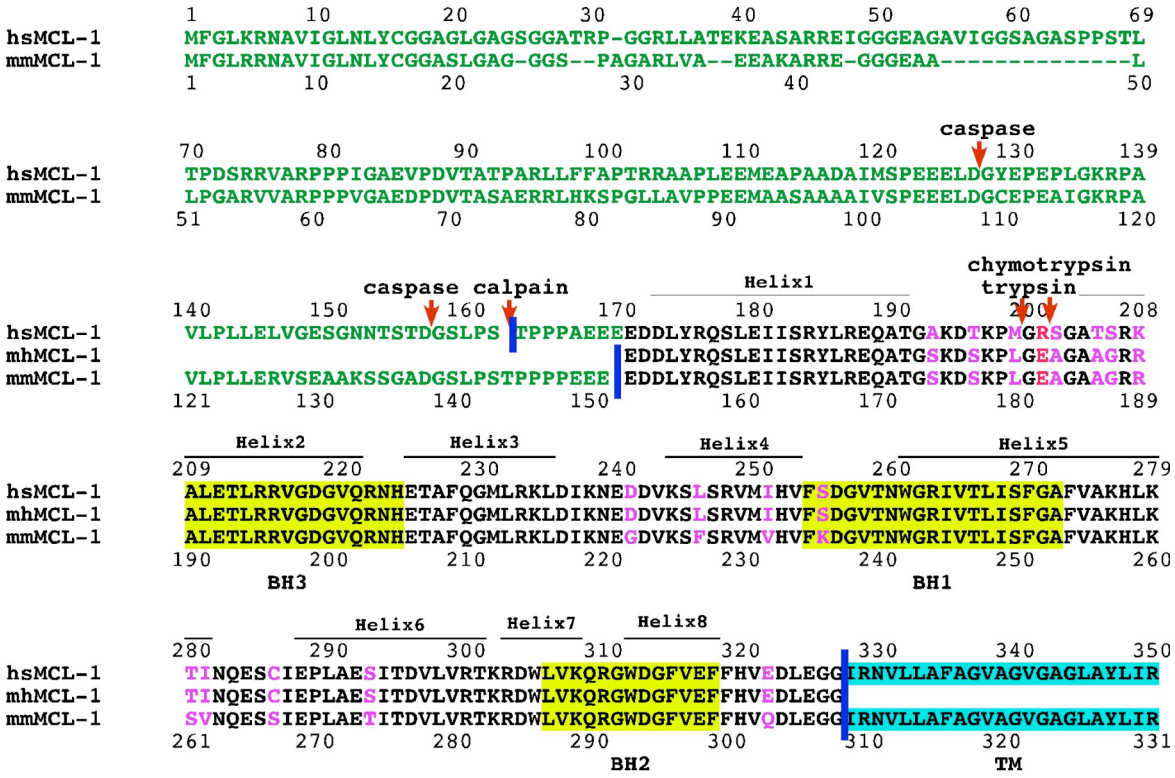

Figure 2.1: The sequence alignment of mouse and human MCL-1. Residue numbers, secondary structures, and sites of limited proteolysis (including trypsin, chymotrypsin, calpain, caspases (Weng et al., 2005)) in human (hsMCL-1; NCBI:AAF64255) and mouse (mmMCL-1; NCBI:AAC31790) and a chimeric protein (mhMCL-1) are labeled. The BH regions and TM region are highlighted by yellow and cyan, respectively. The region between the blue bars represent the constructs used in structural studies.

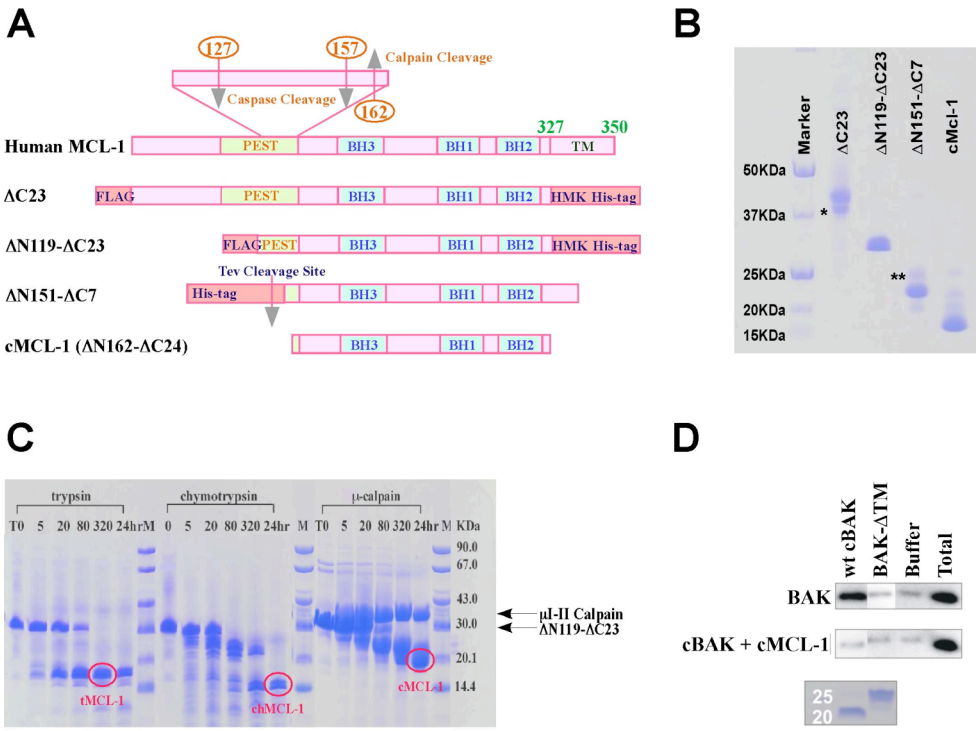

Figure 2.2: Maps and purification of four different human MCL-1 constructs. (A) Representation of the four studied human MCL-1 constructs showing the domain organization. Residues are numbered according to full-length MCL-1 (NCBI:AAF64255) and indicate the site of caspase cleavage (Weng et al., 2005) and fragment boundaries. (B) Coomassie-stained protein gel showing the proteins after purification. A single asterisk (*) indicates a degradation product from the FL construct, and a double asterisk (**) indicates an impurity that copurified with MCL-1 ΔN151-ΔC7. (C) Limited proteolysis of human MCL-1 ΔN119-ΔC23 by trypsin, chymotrypsin and the protease core of μ-calpain (μI-II). Digestion reactions were stopped after 0, 5, 20, 80, 320 minutes and 24 hours. The black arrows indicate the positions of μI-II and MCL-1 ΔN119-ΔC23, and the red ovals indicate proteolysis resistant fragments: tMCL-1, chMCL-1 and cMCL-1. (D) cMCL-1 inhibits the activity of cBAK in releasing cyt *c* from mitochondria purified from KB cells. Cyt c release was detected by SDS-PAGE and immunoblotting. The upper panel shows the release mediated by cBAK. The middle panel shows the inhibition of release by addition of 0.05 μM cMCL-1. The lower panels shows a Coomassie-stained SDS-PAGE of purified cBAK.

as a fusion protein bearing histidine or glutathione S-transferase (GST) tags for affinity purification when subcloned in bacterial expression vectors (data not shown), and therefore subsequent studies were carried out on samples obtained by calpain digestion of purified MCL-1 ΔN119-ΔC23 or ΔN151-ΔC7.

2.3.2 The selectivity of MCL-1 in hetero-dimerizing with BH3 peptides

The anti-apoptotic activity of MCL-1 is largely represented by its binding ability to pro-apoptotic proteins. To illustrate this, we used isothermal titration calorimetry (ITC) to measure the binding affinities between the BH3 peptide and MCL-1. We designed and chemically synthesized a series of BH3 peptides spanning the BH3 regions of the human BH3-only pro-apoptotic proteins, BAD, BIK, PUMA, BID, Noxa, BIM, and MULE (Figure 2.3A), to examine their interactions with recombinant truncated MCL-1 constructs. Figure 2.3B shows a typical titration of MCL-1 ΔN119-ΔC23 with a 20-residue BID peptide, in which negative deflections from the base line indicate exothermic binding. Integration of the peaks and fitting of the resulting thermogram with a 1:1 binding model, yield the Kd of 0.83 μM. Binding affinities for additional MCL-1:BH3 peptide complexes were calculated similarly (Figure 2.3C) and they vary from undetectable to nanomolar, demonstrating a high degree of selectivity of MCL-1 for binding BH3 peptides. Accordingly, MCL-1 did not bind BAD, and bound BIK and PUMA with micromolar affinities, and the BH3 regions from BID, Noxa, BIM and MULE with nanomolar affinities. The wide range of affinities was further confirmed by NMR titrations of ^{15}N-labeled cMCL-1 with unlabeled BH3 peptides (Figure 2.4A and data not shown).

2.3.3 The effects of the N-terminal sequence of MCL-1 on BH3-binding

Comparison of the data for the different constructs shows that, with the intact N-terminus, MCL-1 ΔC23 binds BH3 peptides with significantly lower affinities compared with truncated MCL-1 constructs (Figure 2.3C). Removal of the N-

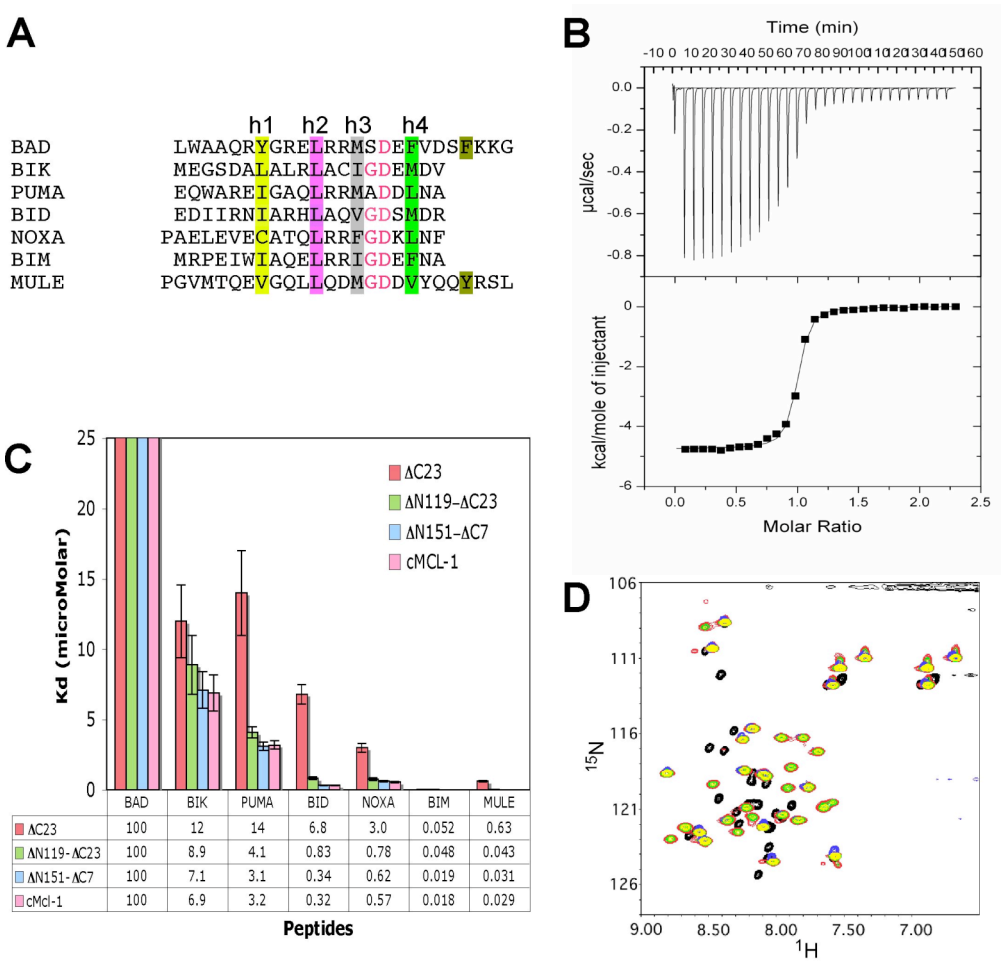

Figure 2.3: Binding affinities of BH3 peptides to human MCL-1. (A) Sequence alignment of BH3 peptides derived from human BH3-only pro-apoptotic proteins: BAD, BIK, PUMA, BID, Noxa, BIM, and MULE. The conserved hydrophobic residues are highlighted. (B) Representative ITC profile for MCL-1 ΔN119-ΔC23 with BID peptide (synthesized BID-BH3). The peaks shown in the thermogram were integrated and then fit to a 1:1 binding model, with a K_d of about 0.83 µM. (C) Graph and table of the ITC-derived dissociation constants (K_d in µM) for BH3 peptides and recombinant MCL-1 constructs lacking the C-terminus with or without engineered deletions of the N-terminal region. Binding between MCL-1 and BAD-BH3 was undetectable. (D) ^{15}N-^{1}H HSQC spectra of human BID-BH3 peptide without MCL-1 (black), with MCL-1 ΔC23 (blue), with ΔN119-ΔC23 (red), with ΔN151-ΔC7 (green) and with cMCL-1 (yellow).

terminus augments the affinities between MCL-1 and BH3 peptides. On the other hand, the BH3-binding selectivity of MCL-1 was not affected by the N-terminus. BAD-BH3 does not bind to any of the four constructs. The N-terminal sequence, which includes a PEST sequence that is likely unfolded, only weakens the binding affinities, but doesn't play a role in regulating the binding selectivity. To further test the effect of the N-terminal sequence on the ligand-binding properties of MCL-1, we carried out titrations of ^{15}N-labeled BID-BH3 peptide with unlabeled recombinant MCL-1 (Figure 2.3D). The signals in the free peptide spectrum (black) fall in the center of the spectrum, which is indicative of an unstructured conformation. When bound, most of the peaks (colored) dispersed reflecting conformational changes and folding of the peptide. Most importantly, the spectra of the peptide bound to the four MCL-1 constructs were very similar, indicating that the peptide adopted identical conformations and that the shortest and most stable construct, cMCL-1, deserves a name of core MCL-1 for providing the structural features necessary and sufficient for BH3 binding.

2.3.4 BH3 binding site on cMCL-1

We next explored the interactions of MCL-1 with the high affinity peptides from BID, BIM, Noxa and MULE by performing NMR titrations. Chemical shift perturbations in cMCL-1 upon peptide binding were very similar (data not shown); the BID-BH3 titration spectra were selected as a representative to analyze in more detail. The cross-peaks in ^{15}N-^{1}H HSQC spectra of cMCL-1 in both the free and bound forms were assigned, and the calculated chemical shift changes were mapped onto the free human MCL-1 structure model derived from the mouse protein (PDB code 1WSX) by Modeller 9v2 (Sali and Blundell, 1993) (Figure 2.4B and 2.4C). Residues with the biggest chemical shift changes are mainly located in the end of helix 2 (α2), the end of α4 and the beginning of α5, and residues with smaller changes map in the middle of α5, the end of α6 and α8. These residues define a peptide-binding pocket that is consistent with published structures of mouse (mm), human (hs) and chimeric mouse/human (mh) MCL-1.

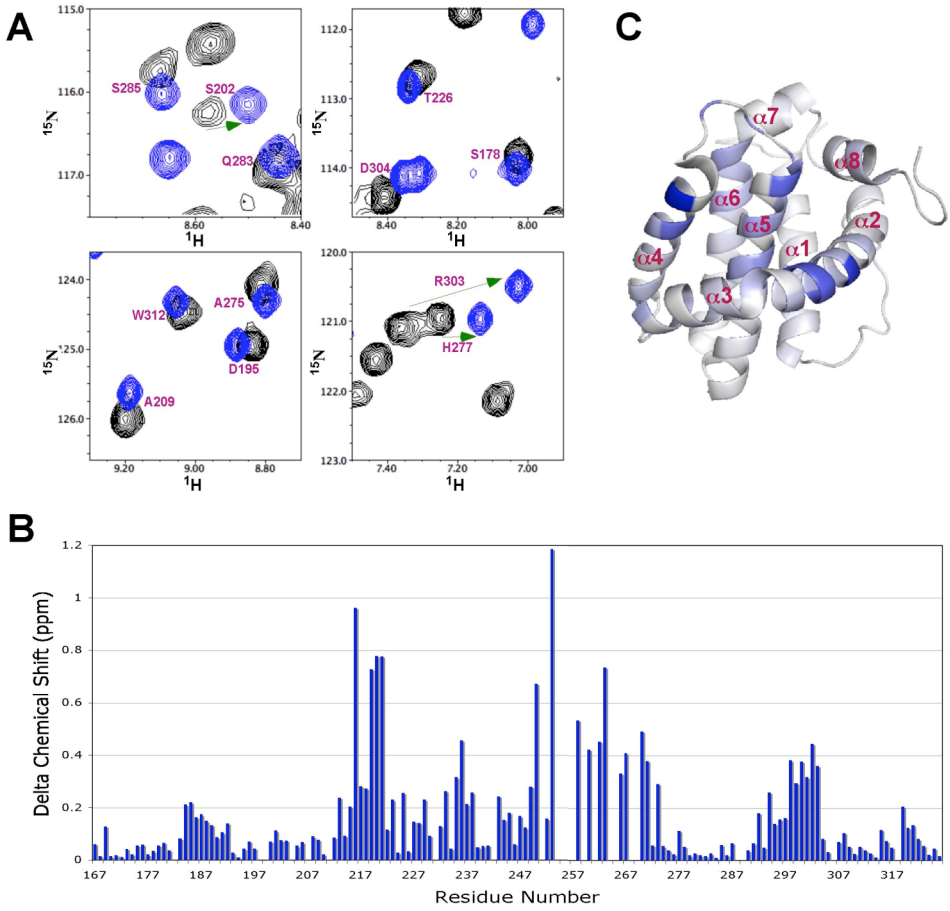

Figure 2.4 Mapping the BH3 peptide binding groove in MCL-1by NMR. (A) Slices of ^{15}N-^{1}H HSQC spectra of cMCL-1 without peptide (black), and with BID-BH3 (blue). The arrows show the direction of chemical shift changes upon BID-BH3 binding.(B) Plot of chemical shift changes (calculated as $((\Delta^{1}\text{H ppm})^2 + (0.2 \times \Delta^{15}\text{N ppm})^2)^{0.5}$) of cMCL-1 amide signals upon titration with BID-BH3 peptide as a function of residue number.(C) Cα trace on free human cMCL-1 model (calculated by Modeller 9v2 (Sali and Blundell, 1993) based on the free mmMCL-1 structure 1WSX) colored according to the chemical shift changes upon BID-BH3 binding. The more intense the blue shading is, the greater the chemical shift difference that was observed upon BID-BH3 binding.

These are mmMCL-1:mmPUMA, PDB code 2ROC; mmMCL-1:mmNoxa-A, PDB code 2ROD; mmMCL-1:mmNoxa-B, PDB code 2JM6; mhMCL-1:mmNoxa-B, PDB code 2NLA; mhMCL-1:hsBIM PDB code 2NL9)(Czabotar et al., 2007; Day et al., 2008).

2.3.5 Calpain cut BID (cBID) initiates mitochondrial cytochrome c release

BID initiates mitochondrial apoptosis via a proteolytically activated, truncated form, termed tBID. Due to the difficulty in directly expressing tBID, we expressed the full-length protein as a glutathione S-transferase (GST) fusion, and again performed limited proteolysis. Calpain cleaves BID in the unfolded loop region following helix $\alpha 2$ (Mandic et al., 2002), generating a truncated form cBID (Figure 2.5A, 2.5B). As observed in caspase cleavage (Chou et al., 1999), the N-terminal and C-terminal fragments following calpain treatment remain associated and copurify resulting in two bands on a Coomassie-stained gel (Figure 2.5C). The pro-apoptotic activity of cBID was demonstrated by adding it to mitochondria purified from KB tumor cells, where it initiated the release of cyt c (Figure 2.5D).

2.3.6 The interaction between cBID and cMCL-1

MCL-1 and tBID interact both in vivo and in vitro (Clohessy et al., 2006). Here, we examined whether cMCL-1 interacts with cBID using NMR spectroscopy. Following addition of an excess of unlabeled cBID to ^{15}N-labeled cMCL-1, ^{15}N-^{1}H HSQC spectra were recorded every four hours. Although some specific chemical shift perturbations started to appear four hours after the titration, the complete transition was only observed at a time-point of 16 hours (Figure 2.6B). The HSQC spectra show two sets of signals that arise from the free and bound forms of cMCL-1 (Figure 2.6C). The surprisingly slow process of cBID binding is likely due to the slow dissociation of the two halves of the cleaved cBID molecule to expose the BID-BH3 region. Comparison of titrations of cMCL-1 with cBID

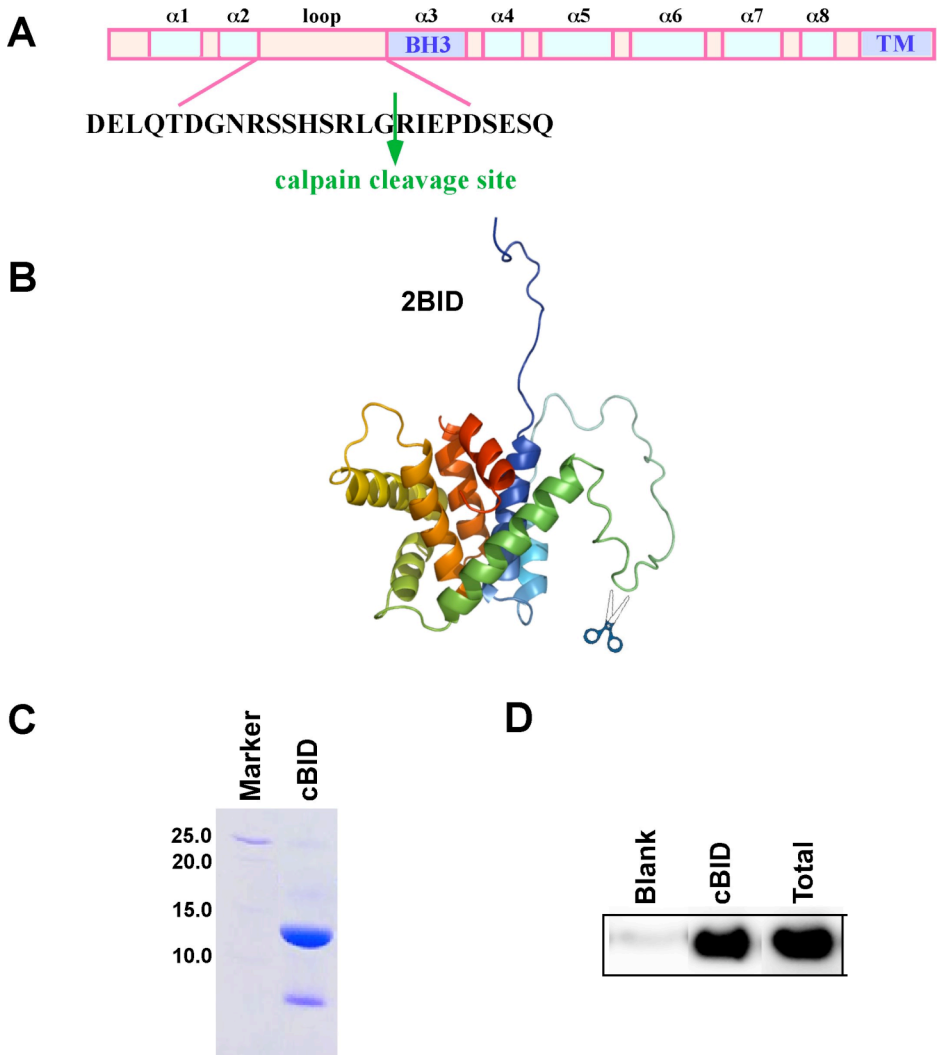

Figure 2.5 Preparation of cBID. (A) Primary and (B) 3D structure of human BID (PDB code 2BID). The green arrow and the scissors indicate the calpain cleavage site. (C) Coomassie-stained protein gel for cBID after purification. (D) Western blot of cyt c released by cBID from mitochondria purified from KB cells.

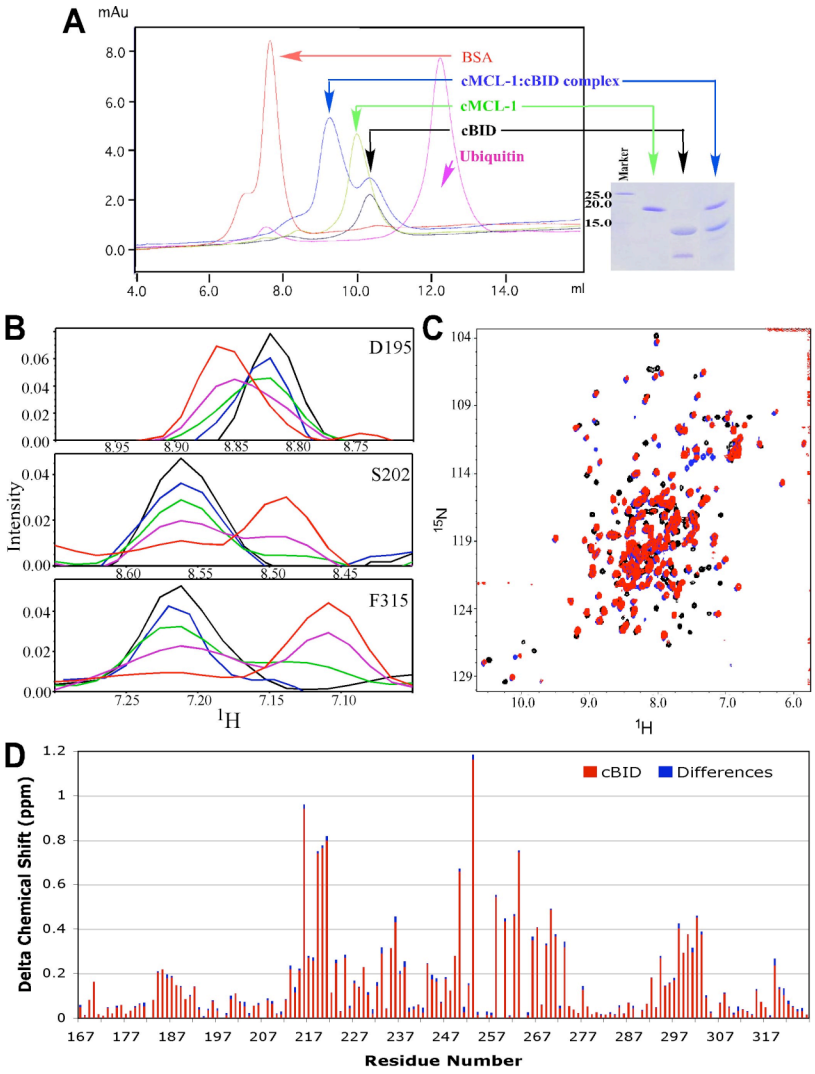

Figure 2.6: Interaction between cMCL-1 and cBID. (A) Size exclusion chromatography profile of BSA (red), ubiquitin (pink), cBID (black), cMCL-1 (green) and overnight mixture of cMCL-1 and cBID (blue). (B) 1D views from the ^{1}H dimension of ^{15}N-^{1}H HSQC spectra, representing specific residues (D195, S202 and F315). The black, blue, green, purple and red spectra were recorded respectively 0 h, 4 h, 8 h, 12 h and 16 h after the addition of unlabeled cBID to ^{15}N-labeled cMCL-1. (C) ^{15}N-^{1}H HSQC spectra of cMCL-1 without peptide (black), with BID-BH3 (blue), and with cBID protein (red). (D) Plots of chemical shift changes (calculated as $((\Delta^{1}H \text{ ppm})^{2} + (0.2 \times \Delta^{15}N \text{ ppm})^{2})^{0.5}$) of cMCL-1 amide signals upon titrations with cBID (red) and the differences (blue) between the spectra with BID-BH3 and cBID as a function of residue number.

and BID-BH3 showed similar patterns of chemical shift changes, which confirms that cBID interacts with the BH3 binding pocket of cMCL-1 (Figure 2.6C and 2.6D). To exclude the possibility of protein degradation, we performed analytical size exclusion chromatography using BSA and ubiquitin as protein standards (Figure 2.6A). Free cMCL-1 (green) and cBID (black) eluted at 9.9 ml and 10.3 ml respectively, while the overnight mixture of cMCL-1 and cBID in 1:2 ratio (blue) gave two elution peaks: one at 10.3 ml, confirming the existence of excess, free cBID, and a second, higher molecular weight peak at 9.2 ml representing the cMCL-1:cBID complex.

2.3.7 Solution structure of cMCL-1:BID-BH3 complex

Using a variety of NMR data, over 95% of backbone and side chain resonances were assigned for the ^{1}H, ^{15}N and ^{13}C atoms in both cMCL-1 and BID-BH3 in the complex. The secondary structure chemical shift indices (CSIs) based on Cα and Hα, and the analysis of the sequential and medium-range NOE connectivities were used to determine the secondary structure. In the complex, cMCL-1 is composed of 8 helices (α1: 173-192; α2: 204-225; α3: 226-236; α4: 239-255; α5: 260-281; α6: 286-302; α7: 303-309; α8: 312-319). The BID-BH3 peptide forms one α-helix (α1': residues 79-99). The limits of the folded regions of the structure were verified by the measurement of $^{15}N\{^{1}H\}$ heteronuclear NOEs values greater than 0.6 (Figure 2.8A, bottom). By comparing the regular NOESY spectra with ^{15}N, ^{13}C-filtered, ^{13}C-edited NOESY and ^{15}N, ^{13}C-filtered, ^{15}N-edited NOESY respectively, 197 inter-molecular NOEs were determined (Figure 2.7A) between protons from the two different molecules (Figure 2.7B). In the final structure calculation, 3563 constraints were invoked using standard molecular dynamics protocols (Table 1). The final ensemble (Figure 2.7C) of structures with the lowest energies and the fewest violations had a mean RMSD from the average of 0.38 Å for backbone atoms, excluding the residues at the termini (residues 167-172 and 320-326 in cMCL-1; residues 76-78 and 100-106 in BID-BH3) and the ones in the disordered loop between helices α1 and α2 (cMCL-1 residues 193-

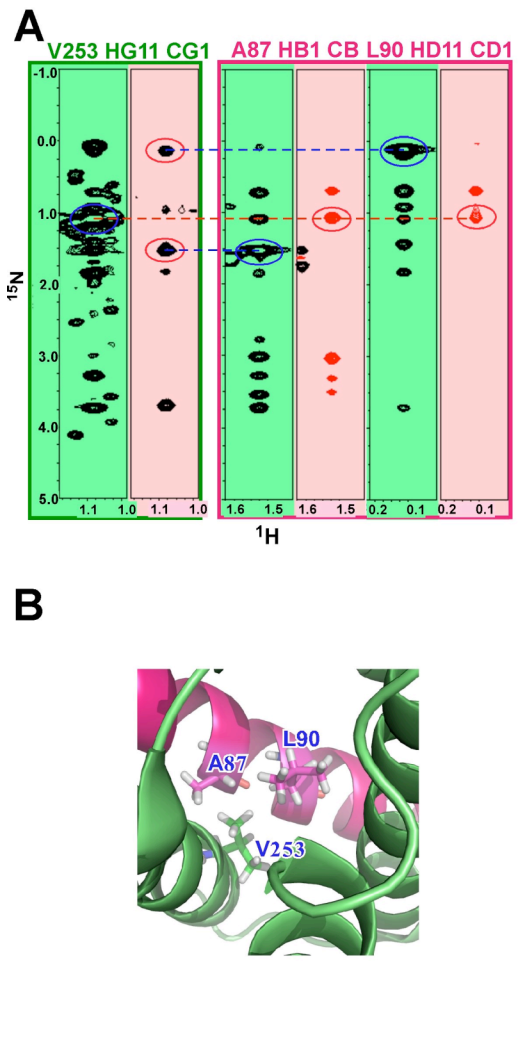

Figure 2.7: Solution structure of the cMCL-1:BID-BH3 complex. (A) Determination of inter-molecular NOEs in the complex. Slices of ^{1}H-^{1}H planes are compared between a 3D ^{13}C-edited NOESY (green background) and a ^{15}N, ^{13}C-filtered, ^{13}C-edited NOESY (red background) spectrum. The first pair of strips (green frame) show NOEs for Val253 HG11 from cMCL-1. The following pairs (red frames) show NOEs for Ala87 HB1 and Leu90 HD11 from the BID-BH3 peptide. The inter-molecular NOEs are indicated by blue and red ovals and correlated by dashed lines. (B) Detail of the structure showing residues responsible for the NOEs identified in panel A. cMCL-1 is in green and BID-BH3 is in magenta. (C) Ribbon diagram of the 10-structure ensemble of the complex cMCL-1:BID-BH3, with cMcl-1 in blue and BID-BH3 peptide in magenta. (D) Schematic representation of the complex. The BH1, BH2 and BH3 regions in cMcl-1 are colored green, beige and blue respectively. The peptide is colored magenta. N, C, N', C' are used to label the termini of the molecules.

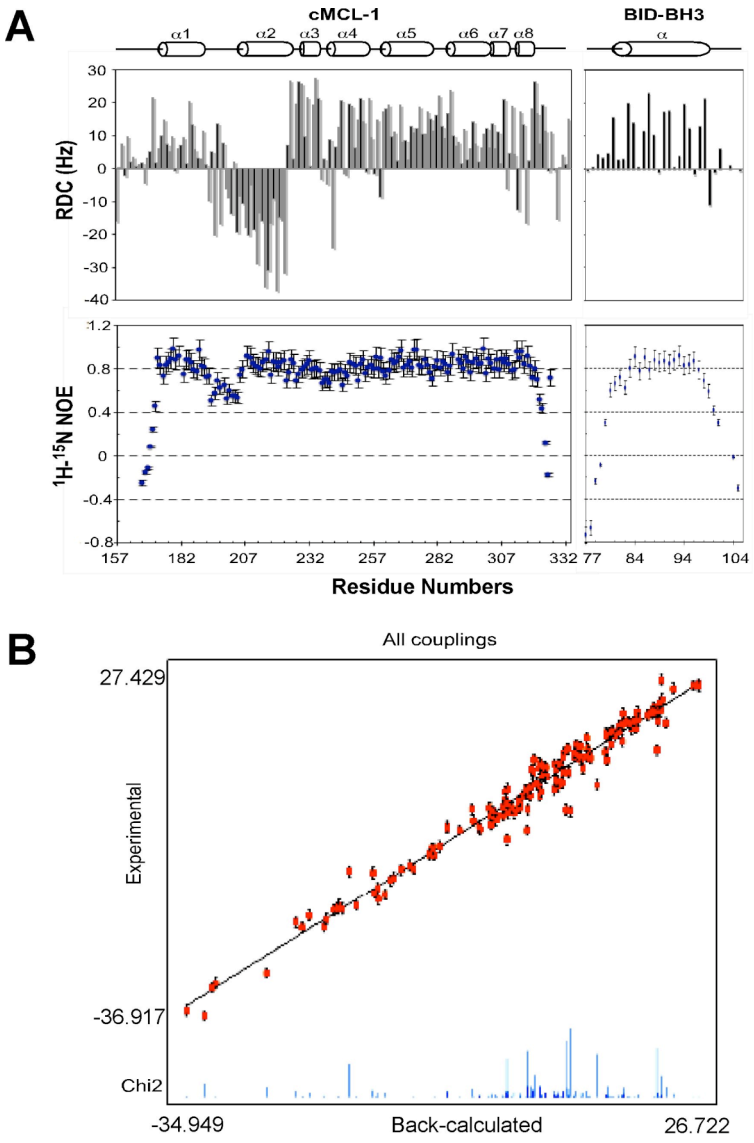

Figure 2.8: Plots of ^{15}N-^{1}H RDCs, ^{15}N{^{1}H} Heteronuclear NOE values and back correlation of the RDCs for the cMCL-1:BID-BH3 complex. (A) Backbone amide ^{15}N-^{1}H RDCs (top) and ^{15}N{^{1}H} heteronuclear NOE values (bottom) plotted against residue number for the cMCL-1:BID-BH3 complex. The cylinders above the graph represent α-helices. (B) Correlation of the experimental couplings (vertical axis) plotted against RDCs back-calculated from the structure (horizontal axis). The correlation factor R is 0.974. Red squares are data points; blue bars on the bottom represent the magnitude of deviations between the measured and back-calculated values.

203). A schematic representation of the structure closest to the average structure is presented in Figure 2.7D.

As part of structure determination, a set of 182 ^{15}N-^{1}H residual dipolar couplings (RDCs) were measured on two complexes with ^{15}N-labeling of either cMCL-1 or the BID-BH3 peptide in Pf1 phage (Figure 2.8A top). For proline residues and residues with significant overlap (P198, P289, I182, and R207 in cMCL-1; P102 and P103 in BID-BH3), the RDC values were not obtained. Normally, RDCs cannot be used to refine mobile regions (Meiler et al., 2001) including the N, C-terminal regions and the ULR in this case. However, the RDCs for the residues in the partially disordered loop fit the structure well, indicating that the loop following helix α1 of cMCL-1 is fixed to some degree. Thus, 157 RDCs including those for that loop were included in the final refinement, which decreased the backbone RMSD from 0.52 Å to 0.38 Å, and dropped the RDC Rdip from 0.55 to 0.127 (Figure 2.8B).

The structure of cMCL-1:BID-BH3 (PDB code 2KBW) shows a very similar topology to other BCL-2 complexes. The central helix α5 is surrounded by other α-helices, and the hydrophobic groove defined by α2-α5 and α8 is occupied by the α-helix of the BID-BH3 peptide. This is consistent with the BH3-binding site as detected by NMR titrations. By aligning our structure with other MCL-1 complexes using the DALI program (Figure 2.9A), the pairwise Cα atomic coordinate RMSDs for the secondary structure elements range from 1.4 Å to 1.6 Å, and the DALI Z factors range from 16.6 to 18.0 (Figure 2.9B). In the cMCL-1 structure, the major difference is that helix α4 is shorter comprising residues 239-255 instead of 239-257. The side chains of the residues in hydrophobic peptide-binding pocket adopt similar conformations across the family of structures but with minor differences due to variation in the sequences of the bound peptides (Figure 2.9C). The hydrophilic interactions between BID-BH3 and cMCL-1 are mainly present at both ends of the peptide (Figure 2.9D). At the peptide N-terminus, Q79 interacts with the side chain of D242 in cMCL-1. At the peptide C-

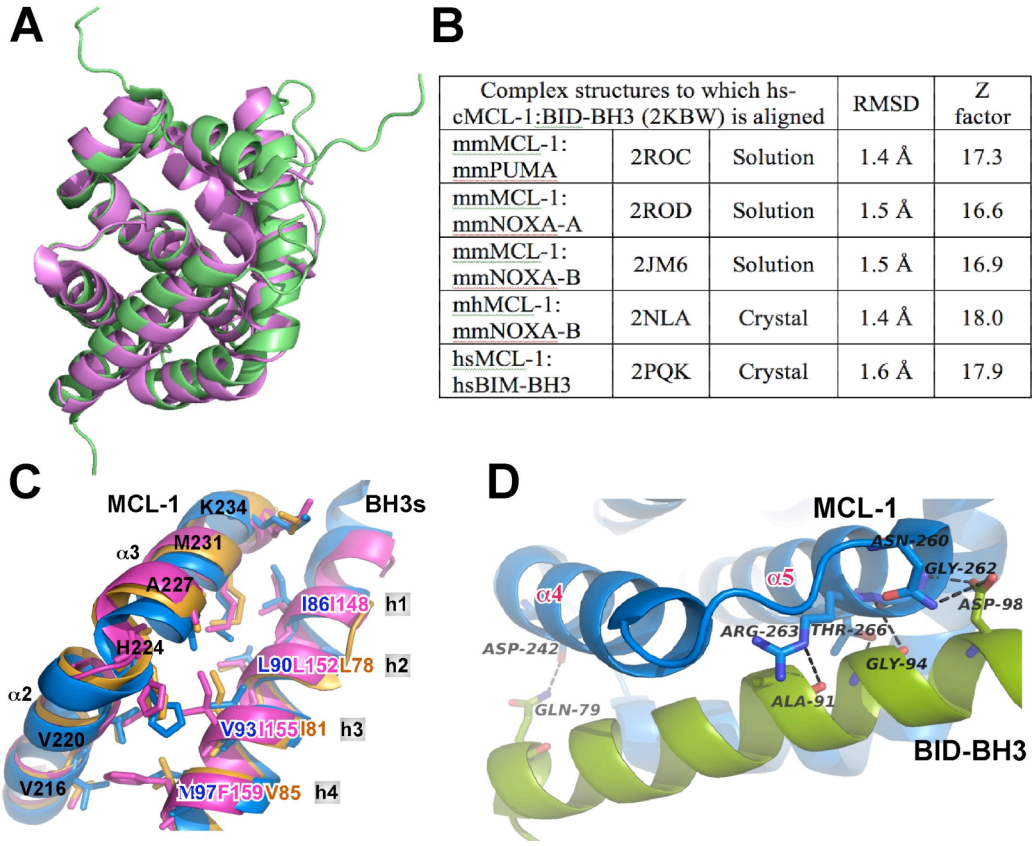

Complex structures to which hs-cMCL-1:BID-BH3 (2KBW) is aligned			RMSD	Z factor
mmMCL-1: mmPUMA	2ROC	Solution	1.4 Å	17.3
mmMCL-1: mmNOXA-A	2ROD	Solution	1.5 Å	16.6
mmMCL-1: mmNOXA-B	2JM6	Solution	1.5 Å	16.9
mhMCL-1: mmNOXA-B	2NLA	Crystal	1.4 Å	18.0
hsMCL-1: hsBIM-BH3	2PQK	Crystal	1.6 Å	17.9

Figure 2.9: Comparison of cMCL-1:BID-BH3 with other BH3 complexes of MCL-1. (A) Superimposition of cMCL-1:BID-BH3 (green, this work - PDB code 2KBW) and MCL-1:BIM-BH3 (purple, PDB code 2PQK). The complex is shown in the same orientation as in Fig 4D. (B) Table listing the RMSDs and Z-factors for the alignment by the program DALI of hs-cMCL-1:BID-BH3 with other MCL-1 complexes. Protein/BH3 peptide names are prefaced by their sequence origin: *mm*, mouse; *hs*, human; *mh*, chimeric mouse/human. (C) Aligned key hydrophobic residues in helices α2/α3 of MCL-1 and the BH3 peptides from the complexes: cMCL-1:BID-BH3 (blue, this work), hsMCL-1:hsBIM-BH3 (magenta, 2PQK) and mhMCL-1:mmNoxa-B (yellow, 2NLA). Selected amino acids side chains are shown and labeled in black for MCL-1 and color-coded for the three different BH3 peptides. (D) Details of the hydrophilic interactions between the BID-BH3 peptide and the peptide-binding groove of cMCL-1.

terminus, the backbone amides of A91 and G94 interact with the side chains of R263 and T266 in cMCL-1. The side chain of one of the last ordered BID-BH3 residues, D98, makes hydrogen bonds with the side chain of N260 and the backbone amide of G262.

2.4 Discussion

MCL-1 plays a notable pro-survival role *in vivo* and its elimination in response to cytotoxic signals is critical in promoting cell death (Brunelle et al., 2007; Craig, 2002; Willis et al., 2005). Accordingly, it has become an important target in the search for new anti-cancer drugs. Although the development of ABT-737 and its derivatives have validated the approach of using BH3 mimetics for treating tumors (Oltersdorf et al., 2005), their low affinities for MCL-1 precludes their use in combating malignancies driven by high MCL-1 levels (Chauhan et al., 2007; Konopleva et al., 2006; Trudel et al., 2007). Multiple structures of MCL-1 in complex with BH3 peptides are crucial for the development of small molecule inhibitors specifically targeting MCL-1 or capable of broadly interacting with all anti-apoptotic BCL-2 proteins.

The first obstacle to structural studies of MCL-1 is the difficulty in producing stable protein due to heterogeneity brought about by degradation during bacterial expression and subsequent purification. The problem of degradation was solved by the deletion of the N-terminal sequence (Czabotar et al., 2007; Day et al., 2005; Day et al., 2008); however, the mouse/human chimera construct failed to produce high-resolution NMR spectra (Czabotar et al., 2007). These are a requirement not only for solving the solution structure, but also for drug screening by NMR. In this study, we report the use of limited proteolysis to produce a calpain cleavage product (cMCL-1) that is the first human construct suitable for NMR studies. In its free form, 95% of the cMCL-1 backbone signals could be assigned and this will enable future screening for compounds that specifically target MCL-1.

We took advantage of the high quality NMR spectra to study ligand binding by cMCL-1. All tested peptides that bound MCL-1 with micromolar to nanomolar affinities perturbed the NMR signals of cMCL-1 similarly (data not shown), which indicates that they induce the same conformational change in cMCL-1 upon binding. Detailed analysis of the chemical shift changes showed that the cMCL-1 residues with largest changes are mainly located in the hydrophobic groove of cMCL-1 formed by the BH1-3 regions (Figure 2.4B and 2.4C). This represents a universal feature of all pro-survival BCL-2 complexes. We determined the selectivity of MCL-1 for BH3 ligands by comparing the binding affinities measured by ITC (Figure 2.3B and 2.3C). The failure of MCL-1 to bind BAD-BH3 and its strong preference for BIM-BH3, Noxa-BH3, and MULE-BH3 are consistent with results reported by other groups, although the values vary somewhat due to differences in the methods and peptides used (Certo et al., 2006; Chen et al., 2005; Day et al., 2008). For example, the shorter PUMA-BH3 (residues 131-150, our work) has a much lower affinity to human MCL-1 than reported for a longer peptide (residues 130-155) binding to mouse MCL-1 (Day et al., 2008).

The higher affinity of longer peptides may be due to their greater helical propensity or the presence of binding elements outside of the consensus BH3 region. In the case of BID-BH3 binding to human MCL-1, we observed almost 10-fold higher affinity for a longer biosynthetically prepared peptide comprising residues 76-106 than for the chemically synthesized peptide comprising residues 80-99 (Figure 2.3C). ITC measurements with the longer BID-BH3 peptide yielded affinities of 85 nM to MCL-1-ΔN119-ΔC23 and 40 nM to MCL-1-ΔN151-ΔC7. These are similar to the values reported for a 34-residue mouse BID peptide binding to mouse MCL-1 (Day et al., 2008).

A detailed examination of the cMCL-1:BID-BH3 structure shows that there is an extra hydrophilic interaction between the side chains of Q79 in the N-terminus of the peptide and D242 in the binding pocket of cMCL-1 (Figure 2.9D). This

interaction may contribute to the higher affinity observed for the longer BID-BH3 peptide. The structure also explains the low affinities of MCL-1 in binding BAD-BH3 and ABT-737, the hotly studied BCL-2 inhibitor. The overlay of our structure and the crystal structure of BCL-X_L:BAD-BH3 (2BZW) reveals that the biggest conformational difference between MCL-1 and BCL-X_L lies in helix α3 (Figure 2.10A). The better formation of helix α3 in MCL-1 leads to its restriction in peptide binding (Czabotar et al., 2007). Figure 2.10B presents that the conformations of the first hydrophobic residues (h1) in BH3 peptides varies largest, and M231 in MCL-1 helix α3 prevents the engagement of Y105 in BAD-BH3 by spatial confliction. Superimposing our structure with the crystal structure of BCL-X_L:ABT-737 complex (Figure 2.10C) clearly shows that the hydrophobic groove in BCL-X_L is narrow and deep, whereas the one in cMCL-1 is wider and shallower. As a result, the pocket formed by F228, M231 and F270, which accommodates the binding of L90 in BID-BH3, results in a spatial restriction that blocks binding of the chloral-biphenyl group in ABT-737 (Figure 2.10D). Similarly, the side-chain of V216 hinders the engagement of the nitrophenyl and the thiophenyl groups in ABT-737 spatially.

The N-terminal sequence of MCL-1 has always been deleted in structural studies due to its lack of structure; however, its regulatory functions have garnered attention recently. With two PEST regions, it not only plays a vital regulating role in the subcellular localization of MCL-1 (Germain and Duronio, 2007), but also provides critical sites for poly-ubiquitination (Warr et al., 2005; Zhong et al., 2005), limited proteolysis (Han et al., 2005; Weng et al., 2005), and phosphorylation (Ding et al., 2008) that modulate the degradation and turnover of MCL-1. It has been reported calpain inhibitors can prevent the degradation of MCL-1, indicating that calpain digestion of MCL-1 could possibly play a physiological role. Here, using four human MCL-1 constructs with different N-terminal deletions, we further explored the effects of this intrinsically unstructured sequence, unique to MCL-1, on BH3-peptide binding. HSQC spectra of the labeled BID-BH3 peptide bound to different unlabeled MCL-1 constructs

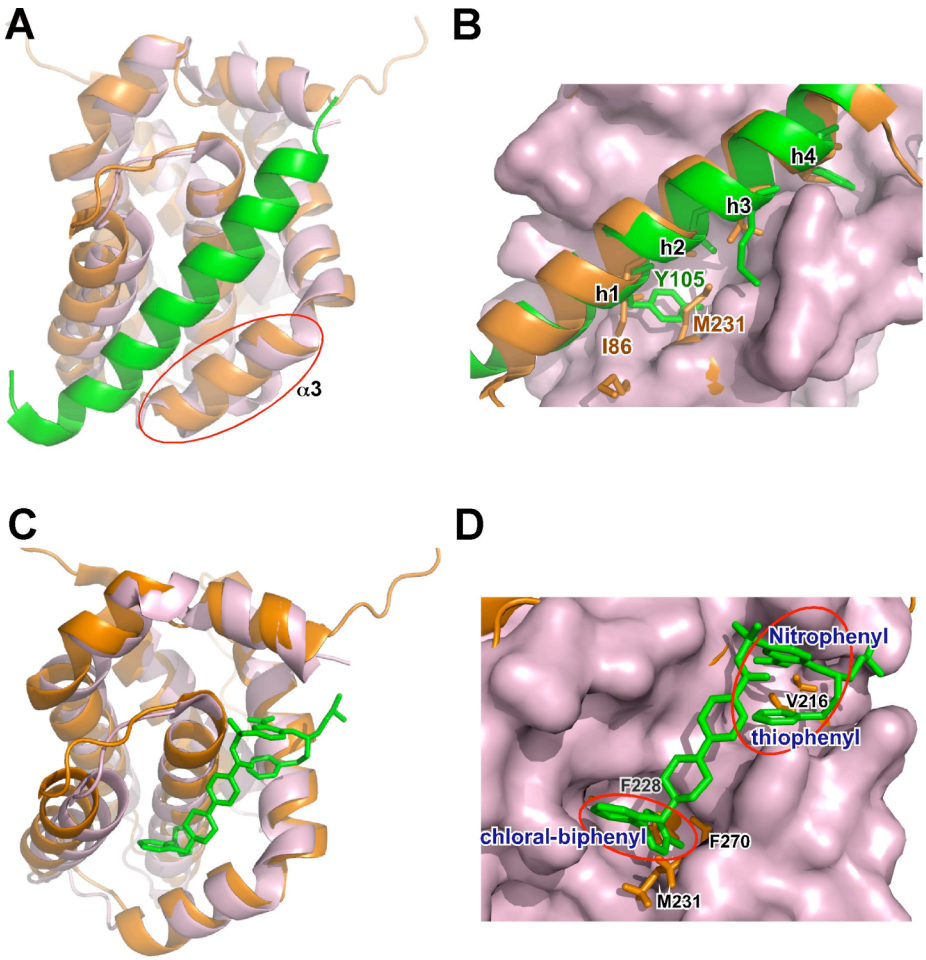

Figure 2.10: The BH3 binding groove of cMCL-1 poorly accommodates BAD-BH3 and ABT-737. (A/B) Overlay of the structures of cMCL-1:BID-BH3 (orange, this work, BID-BH3 is hidden for clarity in A) and BCL-X_L:BAD-BH3 (pink:BCL-X_L, green: BAD-BH3, 2BZW) with the only involvement of the hydrophobic grooves of cMCL-1 and BCL-X_L for alignment. The significant difference in α3 is circled in A, and the hydrophobic residues in peptides (h1-4) are labeled in B. (C/D) Overlay of the structures of cMCL-1:BID-BH3 (orange, this work, BID-BH3 is hidden for clarity) and BCL-X_L:ABT-737 (pink:BCL-X_L, green: ABT-737, 2YXJ) with the only involvement of the hydrophobic grooves of cMCL-1 and BCL-X_L for alignment. MCL-1 residues that appear to hinder sterically ABT-737 binding are labeled in black, and the chloral-biphenyl, nitrophenyl, and the thiophenyl groups of ABT-737 are labeled and circled.

were very similar suggesting that the N-terminal sequence does not influence the structure of the bound peptide (Figure 2.3D). In addition, while the N-terminal sequence does not alter the binding preference of MCL-1; its deletion always led to higher binding affinity. This may be due to non-specific steric crowding from the N-terminus or it may arise from low affinity binding of the N-terminus to the MCL-1 hydrophobic pocket. Whatever the mechanism, proteolytic processing of MCL-1 by caspase, granzyme, and other proteases may be expected to increase not only the stability but also the affinity of MCL-1 binding of the BH3 regions of pro-apoptotic proteins.

BID, the only pro-apoptotic BH3-only protein known to assume a globular fold, has been widely studied in research on the direct activation of BAX and BAK; however, its regulation by anti-apoptotic proteins is always carried out using BID-BH3 peptide, and whether the protein will behave similarly to the peptide has remained an open question. In 2006, Brady and colleagues reported that MCL-1 directly interacts with tBID *in vivo* to inhibit the release of cyt c (Clohessy et al., 2006). In this study using a calpain-activated form, we were able to detect the direct interaction between cBID and cMCL-1 *in vitro*. This interaction is very slow in solution and requires 16 h for completion as detected by NMR. This is most likely due to the kinetic barrier for the dissociation of the N-terminal and C-terminal fragments, which is postulated to increase the accessibility of the BH3 region. In the undissociated complex, the cBID BH3 region is not available for cMCL-1 binding. The interaction of cBID and cMCL-1 can be accelerated by conditions that destabilize cBID. Addition of 0.1% of the detergent IGEPAL decreased the interaction time to less than 1 h (data not shown). The HSQC NMR spectra of cMCL-1 (Figure 2.6B) suggest that cBID binds cMCL-1 very tightly. And the strong similarity of cMCL-1 spectra in complex with BID-BH3 or cBID (Figure 2.6C and 2.6D) confirm that cBID forms a stable hetero-dimer by engaging its BH3 region in the hydrophobic pocket of cMCL-1. This result is consistent with the recently reported direct interaction between tBID and BCL-X_L (Yao et al., 2009).

In conclusion, we report a human MCL-1 construct (cMCL-1) suitable for NMR studies, the solution structure of a human MCL-1:BH3 complex, and critical features of the highly anticipated MCL-1:activated BID complex. By NMR and ITC, we show that the N-terminal sequence of MCL-1 affects its binding affinity but not selectivity. Together these results will be valuable for future drug screening and design of compounds that specifically target human MCL-1.

2.5 Materials and methods

2.5.1 Protein expression and purification

Constructs of human MCL-1 cDNA lacking the C-terminal transmembrane region were expressed as His-tagged fusion proteins (Figure 2.2A). The complete soluble portion (ΔC23) and an N-terminal truncated fragment (ΔN119-ΔC23) were subcloned in vector pET29b(+) with a C-terminal His-tag, and ΔN151-ΔC7 was subcloned in vector pET32a with an N-terminal His-tag (Figure 2.2A). E. coli strain BL21 (DE3) containing the corresponding plasmid was grown in LB media at 37 °C to an optical density of 0.8 at 600 nm, and then induced by 1 mM isopropyl-β-D-thiogalactoside (IPTG) at 30 °C for 4 hours. For NMR samples, cells were grown in M9 media supplemented with ^{15}N ammonium chloride and/or ^{13}C glucose to produce uniformly ^{15}N- or ^{15}N-, ^{13}C-labeled proteins. The soluble human MCL-1 proteins (ΔC23, ΔN119-ΔC23, ΔN151-ΔC7) were purified through batch Ni-NTA affinity chromatography (Qiagen), Sephadex G-75 size exclusion chromatography (GE Healthcare), and Q-Sepharose anion-exchange chromatography (GE Healthcare). A calpain digestion step was further applied to ΔN119-ΔC23 or ΔN151-ΔC7 to produce cMCL-1 (ΔN162-ΔC24), and calpain was removed by Q-Sepharose anion-exchange chromatography. cBID (Moldoveanu et al., 2006), human BID-BH3 peptide (Denisov et al., 2006) (residues 76-106 with four extra residues on N-terminus GPLG-SESQEDIIRNIARHLAQVGDSMDRSIPPGLV) and rat μI-II calpain (Moldoveanu et al., 2002) were purified as previously described. The cMCL-

1:BID-BH3 complex was prepared by mixing protein and peptide at 1:1.2 ratio, and unbound peptide removed by Q-Sepharose chromatography. The BH3 peptides for BAD (residues 104-128 from NCBI:CAG46757), BIK (residues 51-70 from NCBI:CAG46681), PUMA (residues 131-150 from NCBI:AAK39542), BID (residues 80-99 from NCBI: NP_001187), Noxa (residues 18-38 from NCBI:AAH13120), BIM (residues 82-101 from NCBI:AAH33694), and MULE (residues 1969-1994 from NCBI:AAY98258) were synthesized by the Sheldon Biotechnology Centre (McGill University), and purified by C18 reverse-phase chromatography. The chemically synthesized BID peptide was used for ITC. Elsewhere, BID-BH3 refers to the purified BID 35mer produced biosynthetically. All proteins and peptides were stored in 20 mM HEPES (pH 6.5), 1 mM DTT buffer by flash freezing at -80 °C.

2.5.2 Limited proteolysis and N-terminal sequencing

Analytical limited proteolysis for MCL-1 ΔN119-ΔC23 or ΔN151-ΔC7 were performed at a concentration of 5 mg/ml, in 50 mM HEPES (pH 7.6), at room temperature (22 °C), in the presence of 0.001 mg/ml trypsin (Sigma), 0.01 mg/ml chymotrypsin (Sigma), or 5 mg/ml μI-II calpain (supplemented with 50 mM CaCl2) for different time intervals. Reactions were quenched by 4×SDS sample buffer and applied on an SDS-PAGE gel. Proteolysis resistant bands were blotted onto PVDF membranes, and N-terminal sequenced by the Sheldon Biotechnology Center (McGill University).

2.5.3 Mitochondria purification and in-vitro cyt c Release

Mitochondria of KB tumor cells were purified as described previously (Goping et al., 1998). Purified proteins (cBAK and/or cMCL-1) were used at 0.05 μM (final concentration) in the cyt c release reactions at 37 °C for 1 hour. Centrifugation at 9,000 rpm (4 °C) was applied to separate mitochondria from the supernatants and to stop the reactions. The supernatants and pellets were analyzed for cyt c by

western blotting using antibody #556433 (BD Biosciences) and secondary anti-mouse (111-035-008) antibody (Jackson Immunoresearch labs).

2.5.4 Isothermal Titration Calorimetry (ITC) measurements

ITC was carried out on a MicroCal VP-ITC titration calorimeter controlled by VP Viewer software (MicroCal Inc., Northampton, MA). Experiments performed in 50 mM HEPES (pH 7.0) at 23 °C, consisted of 37 injections (8 μL) of 0.1 mM BH3 peptides into 1.45 ml of 0.01 mM human MCL-1 (four different constructs) to obtain a final peptide/protein ratio of 2:1. The calorimetric data were analyzed by the ORIGIN software to determine the thermodynamic binding constants.

2.5.5 NMR titrations

The backbone and side chain assignments for free cMCL-1 and free BID-BH3 were determined with ^{15}N, ^{13}C- labeled samples and standard triple-resonance NMR experiments: HNCACB, CBCA(CO)NH, HNCA, HNCO, CCH-TOCSY and HCCH-COSY (Cavanagh, 1996). In titration studies, unlabeled ligands were added to ^{15}N-labeled cMCL-1 or cBID until saturation. The ^{15}N-^{1}H HSQC spectra were recorded on a Bruker Avance DRX600 MHz spectrometer, processed by NMRPipe (Frank Delaglio, 1995) and visualized by NmrViewJ (Johnson and Blevins, 1994). Changes in chemical shifts of amide signals were plotted as a function of the residue numbers and mapped onto the 3D structure.

2.5.6 Analytical gel filtration chromatography

cMCL-1, cBID, cMCL-1:cBID (mixed overnight at 30 °C) were prepared at 2 mg/ml in 20mM HEPES (pH 6.5) and 1mM DTT. The size exclusion running buffer contains 25 mM HEPES (pH 6.5), 150 mM NaCl, and 1mM DTT. 100μL sample was injected when performing analytical runs on Superdex 75 (10/30).

2.5.7 NMR Data Collection, Analysis and Spectral Assignments

For structure calculation, a series of samples, 0.5 mM ^{13}C, ^{15}N- double-labeled cMCL-1:unlabeled BID-BH3 and 0.5 mM unlabeled cMCL-1:^{13}C, ^{15}N- double-labeled BID-BH3, were prepared in 20 mM HEPES (pH 6.5), 1 mM DTT in either 10% D_2O or 100% D_2O. NMR experiments were recorded at 30 °C on Varian Unity Inova 800 MHz or 500 MHz spectrometers. ^1H homonuclear NOEs were measured from ^{15}N-edited NOESY and ^{13}C-edited NOESY spectra acquired with a 90 ms mixing time (Clore and Gronenborn, 1994), and the inter-molecular ^1H homonuclear NOEs were detected from ^{15}N, ^{13}C- filtered, ^{13}C-edited NOESY and ^{15}N, ^{13}C- filtered, ^{15}N-edited NOESY. Amide heteronuclear $^{15}N\{^1H\}$ NOEs were used for determination of high mobility regions of protein (Peng and Wagner, 1994). IPAP-HSQC experiments were recorded for both an isotropic sample and a sample with 7 mg/ml Pf1 phage to measure ^{15}N-^1H residual dipolar couplings (RDCs) (Ottiger et al., 1998). All spectra were processed by NMRPipe (Frank Delaglio, 1995) and analyzed with NmrViewJ 8.0 (Johnson and Blevins, 1994). ϕ and φ backbone torsion angles were derived by TALOS (Gabriel Cornilescu, 1999).

2.5.8 Structure Calculation and Analysis

Typical α-helical regions were identified by chemical shift indexing (CSI) of Cα and Hα, and confirmed by the identification of Hα(i) - HN (i+3) medium range NOEs. CYANA 2.1 software (Guntert, 2004) was used to generate the initial structures of hcMCL-1:hBID-BH3 complex with optimization to obtain low target functions. The structure was refined with CNS version 1.2 (Brunger et al., 1998) using the standard protocol with a total set of 3563 unambiguous constraints listed in Table 1. Ten structures were selected based on lowest overall energy and least violations to represent the final structures. These were evaluated with PROCHECK (Laskowski et al., 1996) to check the protein's stereochemical geometry. The atomic coordinates of the complex have been deposited in the

Protein Data Bank under accession code 2KBW. Structure figures were generated with MacPymol (Delano, 2008).

2.6 Acknowledgements

This work was supported by Canadian Institute of Health Research grant MOP-81277 to K.G. We would like to acknowledge GeminX for providing us the human MCL-1 expressing plasmids and the cells for mitochondria import assays. We also thank Dr. Guennadi Kozlov, Dr. Alexeij Denisov, and Dr. Jean-Francois Trempe for their assistance and helpful discussions.

Table 2.1: Structural Statistics for cMCL-1:BID-BH3 Complex

Constraints used for structure calculation		
Intraresidue NOEs	(n=0)	973
Sequential NOEs	(n=1)	747
Medium range NOEs	(n=2,3,4)	631
Long range NOEs	(n>4)	386
Intermolecular NOEs		197
Dihedral angle constraints		282
Hydrogen bonds		190
^{15}N–^{1}H residual dipolar couplings		157
Total number of constraints		3563
Average energy values (kcal mol^{-1})[1,2]		
E_{total}		353.97 ± 10.23
E_{bond}		13.40 ± 0.69
E_{angle}		123.19 ± 3.40
$E_{improper}$		14.86 ± 0.87
E_{VdW}		84.26 ± 3.97
E_{NOE}		71.60 ± 5.03
E_{cdih}		0.51 ± 0.13
E_{sani}		46.15 ± 2.92
RMSD from idealized covalent geometry[1,2]		
Bonds (Å)		0.0021 ± 0.00005
Angles (º)		0.3734 ± 0.0052
Improper (º)		0.2452 ± 0.0071
RMSD from experimental restraints[1,2]		
Distance restraints (Å)		0.0175 ± 0.0006
Dihedral angle restraints (º)		0.1206 ± 0.0159
Residual dipolar couplings[2]		
RMSD (Hz)		2.71 ± 0.09
R_{dip}		0.127 ± 0.005
Average RMSD to mean structure[1,2] (Å)		
Backbone atoms		0.38 ± 0.05
All heavy (non-hydrogen) atoms		1.04 ± 0.06
Average Ramachandran statistics[1,2]		
Residues in most favored regions		85.6%
Residues in additional allowed regions		11.1%
Residues in generously allowed regions		2.5%
Residues in disallowed regions		0.7%

[1] Residues 173–192, 204–319, and 79–99
[2] 10 lowest energy conformers

Chapter 3

BAK's Regulation through Two Forms of Homo-Dimers

1. T. Moldoveanu, Q. Liu, A. Tocilj, M. Watson, G. Shore, and K. Gehring, The X-ray structure of a BAK homodimer reveals an inhibitory zinc-binding site. Mol Cell 24 (2006) 677-688.

2. T. Moldoveanu, Q. Liu, M. Watson, D. R. Green and K. Gehring, Disulphide-Bonded BAK Homodimers Escape Inhibition by Zinc. (Manuscript in preparation).

MCL-1 is an endogenous inhibitor of BAK. To understand its regulation more thoroughly, it is necessary to study the regulatory mechanisms of BAK. In this chapter, two crystal structures of BAK will be presented, upon which more activity assays in native membrane environments (mitochondria) were conducted, and a zinc-mediated regulatory model was raised.

3.1 Abstract

BAX and BAK are the major mediators of apoptosis that act to permeablize the MOM and release cyt *c*. The mechanisms by which they are activated and regulated are still not completely known. Here, we identified the crystal structures of two homo-dimeric forms of BAK: one zinc-mediated dimer (calpain-proteolysed BAK, cBAK) at a resolution of 1.5 Å, and one disulphide-bond-linked dimer (cBAK-o) at 3.0 Å. The monomer units in each dimer structure resemble each other and reveal an occluded BH3-peptide binding pocket. They dimerize through residues D160 and H164 in cBAK and C166 in cBAK-o. In activity assays using mitochondria purified from *bak/bax* double-knockout (DKO) mouse embryonic fibroblasts (MEFs), $bax^{-/-}$ MEFs, and human tumor KB cells, both cBAK and cBAK-o can actively initiate cyt *c* release; however, compared to cBAK, whose activity can be inhibited by low micromolar levels of zinc, cBAK-o shows resistance to zinc inhibition, suggesting a unique regulatory element for BAK's activity formed by zinc-binding site and oxidation site.

3.2 Preface

BAK and BAX are the multi-region pro-apoptotic BCL-2 effectors. Upon activation they permeablize the MOM to release cyt *c* and initiate the caspase cascade (Lindsten et al., 2000; Wei et al., 2001). Thus how they are activated is central the understanding of BCL-2 regulated apoptosis.

Inactive BAX locates in the cytosol in a soluble form (Wolter et al., 1997), which facilitated the structural studies. Its solution structure (Suzuki et al., 2000) in turn, provided useful information for further *in vivo* and *in vitro* studies, resulting in a better understanding of BAX activation. It was reported that its BH1 and BH3 regions (α4 and α2) play important roles in BAX oligomerization (George et al., 2007; Nie et al., 2008; Zhou et al., 2007), and there is complicity between its oligomerization and activation (Ivashyna et al., 2009; Valentijn et al., 2008).

In comparison, BAK is much less understood. Our understanding of BAK's activation mostly came from speculation based on the knowledge of BAX. When we started this project, the BAK structure was unknown, probably due to its membrane-association. Therefore, any structural information revealing BAK's conformation should accelerate studies on its activation.

We set our original goal as solving the structure of BAK. In this chapter, we report the unique structural character of a calpain-cleaved form of human BAK (cBAK). The structures show a constricted putative BH3-peptide-binding pocket in BAK, which is different from the ones blocked by the C-terminal TM region in BAX (Suzuki et al., 2000) and BCL-w (Denisov et al., 2003; Hinds et al., 2003). The two crystal structures of BAK reveal different homodimeric interfaces: one accommodates a tetrahedrally coordinated zinc ion, and the other forms a disulphide bond. The effects of zinc and oxidation on BAK's activity are studied and indicate a distinct element in BAK's regulation.

3.3 Results

3.3.1 Screening of suitable constructs for structural studies on BAK

Both studies by NMR spectroscopy and crystallography demand a highly purified protein sample, thus the expression of human BAK protein in *E.coli* was first optimized (Figure 3.1A). Starting from a FLAG-BAK-HMK-ΔTM-His_6 construct provided by GeminX, we screened a series of variants. The full-length protein BAK and the construct with the deletion of TM region BAK-ΔTM induced the lysis of *E.coli* after induction and resulted in a lack of expression, while success was observed in expressing FLAG-BAK-HMK-ΔTM-His_6, FLAG-BAK-ΔTM-His_6, MEAS-BAK-ΔTM-His_6, GST-FLAG-BAK-ΔTM and GST-MEAS-BAK-ΔTM, suggesting the importance of the protection by the N-terminal capping with tags in different length (FLAG, octapeptide; MEAS, quadrapeptide; and GSH S-transferase (GST), 220-residue-protein) and the deletion of the C-terminal TM putative α-helical region. Additionally, we found that the 7-residue heavy-chain myosin kinase (HMK) phosphorylation site had little effect on BAK's expression. Following the purification procedures described in section 3.5.1, all five purified BAK proteins were applied in NMR studies and crystallography; however, they failed to produce high-resolution assignable spectra and diffractable single crystals, probably due to the presence of too many flexible residues or to the insufficient purity of the samples.

We then carried out limited proteolysis to search for protease resistant fragments in which the floppy sequences were removed (Figure 3.1B). During a course of 24 hours, trypsin and chymotrypsin both generated a ~15kDa truncated form, while μI-II calpain produced a ~20kDa fragment, which we call cBAK. According to MALDI-MS analysis and N-terminal sequencing, cBAK is 19,161.1 Da, resulted from the cleavage of the C-terminal His_6 tag, the HMK site, the N-terminal Flag epitope and the first 15 residues of BAK. Since this cBAK failed to directly express as a recombinant protein, its was prepared by large-scale calpain digestion

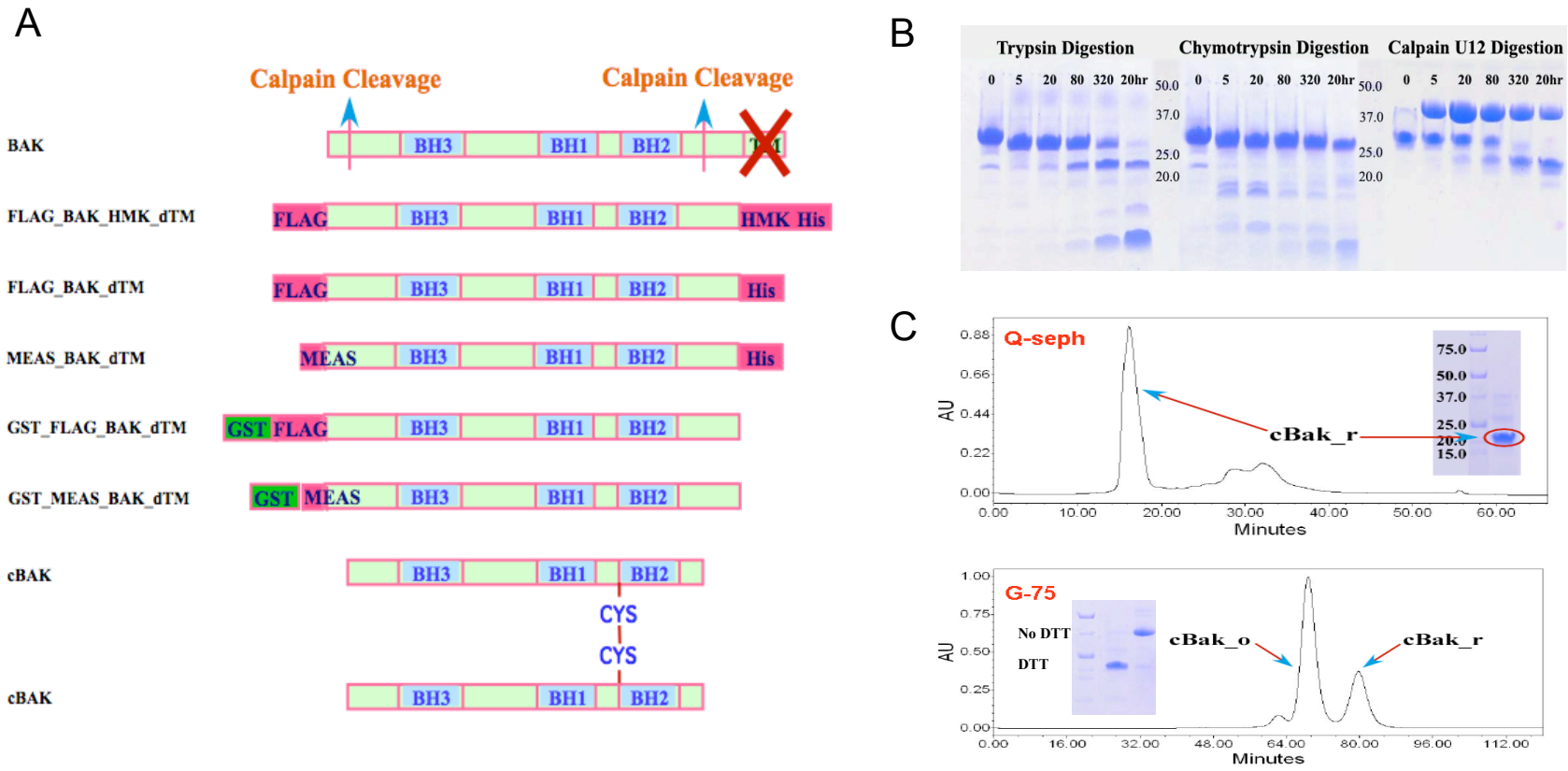

Figure 3.1: Recombinant BAK protein. (A) Constructs screened for BAK's expression. (B) Limited proteolysis on FLAG-BAK-HMK-dTM by trypsin, chymotrypsin, and calpain. (C) Purification of cBAK and cBAK-o.

followed by Q-sepharose chromatography (Figure 3.1C top). Large amounts of cBAK were stored by flash-freezing in -80°C, while small amounts for daily use were kept at 4°C. Although 1 mM DTT was included in the storage buffer, long term exposure in solution led to the oxidation between the single cysteine residue (C166) in each cBAK molecule, resulting in an oxidized cBAK homo-dimer, also called cBAK-o. This oxidation was confirmed by SDS-PAGE using sample buffers with or without DTT. We carried out the purification of cBAK-o by omission of DTT in the storage buffer for 48 h in 4°C followed by size-exclusion chromatography to remove the cBAK monomer (Figure 3.1C bottom).

3.3.2 Optimization of cyt *c* release assays

The activities of BAK and BAX have been monitored by cyt *c* release from purified mitochondria (Goping et al., 1998). Here, we examined the activities of different recombinant BAK proteins using mitochondria from human tumor KB cells, *bax*$^{-/-}$ and *bak/bax* DKO mouse embryonic fibroblasts (MEFs). In the beginning, we only observed very weak cyt *c* release due to the deletion of TM region that helps target the molecules to the membrane. However, as mentioned above, the expression of constructs containing TM promoted the lysis of *E. coli* and led to low expression. Therefore, we needed a method that could improve the recruitment of BAK protein to mitochondria membrane. We considered supplements such as detergents and ions to promote membrane association. IGEPAL is very helpful, but itself in high concentrations will lead to the leakiness of mitochondria (data not shown), so only a low percentage 0.005% was added. Among ions, various Mg^{2+} and Ca^{2+} concentrations were tested, and at ~5mM they both improved the association of cBAK with membrane and facilitated the cBAK-induced cyt *c* release (Figure 3.2A and data not shown). Since Ca^{2+} may cause too many other effects and Mg^{2+} is usually present to maintain mitochondrial integrity and has been used in assays with BAX (Eskes et al., 1998), the assay systems were optimized to include 5 mM $MgCl_2$ and 0.005% IGEPAL.

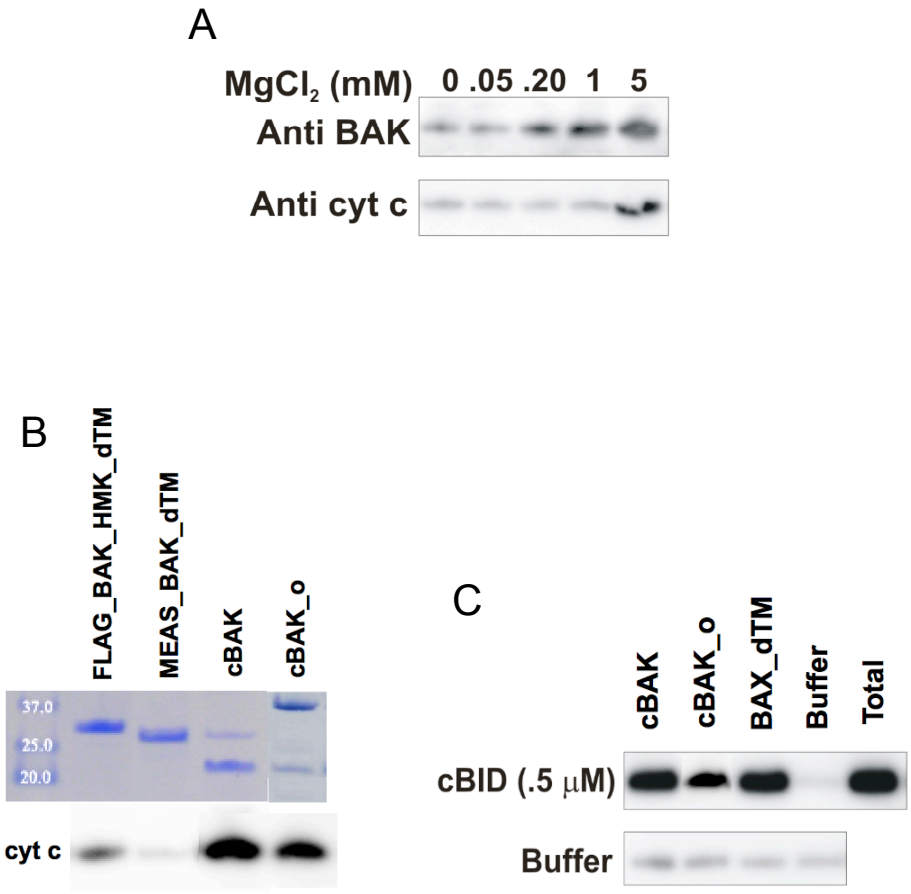

Figure 3.2: cBAK and cBAK-o are active constructs. (A) Optimization for ion supplementation in cyt c release assays, suggesting 5mM Mg^{2+} is necessary to help BAK molecule recruited to MOM and release cyt c. (B) The activities of four different BAK constructs tested using mitochondria purified from KB cells. The purified proteins for importing mitochondria were shown in SDS-PAGE. (C) cBID activates cBAK and cBAK-o to release cyt c from *bax/bak* DKO MEFs mitochondria.

3.3.3 The activities of purified recombinant BAK

In assays using human tumor KB mitochondria, both cBAK and cBAK-o can directly release cyt *c* in the presence of $MgCl_2$ and IGEPAL. cBAK shows more activity than the oxidized form (Figure 3.2B). However, in *bak/bax* DKO mitochondria, significant cyt *c* release was only achieved when truncated BID (cBID) was present (Figure 3.2C). Taking BAX-ΔTM as a positive control, it was shown that cBAK and cBAK-o have comparable abilities in releasing cyt *c* (Figure 3.2C) (Montessuit et al., 1999; Pagliari et al., 2005). This suggests they are bioactive constructs and suitable targets for structural studies. BAK fragments with an intact N-terminal sequence and protective N-terminal cap, such as FLAG-BAK-HMK-ΔTM-His_6 and MEAS-BAK-ΔTM-His_6, were much less active as shown in Figure 3.2B. This is consistent with their reduced toxicity and better expression in *E. coli*, and suggests an inhibitory effect of the N-terminal cap.

3.3.4 Monomeric cBAK crystal structure

cBAK and cBAK-o both developed reproducible crystals in the space groups, C2 and $C222_1$ respectively, diffracting at 1.5 Å and 3.0 Å (Table 3.1). The first structure was solved by a Se-Met SAD dataset collected from cBAK crystal (2IMT), and the structure of cBAK-o was solved by molecular replacement using 2IMT as a model. These two structures both presented homo-dimers, referring to A-A' for cBAK and B-B' for cBAK-o. Overlapping the monomers (A:B, A:B', A':B, A':B') resulted in r.m.s.d. ranging from 0.87 Å to 1.22 Å. The structures present a globular 8-helical bundle structure, which is the BCL-2 "signature" conformation: Helix α5 occupies the central position surrounded by helices α1-α4 and α6-α8 (Figure 3.3A and 3.3B). However, the BAK structure lacked two distinct structural characteristics found in other deposited BCL-2 structures: an unstructured loop region and a hydrophobic groove for BH3-peptide binding. The linkage between helix α1 and α3 (residue 54-69), which is unfolded in the corresponding parts in other BCL-2 members, exhibits a single-turn helix α2

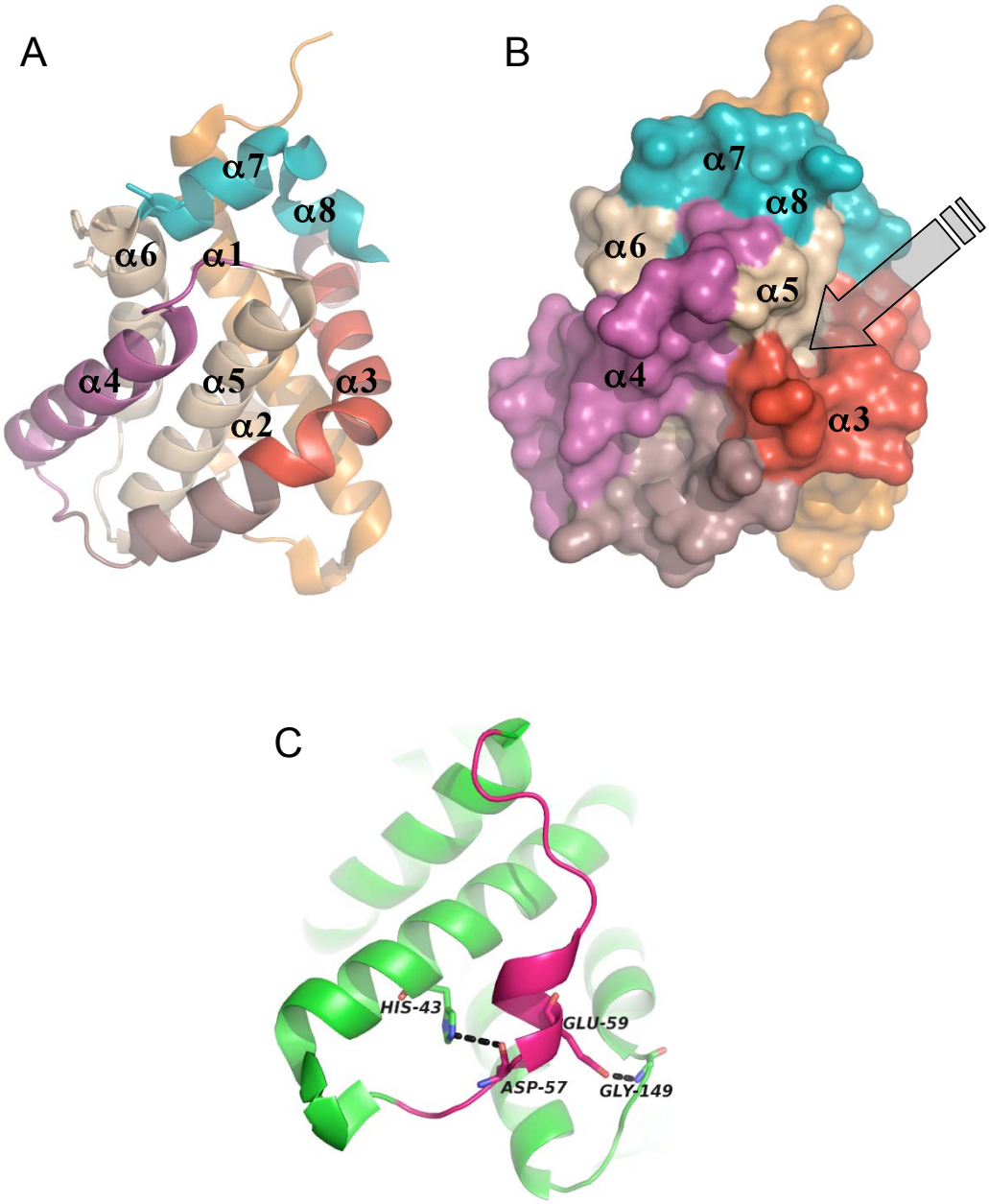

Figure 3.3: The crystal structure of cBAK monomer. The cartoon (A) and surface (B) representation of cBAK crystal structure, in which the BH1-3 regions are highlighted in purple, cyan, and red, and the theoretical hydrophobic groove is pointed with an arrow in (B). (C) The hydrogen bonds of D57 and E59 in α2 (pink) with H43 in α1 (green) and G149 in α6 (green) respectively.

(residue 58-63). In addition, the side chains of D57 and E59 make hydrogen bonds with the side chain of H43 in α1 and the backbone amide of G149 in α6, decreasing the flexibility of this region and reducing the possibility that it regulates BAK's pro-apoptotic activity (Figure 3.3C). For the hydrophobic groove, visible in the surface representation of cBAK (Figure 3.3B), it is a poorly defined short, narrow, and irregular pocket for BH3-peptide binding. This site is hindered by the side chains of R88 and Y89 and leads to BAK's laziness in BH3-binding.

The direct activation of BAK by BH3-only proteins has been extensively debated for lack of structural evidence of a physical interaction. Using either BID-BH3 peptide or cBID, we have tried to detect binding between cBAK and BID by many means, such as co-elution by gel-filtration chromatography, pull-down experiments, isothermal titration calorimetry (ITC) and NMR spectroscopy. Overlaid HSQC spectra recorded by adding a 10-fold excess of unlabeled BID-BH3 peptide or cBAK to 0.2 mM ^{15}N-labeled cBAK or ^{15}N-labeled BID-BH3 only displayed slight line broadening (Figure 3.4C and 3.4D). The affected residues of cBAK mostly mapped to the intrinsically occluded BH3-binding pocket, indicating the occurrence of a very weak interaction. The NMR titrations between cBAK and cBID (Figure 3.4A and 3.4B) gave similar results, supporting the weak binding affinity in solution. Although this is not enough to exclude the direct activation of BAK by truncated BID in the presence of membranes, the occluded hydrophobic pocket does intimate the existence of alternative mechanisms in regulating BAK's activity.

3.3.5 BAK's homo-dimerization

Since cBAK-o was purified as an oxidized dimer, it was not surprising to see a disulphide bond linkage between the two cBAK monomers in its structure (Figure 3.5B). However, the finding of a zinc-mediated homo-dimer was unexpected for the structure of cBAK (Figure 3.5A). Its diffractable crystals were grown in both

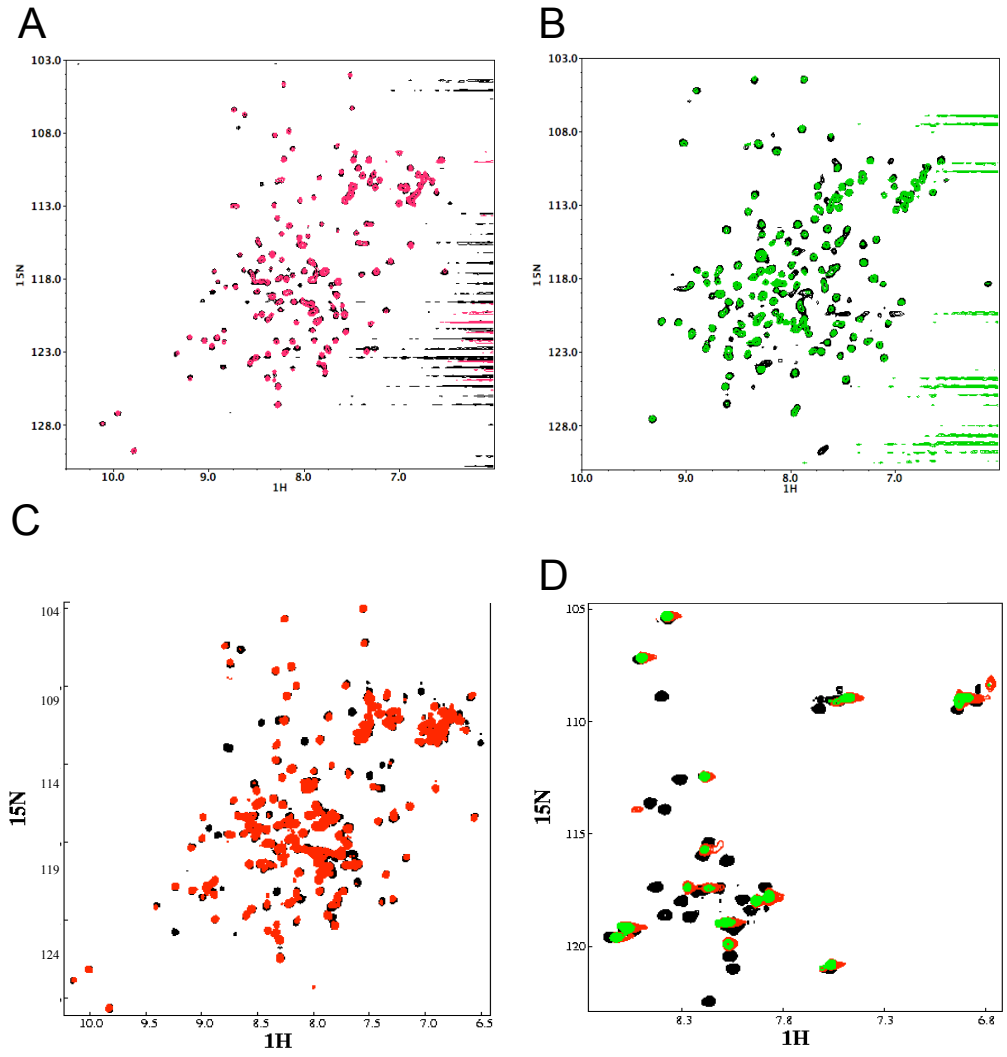

Figure 3.4: Weak interaction between BAK and BID. The HSQC spectra of 4-fold excess unlabeled cBID or cBAK over ^{15}N-labeled cBAK or cBID were shown in (A) and (B). Similar titrations but with 10-fold excess applied on ^{15}N-labeled cBAK or BID-BH3 peptide were presented in (C) and (D).

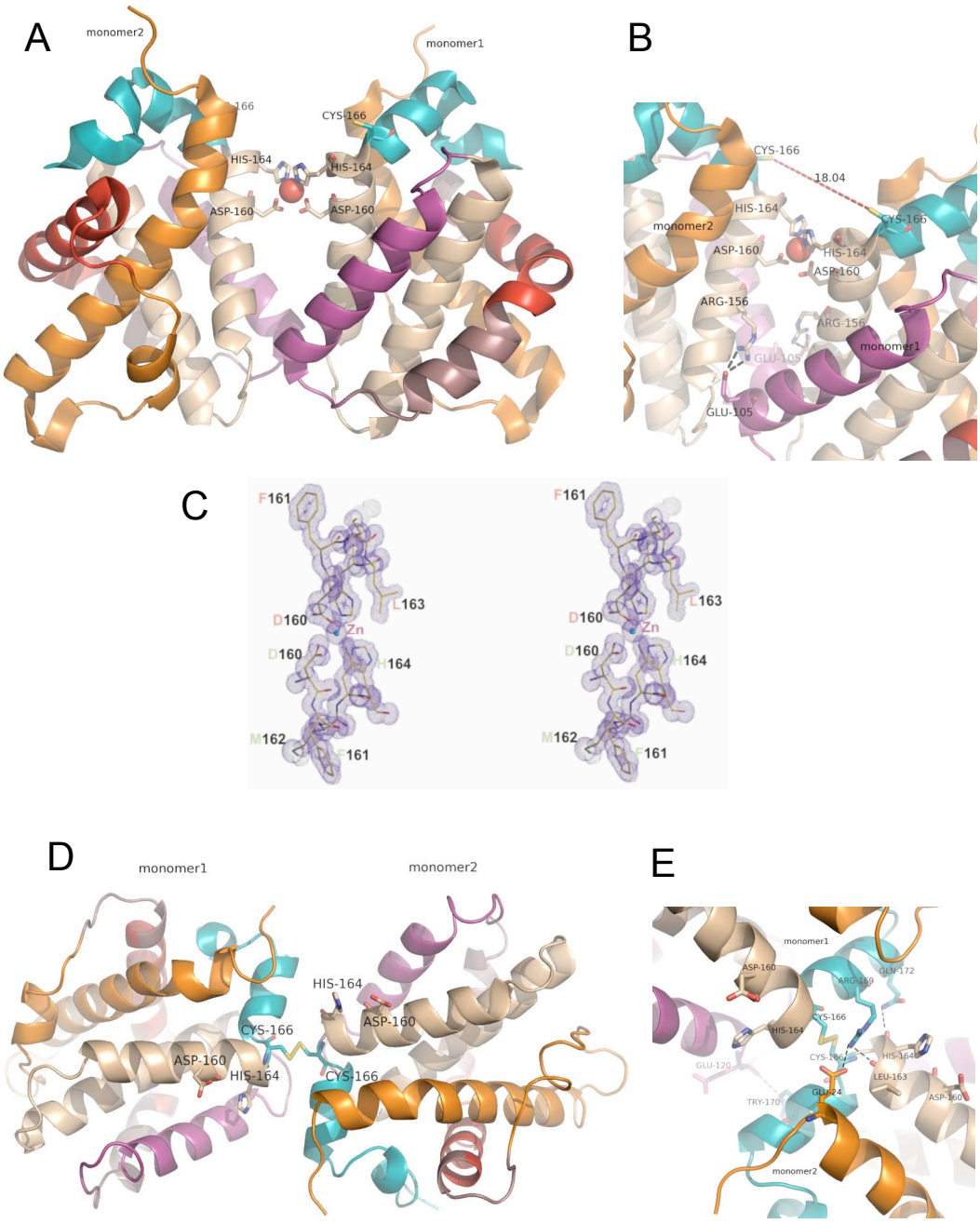

Figure 3.5: Two forms of cBAK homo-dimers. (A/D) Cartoon representation of the Zinc-mediated (A) and the disulpide-bond linked cBAK dimer (D). (B/E) Detailed homo-dimerization interfaces. (C) Stereo view of the Zn^{2+} coordination observed in the ammonium fluoride crystal showing the $2F_o$-F_c (1 sigma level) electron density map.

zinc-containing (polyethylene glycol as precipitant and zinc acetate as additive) and zinc-free conditions (polyethylene glycol as precipitant and ammonium fluoride as additive), and the last step of the purification of cBAK included 5 mM EDTA to chelate trace ions in water. But much to our surprise, we could refine a zinc ion in the structures solved with crystals obtained in both conditions (Figure 3.5C). It is coordinated in a tetrahedral geometry by the side chains of D160 and H164 from two adjacent cBAK monomers, mediating a symmetric dimerization interface (Figure 3.5A and 3.5B). Notably, the distance between the two S atoms in the two C166 residues is around 18.04Å, which is far enough to keep C166 in a reduced form. Opposite to the zinc-binding site, the residues from helices α4 and α6 form an intermolecular crystal contact: the side chain of R156 makes two salt-bridge interactions with the Oε of E105 from the other molecule, stabilizing the intermolecular interface.

In the oxidized dimer, two cBAK monomers are brought together by the S-S bridge formed by C166 from each monomer. Their orientations are stabilized by intermolecular interactions: the side chain of R169 makes salt-bridge with Oε of E24 and hydrogen-bond to the backbone amide of L163; Nε of Q172 interacts with the backbone amide of H164; and the backbone amide of E120 makes hydrogen-bond with the side chain of W170. As a result, the residues contributing to zinc binding, D160 and H164 in helix α6, are no longer aligned in a two-fold quaternary configuration (Figure 3.5C and 3.5D) and unable to bind zinc.

3.3.6 Zinc effects on BAK's activity

Given the striking proximity of C166 to the zinc-binding site (D160 and H164), we postulated that the zinc-dependent non-covalent and the disulphide-bond mediated homodimerization might represent distinct elements in the regulation of BAK's activity. We tested the functional significance in mitochondrial cyt *c* release assays. Low micromolar zinc chloride or zinc acetate inhibited endogenous BAK present in *bax*$^{-/-}$ MEFs mitochondria in response to the

activation by cBID (Figure 3.6A). At a higher concentration of cBID (7.5 μM), complete inhibition was observed using 5 μM $ZnCl_2$, while at a lower concentration of cBID (0.5 μM), strong inhibition was obtained by 1 μM $ZnCl_2$. In mitochondria purified from *bak/bax* DKO MEFs and human KB cells, the cyt *c* release induced by the addition of purified cBAK (5 μM) was similarly inhibited by $ZnCl_2$ (Figure 3.6B and 3.6C). The zinc binding-site mutant of cBAK (H164A) escaped zinc inhibition, suggesting that the zinc-binding site revealed by the crystal structure is necessary for the inhibitory effect of zinc on cBAK-dependent cyt *c* release. Moreover, the activity of cBAK-o was only inhibited at a much higher concentration of zinc (20 μM), and the oxidation-site mutant C166S was almost completely resistant to zinc. These mutants indicate that C166 might play a special role in promoting zinc-mediated homo-dimerization of BAK at the MOM.

3.4 Discussion

The BCL-2 family of proteins regulates intrinsic apoptosis mainly through protein-protein interactions, especially the hetero-dimerization between the BH3 region and the canonical BH3-binding pocket of different BCL-2 proteins (Chen et al., 2005; Liu et al., 2003). As shown in structures deposited in the Protein Data Bank (PDB), BCL-X_L (1MAZ) (Muchmore et al., 1996), BCL-2 (1G5M) (Petros et al., 2001) and MCL-1 (1WSX) (Day et al., 2005) present open hydrophobic grooves that allow peptide binding. In the structures of BCL-w (1MK3) (Denisov et al., 2003) and BAX (1F16) (Suzuki et al., 2000), the groove is blocked by an extra C-terminal helix. BID (2BID) (Chou et al., 1999) displays a shallow and narrow groove that disables ligand binding. Reminiscent of BID, cBAK also presents an occluded BH3-binding pocket, which is achieved by a new conformation of the BH3-containing helix α3. It makes an one-turn earlier bent with the help from the salt bridge between Nη1 in R87 and Oδ1 in D83, and the hydrogen bond between Nε in R87 and backbone amide of D83. Thus helix α3 in BAK is closer to the central helix α5 than in other BCL-2 members, resulting in a

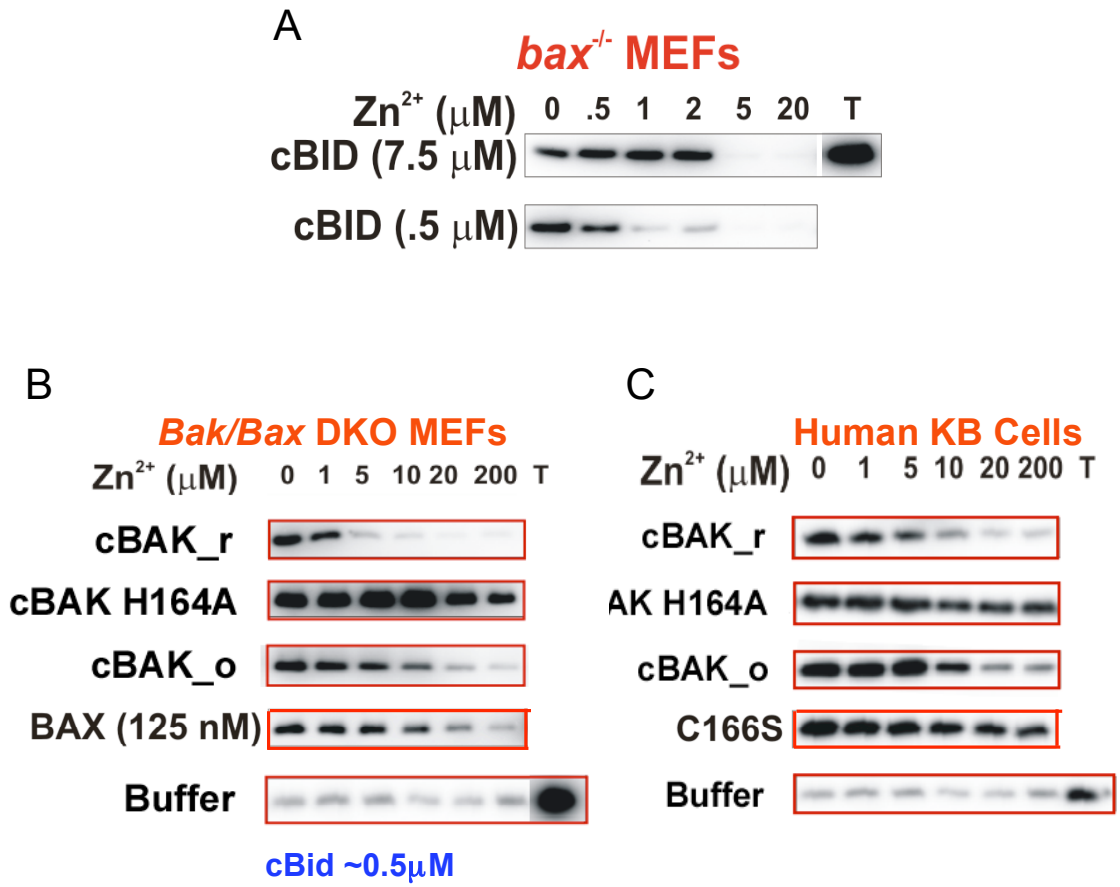

Figure 3.6: Inhibiting effect of Zinc on BAK's activity. Anti-cyt c was used to detect and quantify cyt c released from mitochondria in these western-blots. (A) Zinc inhibition on the activity of endogenous BAK in $BAX^{-/-}$ MEFs, whose activation was initiated by either 0.5μM or 7.5μM cBID (a truncated form of BID processed by calpain). (B) and (C) Zinc effects on the activities of the respective imported purified proteins to release cyt c from mitochondria of *bax/bak* DKO MEFs (B) or human KB cells (C).

shallower groove (Figure 3.7A and 3.7B). On the solvent-exposed side of this pocket, there is a remarkable hydrogen-bonding network that stabilizes the special conformation. This network is composed of Oδ1, Oδ2 in D90, Nε2 in Q94, Nε and Nη1 in R137, and Nη1 in R42 (Figure 3.7B). The residues involved are not conserved throughout the superfamily in a structure-based sequence alignment of solved BCL-2 paralogs (Figure 3.7C). This is consistent with BAK's unique conformation of helix α3. On the nonpolar side, the side chains of R88 and Y89 stack within the pocket (Figure 3.7D compared to BCL-X_L), abolishing any possible helix binding (Figure 3.7E aligned with the structure of BAX).

Recently a novel BH3-binding site in BAX was reported, involving helix α1, α6, and the loop between α1 and α2 (Gavathiotis et al., 2008). This binding by a stabilized alpha-helix of BCL-2 domain, SAHB-BIM-BH3 peptide not only causes a slight conformational change on BAX (Figure 3.8A and 3.8B), but also initiates the oligomerization of BAX, suggesting a novel direct activation site by BH3-only proteins. To address whether BAK involves a similar site in its regulation, we superimposed BAK structure (2IMT) onto the complex of BAX:SAHB-BIM-BH3 (2K7W) (Figure 3.8C and 3.8D). This clearly shows that BAK does not have a similar "trench" formed by the helices corresponding to α1, α2 and α6 of BAX. The side chains of E32, R36, P64 and R156 stretch out on the surface, making apparent spatial conflicts with the bound peptide. Therefore BAK has little likelihood of binding SAHB-BIM-BH3 similarly to BAX. We can assume that in an inactive dormant state, BAK adopts the conformation shown in the crystal structures with its C-terminal TM region associated with membranes (Figure 3.9C). The intrinsic obstruction of the two possible BH3-binding sites prevents BAK from being a BH3-acceptor without major conformational changes.

Although excluded from participating in hetero-dimerization, the two crystal structures reported in this chapter present two models of BAK's homo-dimerization and suggest homo-dimerization is a distinct element in BAK's regulation. This is different from the swapping of the C-terminal regions observed

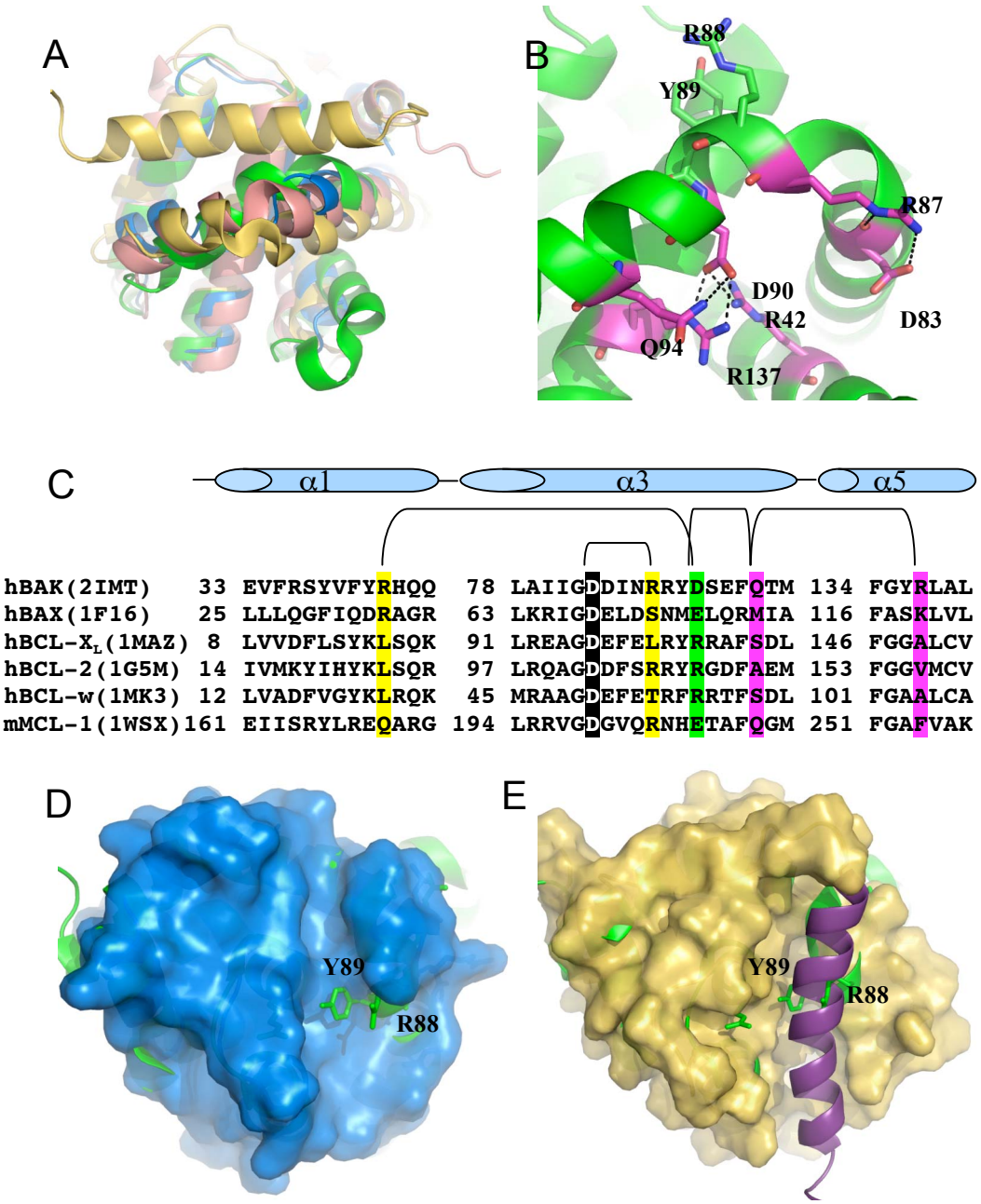

Figure 3.7: Comparison of the hydrophobic grooves in BCL-2 members. Cartoon-surface representations for the structural overlap are shown in (A), (D), and (E): BCL-X_L (blue, 1MAZ), cBAK (green, 2IMT), BAX (yellow with the exception of TM regionin purple, 1F16), and mMCL-1 (pink, 1WSX). (B) A detailed view of the salt bridges and hydrogen bonds on the solvent exposed side of α3: D83-R87, D90-Q94, D90-R42, and D90-R137. (C) Structure-based alignment among the deposited BCL-2 family PDBs, and the involved residues are background-colored according to their identity.

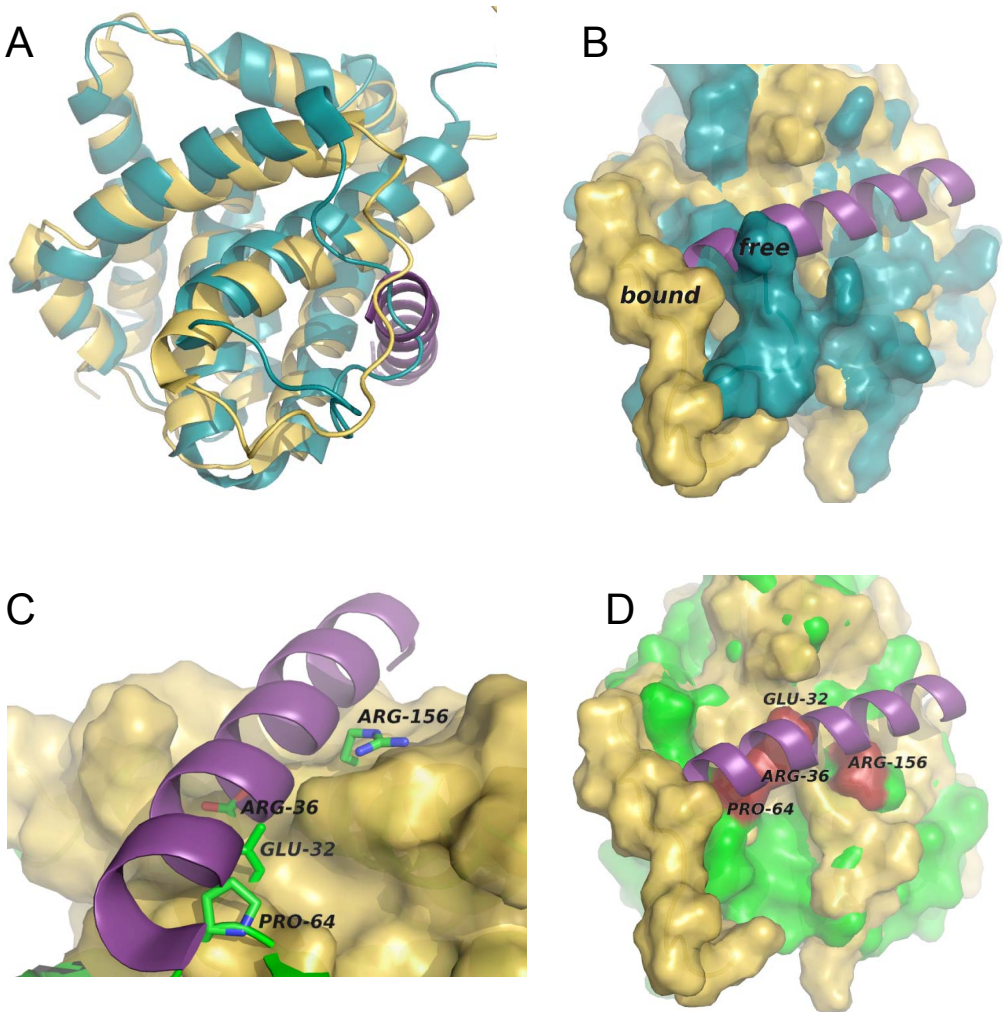

Figure 3.8: Comparison between BAK and BAX at the novel BIM-BH3 binding site of BAX. Cartoon-surface representations for the structural overlap are shown: cBAK (green, 2IMT), free BAX (deepteal, 1F16), and BAX:SAHB-BIM-BH3 complex (yellow except purple for BIM-BH3 peptide, 2K7W). (A) and (B) showed the difference of BAX upon BIM-BH3 binding. (C) and (D) presented the spatial confliction of BAK in BIM-BH3 binding.

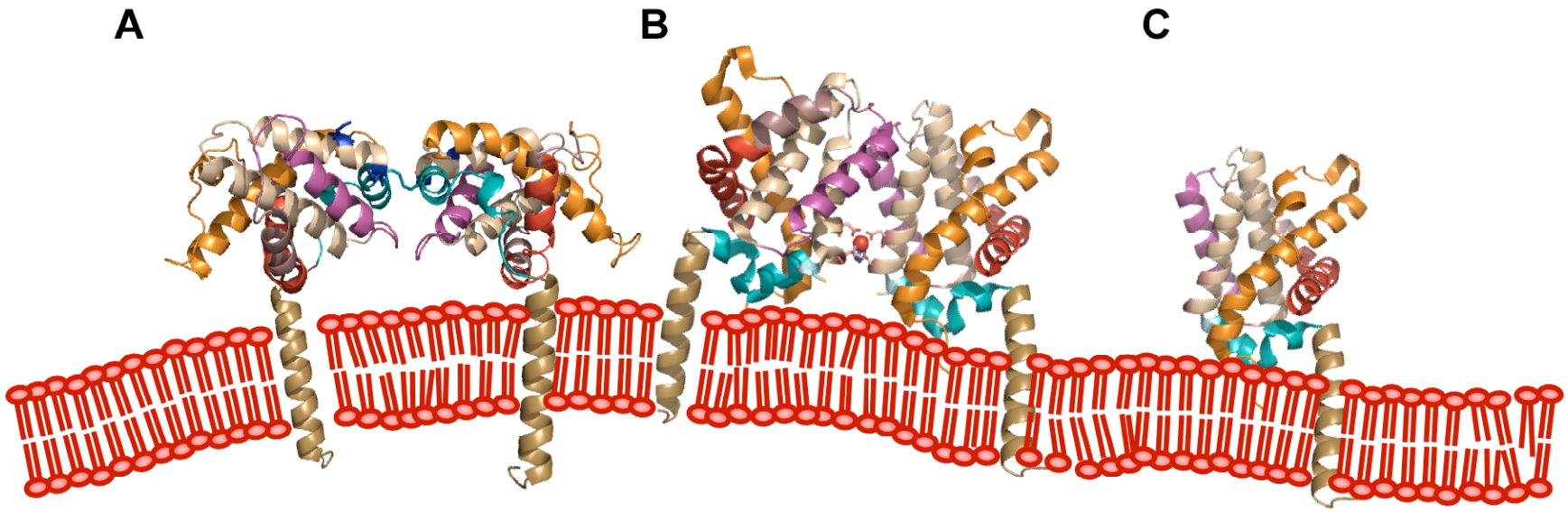

Figure 3.9: Possible conformations of membrane-associated BAK. The cartoon representation shows the TM helices (I188-S212) imbedded in MOM. (A) Disulphide-bond-linked BAK homodimer; (B) Zn^{2+}-mediated BAK homodimer; (C) BAK monomer.

for BCL-X_L (2B48) (Denisov et al., 2007; O'Neill et al., 2006). BAK homo-dimerizes either through a zinc ion held by D160 and H164 or a disulphide bond between two adjacent C166 residues. The zinc dimer is inactive in permeablizing MOM, as shown by the zinc inhibition on the activities of both endogenous and imported BAK at low micromolar levels (Figure 3.6B), indicating that the zinc-binding site might play an important role in switching-off BAK's activity. What's more, the endogenous BAK could be inhibited by 5 to 10 fold lower zinc concentrations compared to the exogenous purified cBAK (1 μM versus 5 μM in *bax/bak* DKO MEFs mitochondria and 10 μM in KB cells mitochondria). This is probably due to the increased two-dimensional alignment to the membrane by targeting via the TM region (Figure 3.9B and 3.9C). As for the oxidation-mediated homo-dimerization, both cBAK-o and the corresponding mutant C166S showed increased tolerance to zinc (Figure 3.6B and 3.6C), suggesting that active -SH might be vital in zinc-binding and oxidation could be a natural pathway for BAK to escape from zinc inhibition. Speculating about possible conformations for the membrane-association of BAK as homo-dimers (Figure 3.9A and 3.9B), we propose that BAK may involve self-control by the unique regulatory element formed by D160, H164 and C166 at the end of helix α6 and the beginning of helix α7.

BAK's N-terminus plays a negative role in its activity. Previous research showed that its exposure could be detected by conformational antibodies before cyt *c* release (Griffiths et al., 1999; Ruffolo and Shore, 2003). Our results on BAK's expression and activity in permeablizing MOM (Figure 3.2B) lead to a similar conclusion: N-terminal capping prevents not only the cell lysis of *E. coli* but also cyt *c* release from mitochondria. On the other hand, the N-terminally deleted construct cBAK could not directly initiate cyt *c* release in *bax*/*bak* DKO MEFs mitochondria without the activation of cBID, indicating that BAK's activity is controlled in multiple levels.

Altogether, the crystal structures of BAK at the monomer and dimer levels reported in this chapter provide novel information about BAK's regulation. Together with the results from cyt *c* release assays, they will facilitate screening and the design of drugs that specifically target BAK for the treatment of multiple diseases including cancer, HIV infection, neurodegeneration, and aging (Green and Kroemer, 2004).

3.5 Materials and methods

3.5.1 Protein cloning, expression and purification

The original construct of human BAK lacking the C-terminal putative TM helix (residues 187-211) was provided by GeminX Biotechnologies. It was cloned in pET29b expression vector to generate a His_6-tag fused protein, and also modified with an N-terminal FLAG epitope tag and a C-terminal kinase recognition site (FLAG-BAK-HMK-ΔTM-His_6). Other constructs listed in Figure 3.1A were generated by ourselves using pRL574 for His_6-tag fusion and pRL296a for GST-fusion, and the used primers were listed in Table 3.2. *Escherichia coli* (BL21 star) containing the corresponding expression plasmid were grown in LB media at 37˚C to an optical density of 0.8 at 600 nm, and then induced by 1mM isopropyl-ß-D-thiogalactoside (IPTG) at 30˚C for 4 hours. For NMR samples, cells were grown in M9 media supplemented with ^{15}N ammonium chloride and/or ^{13}C-enriched glucose to produce uniformly ^{15}N- or ^{15}N,^{13}C-labeled proteins. The soluble human BAK proteins were purified through batch Ni-NTA or GST affinity chromatography (QIAGEN), a following Sephadex G-75 gel-filtration chromatography (GE Healthcare) in running buffer containing 25 mM Tris (pH 7.6), 10 mM EDTA (pH 7.6), 150 mM NaCl, 2% glycerol, 0.01% azide and 1 mM β-mercaptoethanol, and a final Q-sepharose anion-exchange chromatography (GE Healthcare) in 25 mM Tris (pH 7.6), 5 mM EDTA (pH 7.6) and 0-500 mM NaCl gradient. A calpain digestion step was further applied to generate cBAK, and calpain was removed by Q-sepharose anion-exchange chromatography. cBAK-o

was obtained through a slow oxidation step at 4˚C based on the deprivation of reducing reagents and a following size-exclusion purification step. After each step the elution peak of interest was checked by SDS-PAGE electrophoresis. The yield in rich LB medium was 2-3 mg/L of *E. coli*. Full-length human BID was expressed as a GST-fused protein in which GST was removed by thrombin. Similar calpain digestion as above was applied to generate cBID. Human BID-BH3 peptide (residues 76-106 from CAG30275) was co-expressed in E. *coli* as a GST fusion protein (pGEX-6P-1) with mouse BCL-X_L (Denisov et al., 2006; Moldoveanu et al., 2006). The complex of Bcl-X_L/GST-BID-BH3 was first purified through Glutathione (GSH) sepharose-4B (GE Healthcare), and then digested by PreScission protease on column to remove the GST tag leaving four extra residues on N-terminus of the peptide (GPLG-S_{76}ESQEDIIRNIARHLAQVGDSMDRSIPPGLV$_{106}$). The elution fraction from GSH resin was further put on C18 reverse-phase HPLC to separate the peptide before lyophilization. Mass spectrometry was utilized to confirm peptide identity. Rat μI-II (Moldoveanu et al., 2002) were expressed in *E. coli* and purified as previously described. All the purified proteins were stored in 20 mM HEPES (pH 6.5) and 1 mM DTT buffer by flash freezing in -80˚C.

3.5.2 Limited proteolysis and N-terminal sequencing

Analytical limited proteolysis for FLAG-BAK-HMK-ΔTM-His_6, FLAG-BAK-ΔTM-His_6 or MEAS-BAK-ΔTM-His_6 were performed at a concentration of 5 mg/ml, in 50 mM HEPES (pH 7.6), at room temperature (22°C), and in the presence of 0.001 mg/ml trypsin (Sigma), or 0.01 mg/ml chymotrypsin (Sigma), or 5 mg/ml μI-II calpain (supplemented with 50 mM $CaCl_2$), for different time intervals. Reactions were quenched by 4×SDS sample buffer and applied on a 10% SDS-PAGE gel. Proteolysis resistant bands were blotted onto PVDF membranes that were submitted to Sheldon Biotechnology Center (McGill University) for N-terminal sequencing analysis. After conditions were optimized, scaled-up calpain-digestions were carried out with 5mg/ml μI-II calpain in 50 mM

HEPES (pH 7.6), 50 mM $CaCl_2$ at room temperature for over night, and calpain was later removed by Q-sepharose chromatography.

3.5.3 Mitochondria purification and *in vitro* cyt *c* Release

Mitochondria from *bax*$^{-/-}$ and *bak/bax* DKO MEFs and wild-type KB tumor cells were purified using the protocol provided by Dr. Shore's lab (Goping et al., 1998). In brief, cells lifted up by PBS-citrate EDTA buffer (4 g/l citrate and 0.6 mM EDTA in PBS buffer) were resuspended in HIM buffer (200 mM mannitol, 70 mM sucrose, 10 mM HEPES-KOH, 1 mM EGTA, pH 7.5, supplemented with protease inhibitors), and homogenized in a 2 mL Teflon homogenizer (Wheaton). The unbroken cells and nuclei were removed by pelleting at 1,000 rpm for 5 minutes, and the supernatant was spun at 9,000 rpm for 5 minutes to collect mitochondria. Further cleaning steps were applied by repeated resuspending in HIM buffer and spinning at 1,000/9,000 rpm alternatively for 5 minutes. Final mitochondria stocks were prepared in cMRM buffer (250mM sucrose, 10mM HEPES-KOH, 1mM ATP, 5mM Na^+ Succinate, 0.08mM ADP, 2mM K_2HPO_4, 1mM DTT, pH 7.5 supplemented with protease inhibitors) to reach a concentration of about 2mg of mitochondrial protein per ml, which will be half-diluted in import assays. All these purification steps were carried out on ice or at 4°C. Special modifications were made using buffers free of EGTA, and DTT for zinc reactions, and free of DTT for cBAK-o reactions, in order to prevent chelation of Zn^{2+} and reduction of disulphide bond respectively.

In the cyt *c* release assays, purified proteins rather than *in vitro* translated proteins were used, and their final concentrations were 0.05 to 5 μM for cBAK or BAX and 0.05 to 7.5 μM for cBID. The reactions were carried out for 1 hour at 37°C, and were stopped by centrifugation at 9,000 rpm (4°C). The supernatants and pellets were analyzed for cyt *c* by western blots using antibody #556433 (BD Biosciences) and secondary anti-mouse antibody (111-035-008, Jackson Immunoresearch labs). The pellets after 3 additional washes with cMRM buffer

were analyzed by western blots detected with anti-human BAK (sigma) and secondary anti-rabbit antibodies (111-035-008, Jackson Immunoresearch Lab.) to assess the association of BAK with membranes in the presence of divalent cations.

3.5.4 Crystallization and structure determination

Purified cBAK (10 mg/mL) and cBAK-o (10 mg/mL) were crystallized with the hanging drop method by mixing 1μL protein solution with 1μL well-solution. For cBAK, a reproducible crystal form with similar cell dimensions in the C2 space group (Table 3.1) has been obtained with PEG 3350 (15-30%) as precipitant, a pH range from 4.0-6.0, and 1-50 mM zinc acetate or ~0.2 M ammonium fluoride as additives. The native datasets were collected in house and a Se-Met SAD data set (peak) about the selenium K absorption edge was collected at beam line X8C (National Synchrotron Light Source, Brookhaven National Laboratory) using a Quantum-4 CCD area detector (Area Detector Systems Corporation, San Diego, CA) (Table 1) at 100K (Oxford cryosystems). Solve/Resolve was used to produce the initial SAD phases/model which was partially build and refined using arp/warp (Lamzin and Perrakis, 2000) and REFMAC (Collaborative Computational Project, 1994). Subsequent manual model building and fitting in Xfit (McRee, 1992) were complemented with refinement in CNS (Brunger et al., 1998). For cBAK-o, the reproducible crystals in $C222_1$ space group (Table 3.1) were obtained in 2.5-3.3M NaOAc pH 5.0-6.0. The Se-Met cBAK structure (2IMT) was used to find the solutions for cBAK-o structure using Molrep (Vagin and Teplyakov, 2000). Automatic refinement was performed using CNS (Brunger et al., 1998) and REFMAC (Murshudov et al., 1997) with inspection and manual fitting in Xfit (McRee, 1992).

3.5.5 NMR titrations

The backbone assignment of cBAK was determined by combining a series of 3D experiments taken on a $^{15}N,^{13}C$-labeled cBAK sample including HNCACB, CBCA(CO)NH, ^{15}N-edited NOESY, HNCA, HNCO and so on. In titration studies, different concentrations of unlabeled cBID, BID-BH3 peptide or cBAK were added to ^{15}N-labeled cBAK or cBID respectively. The ^{15}N-^{1}H HSQC spectra were recorded on a Bruker Avance DRX600 MHz spectrometer, processed by NMRPipe (Frank Delaglio, 1995) and superimposed by NmrViewJ (Johnson and Blevins, 1994).

3.6 Acknowledgement

This work was supported by grants from Natural Sciences and Engineering Research Council and Canadian Institutes of Health Research to K.G. We would like to acknowledge Dr. Tara Sprules from the Quebec/Eastern Canada High Field NMR Facility for acquiring 3D NMR spectra, Dr. Mai Nguyen and Hannah Heath-Engel of Dr. Shore's lab for technical assistance and advice regarding mitochondria purification and cyt *c* release assays, Youssouf Soumounou at GeminX for cell culture, and Dr. Douglas R. Green of St. Jude Children's Research Hospital for the *bax*$^{-/-}$ cells and helpful discussions.

Table 3.1: Data collection and refinement statistics

	cBAK	cBAK-o
Data collection		
Space group	C2	$C222_1$
Cell dimensions		
a, b, c (Å)	57.33, 53.66, 58.28	69.21, 114.68, 131.56
α, β, γ (°)	90.00, 115.05, 90.00	90.00, 90.00, 90.00
λ	0.98	1.54
Resolution (Å)	100.00-1.47 (1.52-1.47)*	100.0-3.0 (3.11-3.00)*
R_{sym} or R_{merge}[1]	4.0 (48.7)	11.7 (46.8)
I / σI	36.5 (2.2)	22.9 (4.8)
Completeness (%)	98.1 (82.6)	98.1 (82.6)
Redundancy	3.6 (2.4)	7.1 (6.9)
Refinement		
Resolution (Å)	52.70-1.47	65.94-3.00
No. reflections	25,682	11,410
R_{work} / R_{free}[2]	18.6 / 21.0	21.5 / 28.3
No. atoms	1441	4070
Protein	1305	3935
Ligand/ion	1	
Water	135	135
B-factors	22.0	32.0
Protein	21.0	34.5
Ligand/ion	17.0	
Water	31.9	22.6
R.m.s. deviations		
Bond lengths (Å)	0.016	0.067
Bond angles (°)	1.502	3.954

[1] $R_{merge} = \Sigma|I_j - \langle I \rangle|/\Sigma I_j$, where I_j are individual measurements for any on reflection and $\langle I \rangle$ is the average intensity of the symmetry equivalent reflections;

[2] $R_{cryst} = \Sigma|F_o - F_c|/\Sigma F_o$, F_o and F_c are observed and calculated structure factor amplitudes, respectively;

* Outer shell statistics shown in parenthesis.

Table 3.2: Primers used in BAK's subcloning	
Constructs	Primers
FLAG-BAK-dTM	5': AGATATACATATGGACTACAAAGAC
	3': GTGGTGCTCGAGACCATTGCCCAAGTTCAGGGC
MEAS-BAK-dTM	5': GATATACATATGGAAGCTTCAGCTTCGGGGCA
	3': GTGGTGCTCGAGACCATTGCCCAAGTTCAGGGC
GST-FLAG-BAK-dTM	5': AGATATACATATGGACTACAAAGAC
	3': GTGGTGCTCGAGCTAACCATTGCCCAAGTTCAGGGC
GST-MEAS-BAK-dTM	5': GATATACATATGGAAGCTTCAGCTTCGGGGCA
	3': GTGGTGCTCGAGCTAACCATTGCCCAAGTTCAGGGC
D160A	+: CCCGCTTCGTGGTCGCATTCATGCTGCATCACTGC
	-: GCAGTGATGCAGCATGAATGCGACCACGAAGCGGG
H164A	+: CGTGGTCGACTTCATGCTAGCTCACTGCATTGCCCGG
	-: CCGGGCAATGCAGTGAGCTAGCATGAAGTCGACCACG
D160A / H164A (mutated from D160A)	+: CGTGGTCGCATTCATGCTAGCTCACTGCATTGCCCGG
	-: CCGGGCAATGCAGTGAGCTAGCATGAATGCGACCACG
C166S	+: GACTTCATGCTGCATCACTCAATTGCCCGGTGGATTGC
	-: GCAATCCACCGGGCAATTGAGTGATGCAGCATGAAGTC
C14S	+: CCAGGCAGGAGTCCGGAGAGCCTGC
	-: GCAGGCTCTCCGGACTCCTGCCTGG

Chapter 4

BAK Interacts with MCL-1 through Its BH3 Region

Qian Liu and Kalle Gehring. Hetero-dimerization of BAK and MCL-1 activated by detergent micelles. (manuscript submitted to *J. Biol. Chem.* MS ID#: JBC/2010/144857).

The results from the former chapters, the hetero-dimerization of MCL-1 with BH3-only proteins (chapter 2) and the homo-dimerization of BAK (chapter 3), revealed the distinct regulatory mechanisms of MCL-1 and BAK. This following chapter will bridge chapter 2 and 3 by characterizing the interaction between BAK and MCL-1 in the presence of detergent micelles.

4.1 Abstract

BAK is a key protein mediating mitochondrial outer membrane permeabilization (MOMP), however, its behavior in the membrane is poorly understood. Here, we characterize the conformational changes in BAK and MCL-1 using detergents to mimic the membrane environment, and study their interaction by *in vitro* pull-down experiments, size exclusion chromatography, titration calorimetry and NMR spectroscopy. The non-ionic detergent IGEPAL has little impact on the structure of MCL-1, but induces a conformational change in BAK, whereby its BH3 region is able to engage the hydrophobic groove of MCL-1. Although the zwitterionic detergent CHAPS induces only minor conformational changes, it is also able to initiate heterodimerization. The complex of MCL-1 and BAK can be disrupted by a BID-BH3 peptide, which acts through binding to MCL-1, but a mutant peptide, BAK-BH3-L78A, with low affinity for MCL-1 failed to dissociate the complex. The mutation L78A in BAK prevented binding to MCL-1, thus demonstrating the essential role of the BH3 region of BAK in its regulation by MCL-1. Our results validate the current models for BAK's activation and highlight the potential value of small molecule inhibitors that directly target MCL-1.

4.2 Preface

BAX and BAK, also called MOMP effectors, perform their pro-apoptotic activities by directly mediating membrane permeabilization through oligomerization (Lindsten et al., 2000; Wei et al., 2001). The mechanism of their activation and regulation are the biggest mystery in field. Different from BAX, which has to translocate from the cytosol to the OMM during activation (Wolter et al., 1997), BAK is constitutively anchored to the outer membrane of mitochondria and the endoplasmic reticulum through its C-terminal transmembrane (TM) region (Breckenridge et al., 2003; Griffiths et al., 1999; Wei et al., 2000). Its N-terminal domain adopts the α-helical bundle conformation that is conserved across all BCL-2 family members containing multiple BH regions (Moldoveanu et al., 2006). Induced by various factors including staurosporine, etoposide, cisplatin, anti-Fas antibody, and detergents (Griffiths et al., 1999; Mandic et al., 2001; Sawai and Domae, 2009; Zhang et al., 2004), BAK undergoes a conformational change in apoptosis, which is termed BAK activation, and is characterized by the insertion of additional α-helical elements into the membrane and the assembly of BAK into higher-order oligomers (Korsmeyer et al., 2000; Reed, 2006). The conserved BH1 and BH3 regions of BAK have been reported to be important for its role in apoptosis (Dai et al., 2009; Dewson et al., 2008), but their specific functions are not fully understood. MCL-1 has been reported as an endogenous BAK-inhibitor, whose inhibition can be disrupted by the tumor suppressor p53 and NOXA (Gillissen et al., 2010; Leu et al., 2004; Willis et al., 2005). However, the mechanism by which MCL-1 regulates BAK is unclear.

BH3-only proteins are the death-initiators in BCL-2 family. They respond to cellular stress, and activate the effectors (BAX and BAK) to promote apoptosis directly or indirectly or both (Cartron et al., 2004; Kuwana et al., 2005; Kuwana et al., 2002; Letai et al., 2002). There are two popular models for effectors' activation (reviewed in section 1.8). In the case of BAK, the competitively

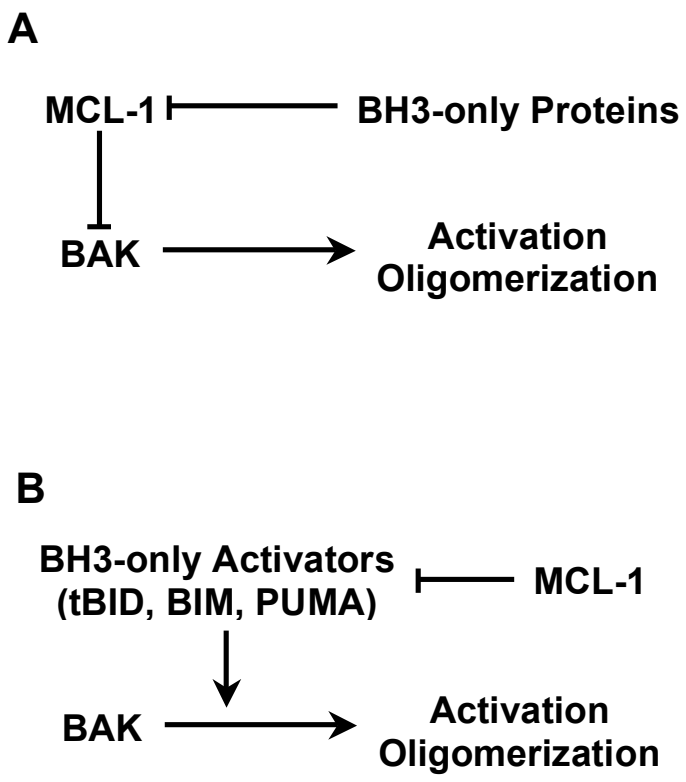

Figure 4.1: Model of BAK activation. (A) Competitively activating model (CAM): BH3-only proteins release BAK from its complexes with MCL-1 or BCL-X_L through competitively binding to the pocket of the anti-apoptotic proteins (Chen et al., 2005; Willis et al., 2005; Willis et al., 2007). (B) Directly activating model (DAM): BH3-only activators including tBID, BIM and PUMA directly bind and activate BAK, and the role of the anti-apoptotic proteins is to sequester the BH3-only activators to prevent apoptosis (Cartron et al., 2004; Kim et al., 2006; Kuwana et al., 2005; Letai et al., 2002; Wei et al., 2000).

activating model (CAM) proposes that BH3-only proteins release BAK from complexes with MCL-1 or BCL-X_L through competitively binding to the pocket of the anti-apoptotic proteins (Figure 4.1A) (Chen et al., 2005; Willis et al., 2005; Willis et al., 2007). The directly activating model (DAM) posits that BH3-only activators including tBID, BIM and PUMA directly bind and activate BAK, and the role of the anti-apoptotic proteins is to sequester the BH3-only activators to prevent apoptosis (Figure 4.1B) (Cartron et al., 2004; Kim et al., 2006; Kuwana et al., 2005; Letai et al., 2002; Wei et al., 2000). The debate over CAM and DAM has lasted for a long time due to difficulties in detecting direct protein-protein interactions and in determining the order in which they proceed (Certo et al., 2006; Chipuk and Green, 2008; Hacker and Weber, 2007; Willis et al., 2007).

To gain a deeper understanding of BAK's regulation, we sought additional information about the structural transitions that BAK undergoes during activation, and models of its heterodimerization that might be involved in its regulation. In this aim, we condensed the BCL-2 regulatory network to a mini-system consisting of BAK, MCL-1, a BID-BH3 peptide, and detergents to mimic the membrane environment of the cell. We used NMR spectroscopy, pull-down assays and size exclusion chromatography to assess protein-protein binding and structural transitions. We find that detergent is required for the direct interaction between BAK and MCL-1 *in vitro* and that heterodimerization occurs through binding of the BH3 region of BAK to the BH3-binding site of MCL-1.

4.3 Results

4.3.1 BAK in aqueous solution is not ready for hetero-dimerization

BAK's regulation by MCL-1 and BCL-X_L has been proposed to occur through the engagement of its BH3 region into the hydrophobic groove of anti-apoptotic proteins (Leu et al., 2004; Willis et al., 2005). However, in the crystal structure of BAK (Chapter 3), the BH3 region is partially buried in the protein interior and

unavailable for binding without a major conformational change. To investigate the interaction of BAK with the inhibitor MCL-1, purified components were mixed in aqueous solution for one hour at room temperature or overnight at 4°C. Neither condition resulted in the formation of a MCL-1:BAK complex, as indicated by the failure of cMCL-1 to be retained on Ni^{++}-NTA resin by Flag-BAK-HMK-ΔTM-His_6 in a pull-down experiment, the absence of elution shifts in analytical size exclusion chromatography, and the absence of chemical shift changes in the NMR spectra of ^{15}N-labeled cMCL-1 or ^{15}N-labeled cBAK upon the addition of unlabeled partner (data not shown). Therefore, under these conditions, we conclude that MCL-1 and BAK do not interact with each other.

4.3.2 Conformational changes of BAK and MCL-1 in the presence of IGEPAL

Pioneering studies on BCL-2 proteins revealed that specific detergents can induce conformational changes leading to conformational changes and/or their oligomerization (Denisov et al., 2006; Hsu and Youle, 1998; Kuwana et al., 2002; Losonczi et al., 2000). Detergents can also induce BAK-mediated apoptosis (Sawai and Domae, 2009). These led us to test the behavior of BAK and MCL-1 in the presence of detergents. We used both IGEPAL (a nonionic detergent) and CHAPS (a zwitterionic detergent) in our tests. Nonionic detergents have been reported to artificially promote the interactions between BCL-2 family of proteins (Hsu and Youle, 1997), while CHAPS has been reported to reduce the dimerization between BAX and tBID (Lovell et al., 2008).

Upon the addition of a range of IGEPAL concentrations from 4 times below its critical micelle concentration (CMC, ~0.02% v/v) to 20 times above, only slight chemical shift changes were observed in ^{1}H-^{15}N HSQC spectra of ^{15}N-labeled cMCL-1 (Figure 4.2A and data not shown). The well-dispersed pattern of peaks indicates that MCL-1 maintained its three-dimensional alpha-helical conformation. Analysis of the titration at 0.1% IGEPAL (Figure 4.2B and 4.2C) showed that the largest shifts, in the range of 0.1 – 0.16 ppm, came from the

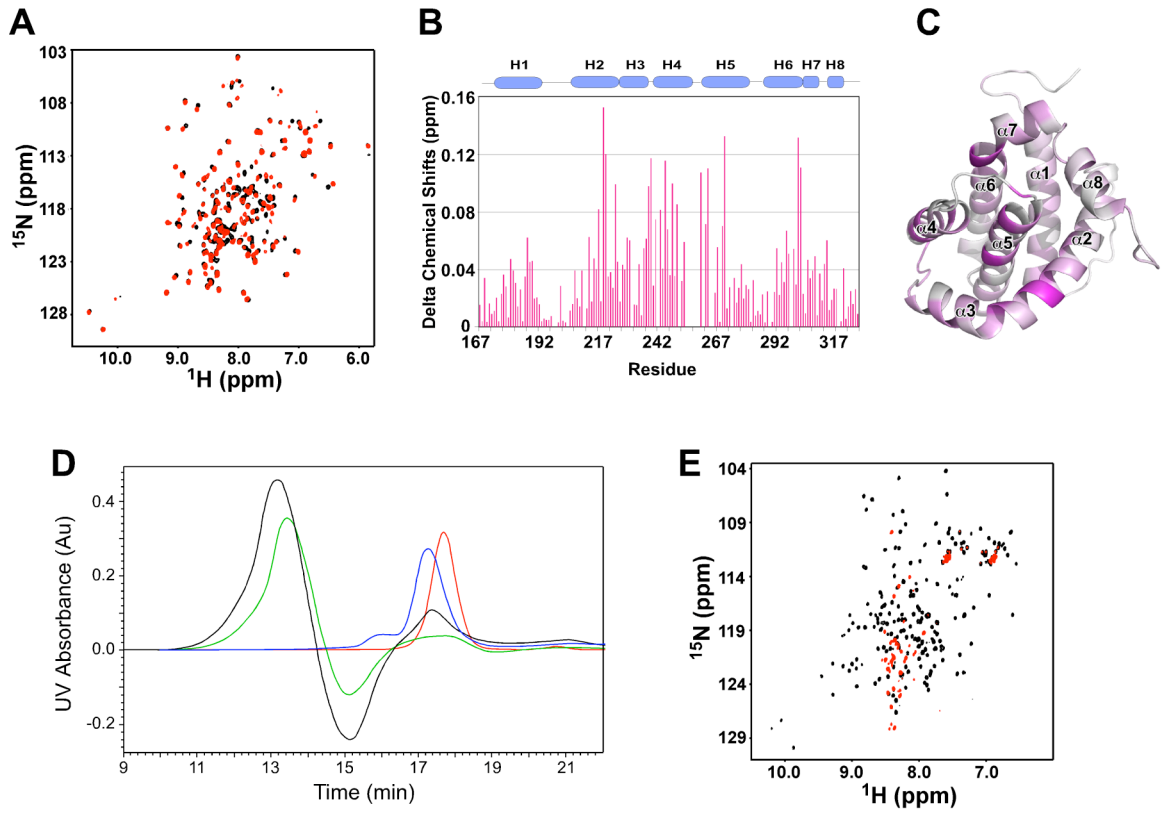

Figure 4.2: Behavior of BAK and MCL-1 in the presence of IGEPAL. (A) ^{1}H-^{15}N HSQC spectra of ^{15}N-labeled cMCL-1 without (black) and with (red) 0.1% (v/v) IGEPAL. (B) Plot of IGEPAL-induced chemical shift changes by residue for cMCL-1. The secondary structure (helices H1 to H8) of cMCL-1 is shown for reference. (C) Three-dimensional model of cMCL-1 colored by the values of their chemical shift changes upon the addition of IGEPAL. (D) Analytical size exclusion profiles for cBAK (red), cBAK in 0.1% IGEPAL (green), cMCL-1 in 0.1% IGEPAL (blue), and cBAK and cMCL-1 mixture in 0.1% IGEPAL (black). (E) ^{1}H-^{15}N HSQC spectra of ^{15}N-labeled cBAK without (black) and with (red) 0.1% (v/v) IGEPAL.

hydrophobic groove for BH3 peptide binding, residues located in helix α2, α4, α5, and the end of α6. The cMCL-1 detergent interaction was transient, and did not involve formation of a protein:micelle complex or the oligomerization of cMCL-1, as shown by the absence of changes in the analytical size exclusion chromatography profile (Figure 4.2D, blue trace, 17.2 minutes).

Similar titrations with cBAK resulted in a very different behavior. At low IGEPAL concentrations, there was a gradual disappearance of peaks in the spectrum of ^{15}N-labeled cBAK, and at 0.05% IGEPAL, the ^{1}H-^{15}N HSQC spectrum started to display a pattern typical of unfolded proteins (Figure 4.2E red, recorded in 0.1% IGEPAL). This suggests IGEPAL unfolds cBAK and the small number of signals observed indicates that the majority of BAK inserts into the large detergent micelles. Additionally, the elution time of cBAK on analytical size exclusion chromatography shifts from 17.8 minutes (Figure 4.2D, red trace) to 13.5 minutes (green trace). This high-molecular weight peak could be either oligomers of cBAK or cBAK associated with IGEPAL micelles. Thus, we observed a strongly altered conformation of BAK in the presence of IGEPAL.

4.3.3 Behavior of BAK and MCL-1 in the presence of CHAPS

In comparison, the application of 2% (w/v) CHAPS generated little effects on both cMCL-1 and cBAK; titrations with CHAPS induced only very minor chemical shift changes in the ^{1}H-^{15}N HSQC spectra of both proteins (Figure 4.3A and 4.4A). Even after overnight incubation, the shifts were under 0.19 ppm for cMCL-1 (Figure 4.3B) and 0.16 ppm for cBAK (Figure 4.4B and 4.4C), which suggests that only minor conformational changes occurred. Perturbations of chemical shifts above 0.10 ppm occurred in the residues located in helices α2 to α5 and the end of α6 in cMCL-1 (Figure 4.3C), and helices α3 to α5 in cBAK (Figure 4.4D), indicating that the CHAPS interacts weakly with both proteins in their putative BH3-binding hydrophobic grooves.

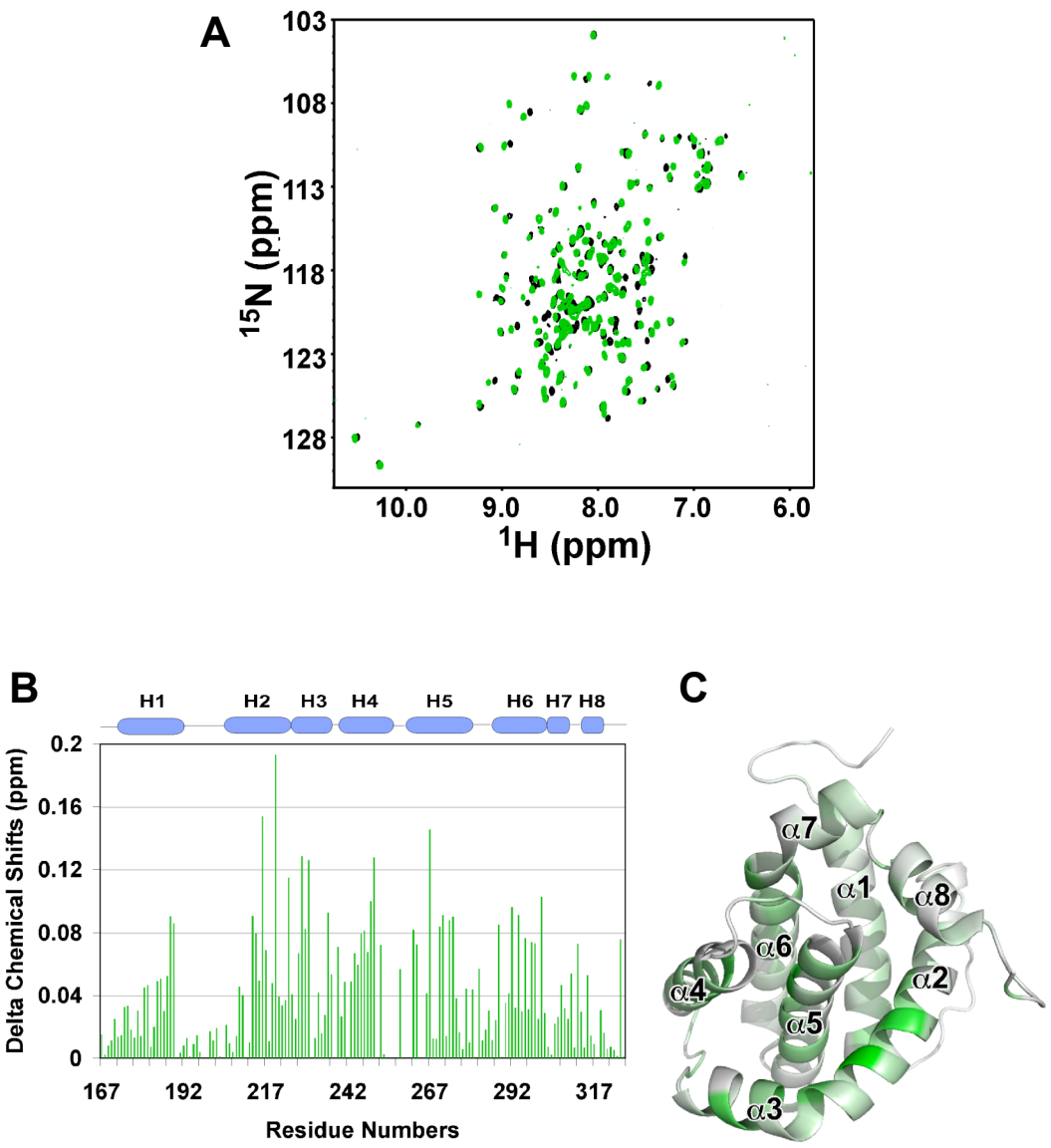

Figure 4.3: Behavior of cMCL-1 in CHAPS. (A) HSQC overlay of ^{15}N-labeled cMCL-1 without (black) and with 2% CHAPS (red). (B) Plots of CHAPS-induced chemical shift changes by residue for cMCL-1. (C) Three-dimensional models of cMCL-1 and colored by the values of their chemical shift changes upon the addition of CHAPS.

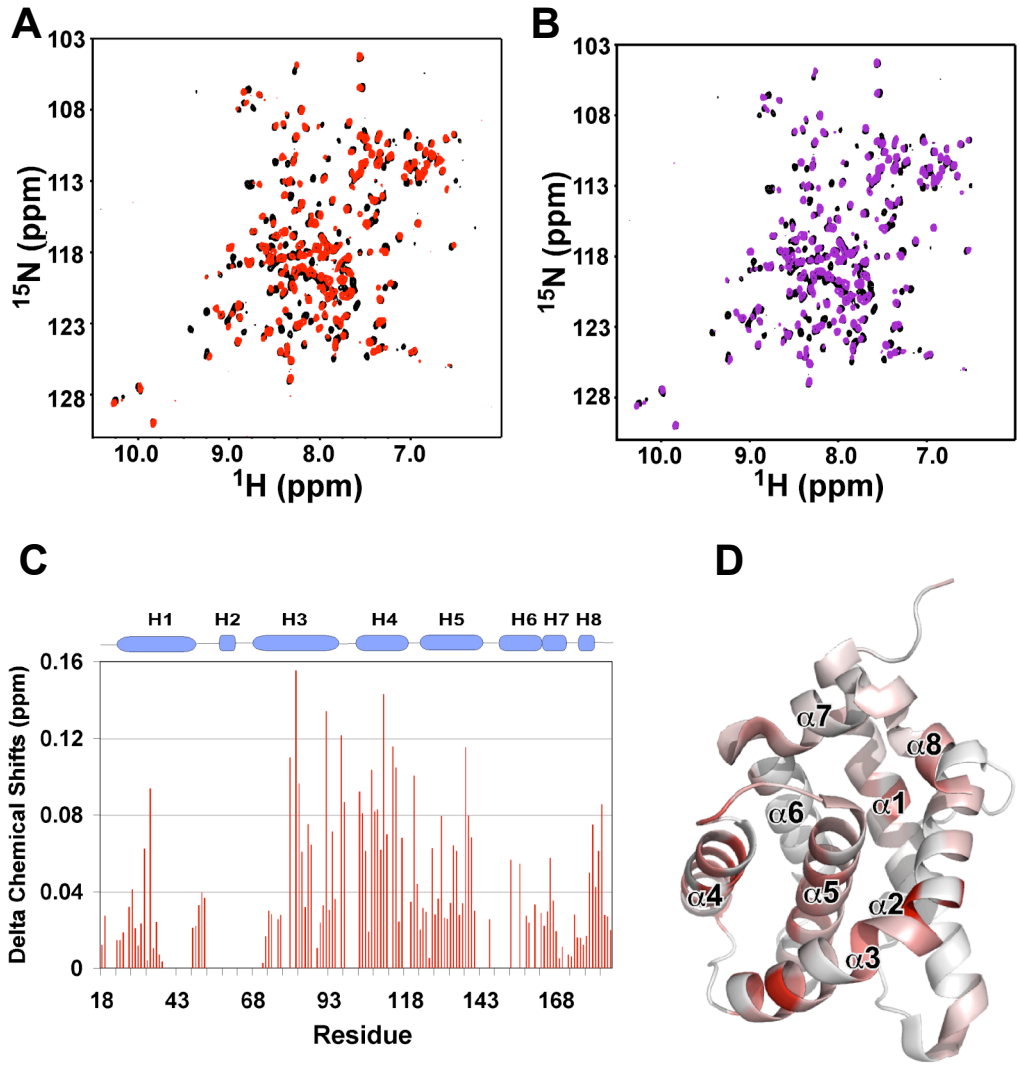

Figure 4.4: Behavior of cBAK in CHAPS. (A/B) HSQC overlay of ^{15}N-labeled cBAK without (black) and with 2% CHAPS in 20 minutes (A, red) and after overnight incubation (B, purple). (C) Plots of CHAPS-induced chemical shift changes by residue for cMCL-1. (D) Three-dimensional models of cMCL-1 and colored by the values of their chemical shift changes upon the addition of CHAPS.

4.3.4 BAK interacts with MCL-1 in the presence of detergents

In light of the IGEPAL-mediated conformational changes in BAK, we tested whether either detergent allows the association of BAK with MCL-1. On analytical size exclusion chromatography (Figure 4.2D), addition of cMCL-1 to cBAK in 0.1% IGEPAL gave rise to a peak that eluted at 13.2 minutes (black trace), which suggests the formation of a cBAK:cMCL-1:micelle complex larger than either cBAK or cMCL-1 alone in IGEPAL. Ni^{++}-NTA resin pull-down experiments showed that 0.1% IGEPAL was sufficient for Flag-BAK-HMK-ΔTM-His_6 to retain cMCL-1 on the Ni^{++}-NTA resin at about 1:1 ratio (Figure 4.5A). In NMR titrations (Figure 4.5B), the signals in the HSQC spectrum of ^{15}N-labeled cMCL-1 were strongly disturbed in the presence of both cBAK and IGEPAL. These results confirm a direct interaction between cBAK and cMCL-1.

To our surprise, 2% CHAPS also sufficed to promote the association between MCL-1 and BAK. Figure 4.6A shows that a concentration of CHAPS at 2% (above its CMC of 0.5%) was sufficient for retention of cMCL-1 by Flag-BAK-HMK-ΔTM-His_6 on the Ni^{++}-NTA resin. The well-dispersed ^{1}H-^{15}N HSQC spectra of both proteins in 2% CHAPS allowed us to detect the interaction using either ^{15}N-labeled cBAK or cMCL-1 (Figure 4.6B and 4.6C). In both cases, the formation of a large high-molecular weight complex of cBAK and cMCL-1 led to a loss of the majority of signals in the spectrum.

4.3.5 cBAK interacts with cMCL-1 through its BH3 region

We then asked whether BAK interacts with MCL-1 in detergent through its BH3 region as reported in assays using cell lysates (Leu et al., 2004; Willis et al., 2005). Titration of an unlabeled BAK-BH3 peptide into ^{15}N-labeled cMCL-1, generated many chemical shift changes in the slow exchange regime, which is indicative of tight binding (Figure 4.7A). In agreement with work from Hinds and co-workers (Day et al., 2008), the BAK-BH3 peptide engages the hydrophobic

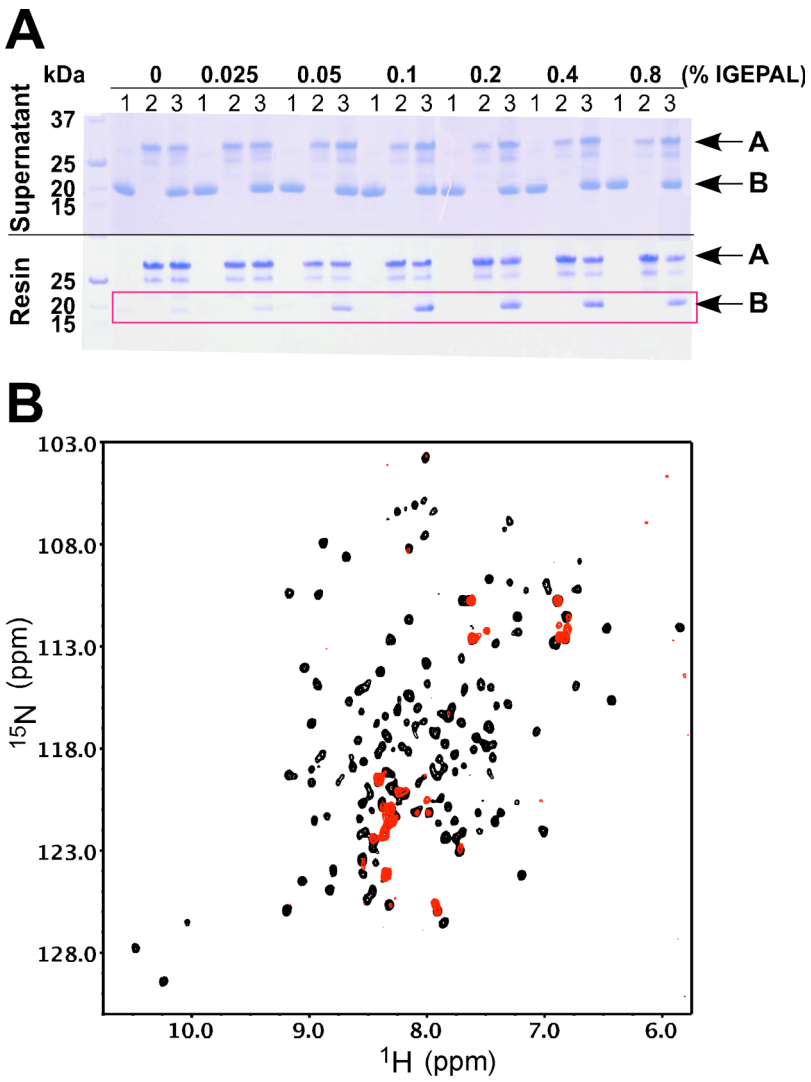

Figure 4.5: Interaction between BAK and MCL-1 in the presence of IGEPAL. (A) Coomassie-stained SDS-gels showing the supernatant (top) and proteins retained by the Ni^{++}-NTA resin (bottom) under the conditions indicated. Conditions 1-3 respectively mean that cMCL-1, Flag-BAK-HMK-His_6, or their combination was loaded. Arrows A show the positions of Flag-BAK-HMK-ΔTM-His_6, and arrows B show the positions of cMCL-1. The red frame highlights the cMCL-1 retained by Flag-BAK-HMK-ΔTM-His_6 in the presence of IGEPAL. (B) ^{1}H-^{15}N HSQC spectra of ^{15}N-labeled cMCL-1 in 0.1% IGEPAL without (black) and with (red) unlabeled cBAK.

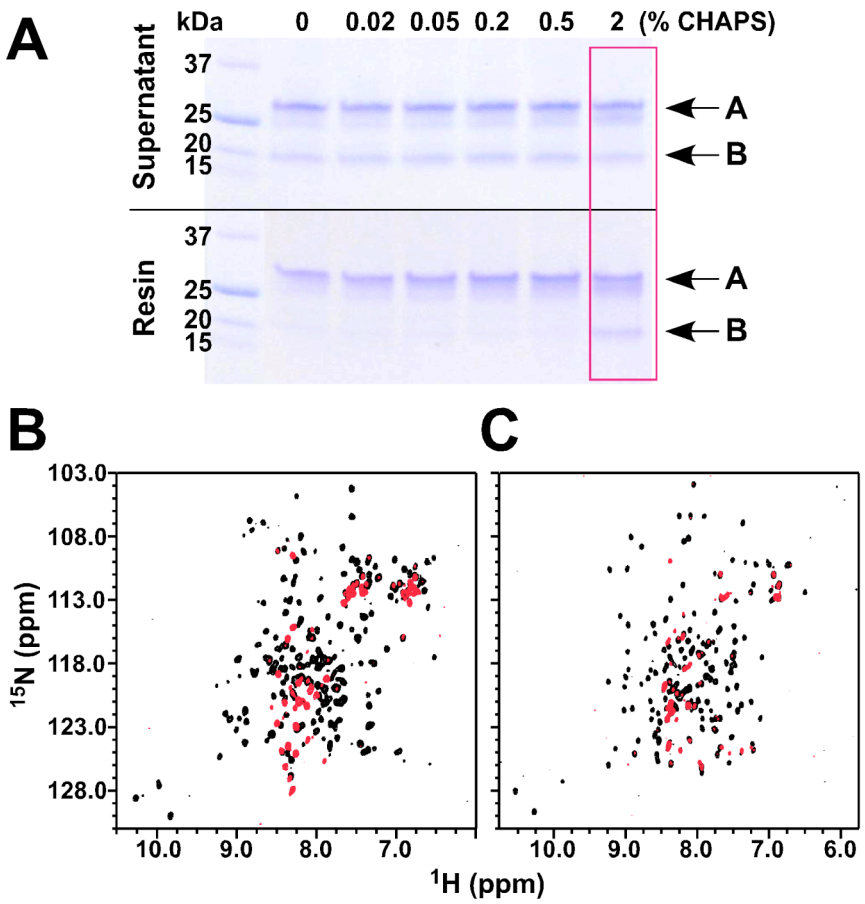

Figure 4.6: Interaction between BAK and MCL-1 in CHAPS. (A) Coomassie-stained SDS-gels showing the supernatant (top) and proteins retained by the Ni^{++}-NTA resin (bottom) in the presence of increasing concentrations of CHAPS as indicated. Arrows A show the positions of Flag-BAK-HMK-ΔTM-His_6, and arrows B show the positions of cMCL-1. The red frame indicates the condition in which the binding between BAK and MCL-1 was observed. (B) Overlay of ^{1}H-^{15}N HSQC spectra of ^{15}N-labeled cBAK in 2% CHAPS without (black) and with unlabeled cMCL-1 (red). (C) Overlay of ^{1}H-^{15}N HSQC spectra of ^{15}N-labeled cMCL-1 in 2% CHAPS without (black) and with unlabeled cBAK (red).

groove of MCL-1. The dissociation constants for MCL-1 constructs with different N-terminal deletions and BAK-BH3 peptides (wild-type and L78A mutant) were further tested by ITC (Figure 4.7B and 4.7C). As observed previously, removal of the N- and C-terminal extensions increased the affinity of MCL-1 for the BH3 peptides (Chapter 2). The wild-type BAK-BH3 peptide bound MCL-1 sixteen times more tightly than BID-BH3. In contrast, the mutation of L78A in BAK decreased the affinity of the BAK-BH3 peptide 160-fold. These data suggested the possibility of testing whether the full-length proteins interacted in same manner as the peptides by using BH3 peptides to inhibit the interaction.

The complex of Flag-BAK-HMK-ΔTM-His_6 and cMCL-1 was immobilized on Ni^{++}-NTA resin and a BID-BH3 peptide was used to compete for binding to cMCL-1. SDS-PAGE analysis of the pull-down experiment showed that increasing concentrations of the BID-BH3 peptide decreased the amount of cMCL-1 that was retained on the resin. When BID-BH3 was present at 4 times the concentration of the complex, cMCL-1 was fully released (Figure 4.8A). This competition was also observed in NMR titrations in 0.1% IGEPAL. Upon the addition of the BID-BH3 peptide at a 4:1 ratio of ^{15}N-cMCL-1:unlabeled-cBAK complex, all the signals for cMCL-1 were recovered and the spectrum was identical to that of the ^{15}N-cMCL-1:unlabeled-BID-BH3 complex (Figure 4.8B and 4.9). Significantly, the mutant peptide BAK-BH3-L78A failed to retrieve these signals, suggesting that the engagement of the BH3 peptide into MCL-1 is necessary to disrupt its interaction with BAK. Parallel experiments with mutant cBAK-L78A showed that the mutant protein could no longer recruit cMCL-1 into IGEPAL micelles (Figure 4.8B and 4.9). This confirms that the BAK BH3 region interacts with MCL-1. Similar conclusions were also drawn from the NMR titrations in 2% CHAPS. The complex could be disrupted by BID-BH3 peptide (Figure 4.10A), and upon release ^{15}N-cBAK gave rise to a spectrum typical of an unfolded protein (Figure 4.10B). This suggests that BAK loses its original α-helical fold when bound to MCL-1with its exposed BH3 region and is unable to refold when released.

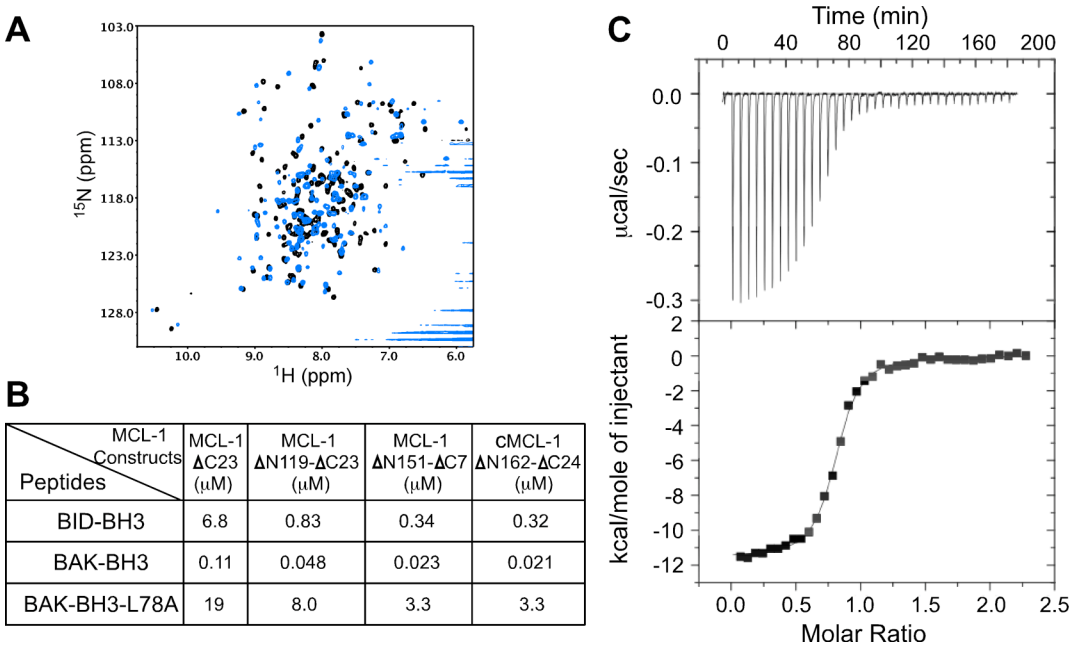

B

Peptides \ MCL-1 Constructs	MCL-1 ΔC23 (μM)	MCL-1 ΔN119-ΔC23 (μM)	MCL-1 ΔN151-ΔC7 (μM)	cMCL-1 ΔN162-ΔC24 (μM)
BID-BH3	6.8	0.83	0.34	0.32
BAK-BH3	0.11	0.048	0.023	0.021
BAK-BH3-L78A	19	8.0	3.3	3.3

Figure 4.7: MCL-1 interacts with BAK-BH3 peptide. (A) ^{1}H-^{15}N HSQC spectra of cMCL-1 without (black) and with (blue) unlabeled BAK-BH3 peptide. (B) Table of binding affinities between MCL-1 and BH3 peptides measured by ITC. Values for BID-BH3 bindings are from (Liu et al., 2010). (C) The ITC profile for BAK-BH3 peptide titrated into MCL-1-ΔC23.

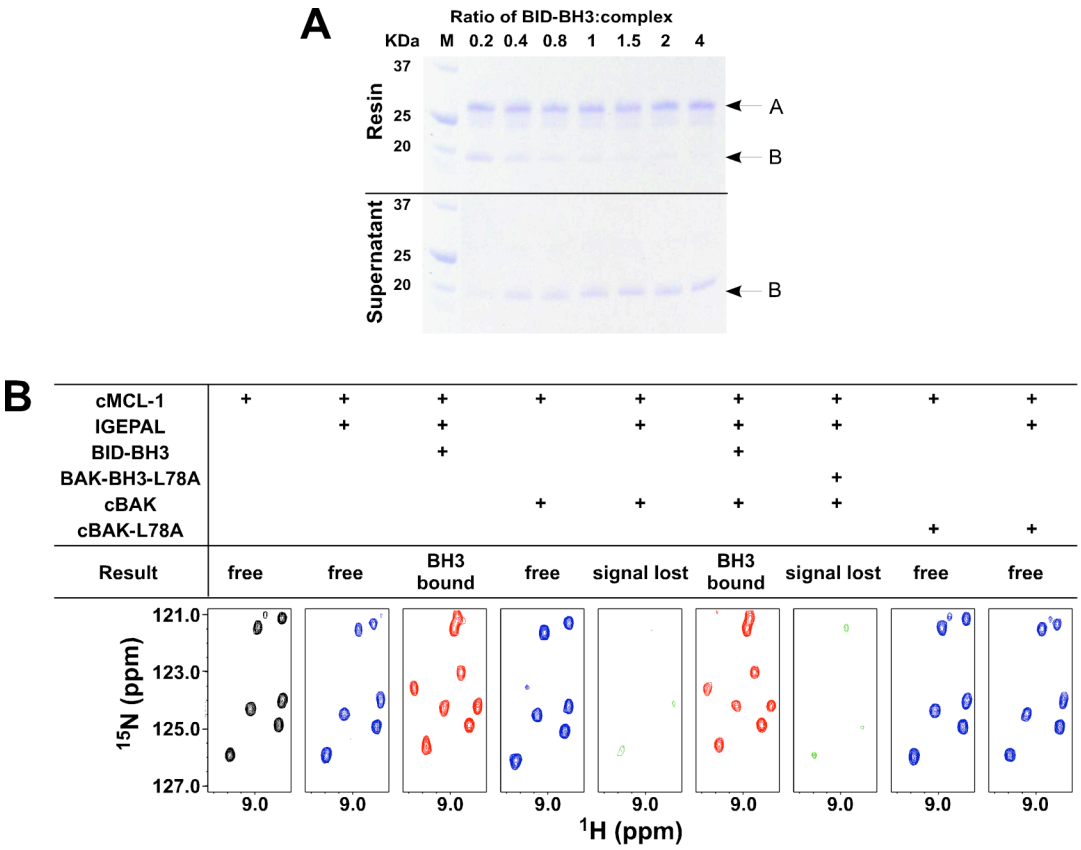

Figure 4.8: BID-BH3 peptide disrupts the complex of BAK:MCL-1. (A) Coomassie-stained SDS-gels showing the results of the competition assay. Upper gel shows proteins that were pulled down by the Ni^{++}-NTA resin, and the lower gel shows proteins that remained in the supernatant. The numbers above the gel show the ratio of BID-BH3 peptide to Flag-BAK-HMK-ΔTM-His_6:cMCL-1 complex when added for competition. The arrow with A show the position of Flag-BAK-HMK-ΔTM-His_6, and arrows with B show the positions of cMCL-1. (B) Slices of ^{1}H-^{15}N HSQC spectra (bottom) of ^{15}N-labeled cMCL-1 in different conditions as shown in the table (Spectrum for free cMCL-1: black, spectra with little chemical shifts: blue, spectra with significant changes: pink, and spectra with signals disappeared: green).

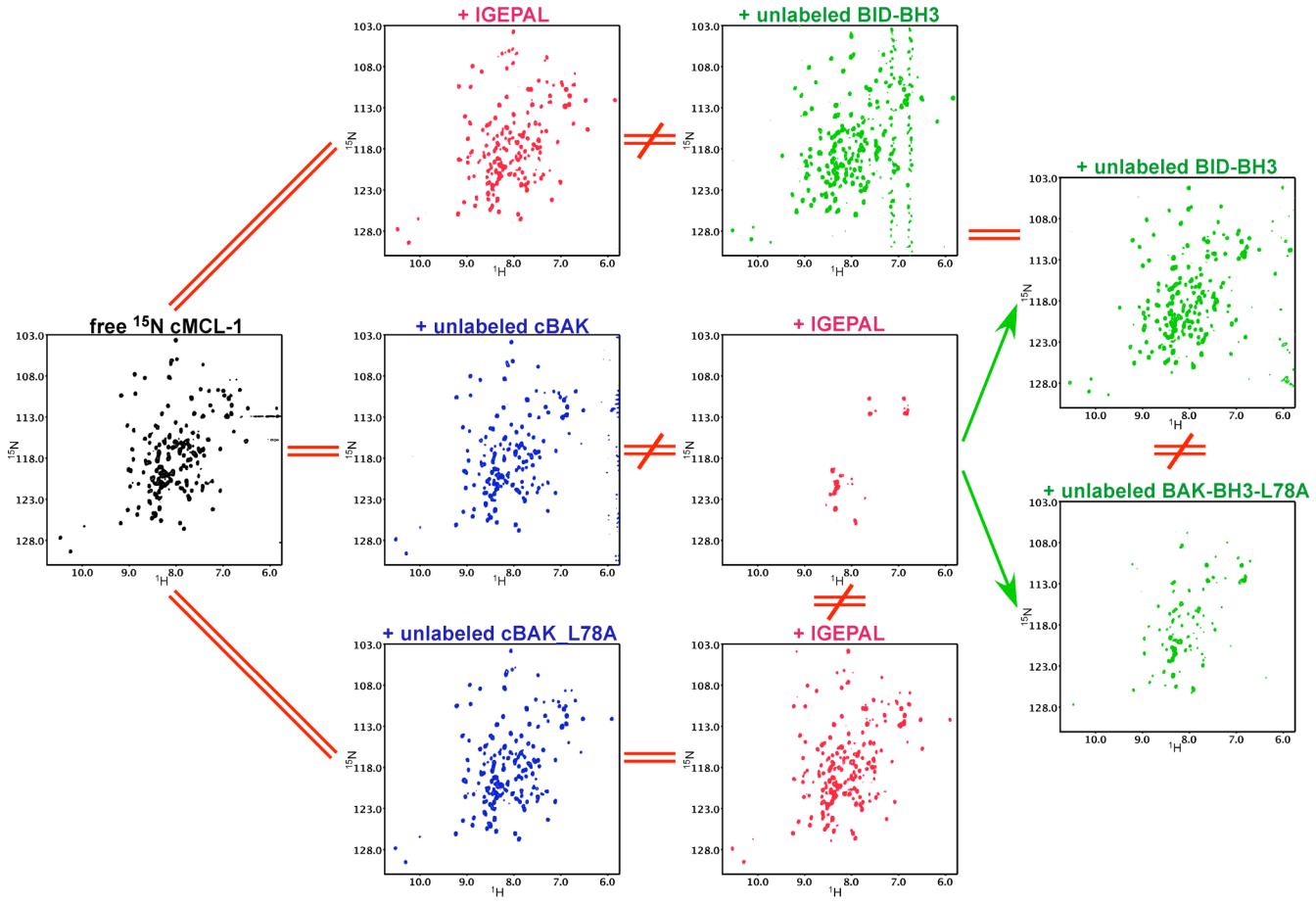

Figure 4.9: NMR titrations in IGEPAL. ^{1}H-^{15}N HSQC spectra are shown of free ^{15}N-labeled cMCL-1 (black), in 0.1% IGEPAL (red), with wild-type and mutant L78A cBAK protein (blue), and with competing BH3 peptides BID-BH3 and BAK-BH3-L78A (green).

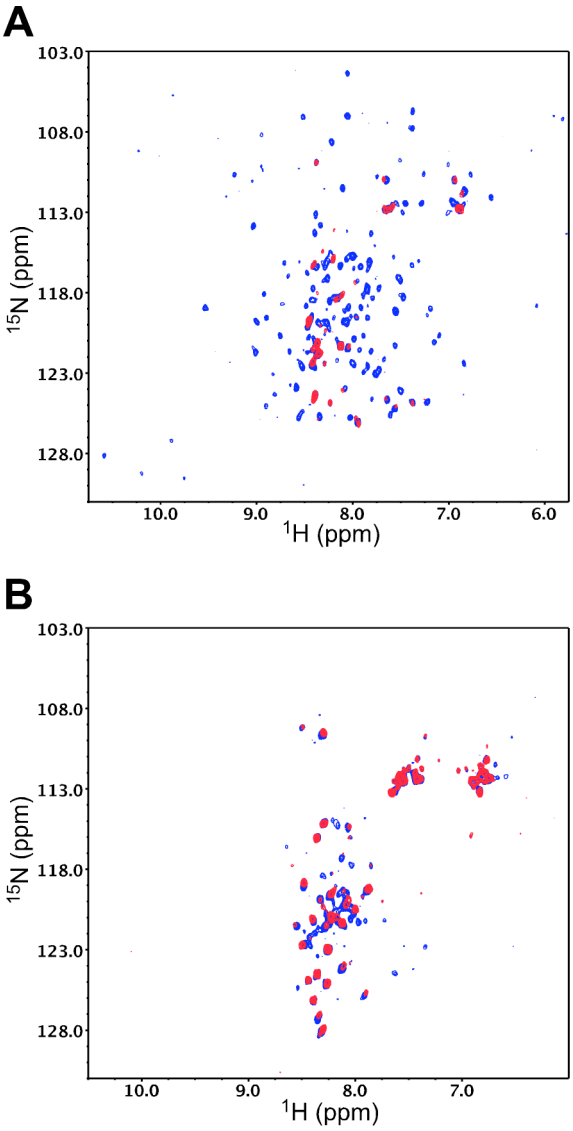

Figure 4.10: NMR titrations in CHAPS. (A) Overlay of ^{1}H-^{15}N HSQC spectra of complex ^{15}N-cMCL-1:unlabeled-cBAK in 2% CHAPS without (red) and with unlabeled BID-BH3 peptide (blue).

4.4 Discussion

BAX and BAK are the major pro-apoptotic effectors that undergo conformational changes and oligomerization to mediate MOMP (Lindsten et al., 2000; Wei et al., 2001). To gain insight into this process, detergents have been used to mimic in the protein's native membrane environment. These studies have shown that BAX can be specifically activated by detergents to form higher-order aggregates (Hsu and Youle, 1998; Ivashyna et al., 2009; Kuwana et al., 2002). Here, we describe BAK's behavior in the presence of detergents. The nonionic detergent IGEPAL (0.1%) induced large changes in the spectrum of BAK (Figure 4.2E), which likely reflects the formation of large complexes as observed for BAX in Triton X-100 (Hsu and Youle, 1997, 1998) and dodecyl-β-D-maltoside (Bleicken et al., 2010). Due to the large size of IGEPAL micelle, which is around 90 kDa and equivalent to a BAK tetramer, it is hard to determine the BAK oligomeric state in this high molecular complex. In contrast, the conformation of BAK was not markedly affected by the zwitterionic detergent CHAPS (2%). Only minor perturbations were detected in the spectrum of BAK (Figure 4.4) even after overnight incubation (Figure 4.4B), which indicates that BAK maintains its global fold with changes restricted to the residues surrounding its putative BH3-binding hydrophobic groove. This result is consistent with reports that CHAPS has little effect on BAX oligomerization (Ivashyna et al., 2009).

In this chapter, we also showed that the anti-apoptotic protein MCL-1 undergoes only minor conformational changes in both detergents as revealed by the small changes in the protein NMR spectrum (Figure 4.2A, 4.2B, 4.2C, 4.3A, 4.3B and 4.3C) and its behavior in size-exclusion chromatography (Figure 4.2D). Similar results were observed for BCL-X_L and BCL-w at concentration of detergents below the CMC, however, BCL-X_L and BCL-w both displayed abrupt spectral changes in concentration of detergents above the CMC (Denisov et al., 2006; Losonczi et al., 2000). This is similar to the behavior we observed for BAK in the

presence of IGEPAL and suggests that resistance to detergent-induced unfolding is not a general feature of anti-apoptotic proteins.

At the level of protein-protein interactions, both IGEPAL and CHAPS were able to promote the association of BAK with MCL-1 (Figure 4.5 and 4.6). To our knowledge, this is the first time the interaction between the intact protein domains has been characterized in vitro. By peptide competition and site-directed mutagenesis, we show that the interaction involves the BH3 region of BAK and the hydrophobic groove of MCL-1 (Figure 4.8, 4.9 and 4.10). The absence of binding without detergent suggests that the BAK:MCL-1 interaction requires the exposure and accessibility of BH3 region in BAK. This is relatively easy to imagine in the case of IGEPAL, where we observe large conformational changes in BAK. CHAPS does not strongly perturb the structure of BAK but likely increases the internal dynamics and decreases the energy barrier for the exposure of the BH3 region. Interestingly, the affinity of BAK for MCL-1 appeared to be less than the affinity of the isolated BAK-BH3 peptide; BAK was efficiently removed by BID-BH3, which has weaker affinity than BAK-BH3 (Figure 4.7B). This suggests that the BH3 region of BAK is not fully accessible in the presence of detergents. This could be due to residual folding, steric hinderance due to the detergent micelles, or competing intramolecular interactions such as observed for MCL-1 where longer constructs display lower affinity than the core cMCL-1 domain (chapter 2).

Our data add valuable information for evaluating the existing models of BAK activation. Taking a look at CAM and DAM in Figure 4.1, we note that both models agree on the interaction between MCL-1 (anti-apoptotic proteins) and BID (BH3-only pro-apoptotic proteins). The difference between these two models centers on whether MCL-1 or BID directly interact with BAK. Our data show that MCL-1 interacts not only with BH3-only proteins as represented by the structures of complexes of MCL-1 with BH3 peptides (Czabotar et al., 2007; Day et al., 2008; Fire et al., 2010; Qian Liu, 2010) but also with BAK. Thus, the function of MCL-1 is not limited to the inhibition of BH3-only proteins, and DAM does not

encompass the whole regulatory pathway. Second, the interaction between BAK and MCL-1 is conditional on the exposure of BAK's BH3 region, thus BAK is not necessarily always kept in check by anti-apoptotic proteins. How free BAK could be initiated to promote apoptosis is not addressed by CAM. In addition to direct activation through BH3-only proteins (especially the BH3-only activators tBID, BIM, and PUMA) in DAM (Kim et al., 2009), our observation of a complex of MCL-1:BAK in CHAPS suggests that any means such as membrane targeting or alignment might activate BAK toward either MOMP or inhibition by anti-apoptotic proteins. Thus, we propose this hybrid activating model (Figure 4.11): BAK can be activated by either the BH3-only activators or other factors (e.g. membrane alignment) that cause conformational changes; MCL-1 interacts with both BH3-only proteins and BAK that has its BH3 region accessible. While our study has been limited to studying the proteins in the presence of membrane mimics, we believe that the requirement for accessibility of the BAK BH3 applies to BAK and MCL-1 in their native environment.

Our finding that a BID-BH3 peptide can displace BAK from MCL-1 highlights the potential therapeutic use of compounds that bind to MCL-1. The disruption of the MCL-1:BAK complex is a critical step to stimulate cells to undergo apoptosis. As an alternative to the well-known tumor suppressor p53 that can disrupt complex formation by binding to BAK (Leu et al., 2004), our data show that the success of BID-BH3 and the failure of BAK-BH3-L78A to displace BAK from its complex with MCL-1 are dependent on their binding affinities to MCL-1 (Figure 4.8B and 4.10A). This is consistent with the finding that obatoclax (GX15-070) is able to overcome MCL-1 mediated resistance to apoptosis (Nguyen et al., 2007; Zhai et al., 2006) while ABT-737 fails to do so (Chen et al., 2007; Oltersdorf et al., 2005; van Delft et al., 2006). Our data suggest the need for high-affinity small molecule inhibitors that target MCL-1. As BAK once released from the complex exists in an unfolded conformation (Figure 4.10B) and may readily be able to undergo oligomerization to promote apoptosis, the therapeutic use of MCL-1 inhibitors should be particularly effective in transiting cells into apoptosis.

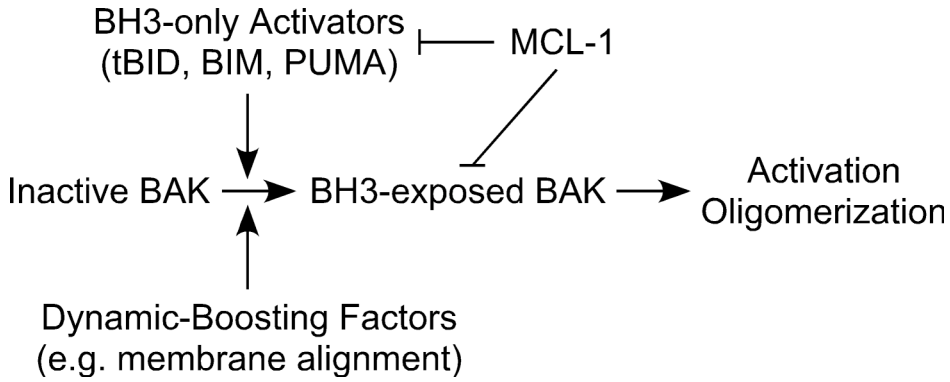

Figure 4.11: Hybrid activating model for BAK activation. Inactive BAK can get initiated for conformational changes by either the BH3-only activators or the dynamic-boosting factors (e.g. membrane alignment), and the inhibition of MCL-1 is performed by interacting with both BH3-only proteins and BH3-accessible BAK.

4.5 Materials and methods

4.5.1 Protein expression and purification

Flag-BAK-HMK-ΔTM-His_6 (residue 2-186 from NCBI:AAA74466), calpain-proteolysed BAK (cBAK, residue 16-186 from NCBI:AAA74466), cBAK-L78A, core domain of MCL-1 (also calpain-proteolysed MCL-1, cMCL-1, residue 163-326 from NCBI:AAF64255) and BID-BH3 peptide (residue 76-106 from NCBI:NP_001187 with four extra residues on N-terminus GPLG) were purified as previously described (Denisov et al., 2006; Moldoveanu et al., 2006; Qian Liu, 2010). *E. coli* strain BL21 (DE3) containing the corresponding plasmid was grown in LB media at 37˚C to an optical density of 0.8 at 600 nm, and then induced by 1 mM isopropyl-*β*-D-thiogalactoside (IPTG) at 30˚C for 4 hours. For NMR samples, cells were grown in M9 media supplemented with ^{15}N ammonium chloride. The soluble proteins were purified by batch Ni-NTA or GST affinity chromatography (Qiagen), followed by Sephadex G-75 size exclusion chromatography (GE healthcare) and Q-Sepharose anion-exchange chromatography (GE healthcare). A calpain digestion step was further applied to produce cBAK, cBAK-L78A, and cMCL-1, and calpain was removed by Q-Sepharose anion-exchange chromatography. BAK-BH3 (TMGQVGRQLAIIGDDINRRY) and BAK-BH3-L78A (TMGQVGRQAAIIGDDINRRY) peptides were chemically synthesized (Sheldon Biotechnology Centre, McGill University) and purified on a C18 reverse-phase column. All proteins and peptides were stored in 20 mM HEPES (pH 6.5), 1 mM DTT buffer by flash freezing in liquid nitrogen and stored at -80˚C.

4.5.2 Site-directed mutagenesis

The mutation L78A in the BH3 region of BAK was generated using the QuikChange Site-Directed Mutagenesis Kit (Stratagene) according to

manufacturer's manual. The mutagenesis was carried out by using Flag-BAK-HMK-ΔTM-His_6 in pET29b(+) plasmid as a template, and using oligonucleotides (CAGGTGGGACGGCAGGCCGCCATCATCGGGGAC) and (GTCCCCGATGATGGCGGCCTGCCGTCCCACCTG) as PCR primers. The construct was confirmed by DNA sequencing.

4.5.3 Analytical size exclusion chromatography

cMCL-1, cBAK, and the mixture of cMCL-1 and cBAK were prepared at 2 mg/ml (for the mixture, the concentration for each protein is 2 mg/ml) in 20 mM HEPES (pH 6.5), 1 mM dithiothreitol (DTT) and with or without 0.1% IGEPAL. The size exclusion running buffer contained 25 mM HEPES (pH 6.5), 150 mM NaCl, 1 mM DTT and with or without 0.1% IGEPAL. A 30 µl sample was injected for Superdex 200 PC (3.2/30) analytical runs. The chromatographs were recorded and analyzed on Waters Millenium HPLC software.

4.5.4 Ni^{++}-NTA pull-down assay

Three buffers: buffer N, buffer W and buffer E, each containing 50 mM Tris (pH 6.8), 500 mM NaCl, 1% glycerol, 1 mM NaN_3, with the addition 10 mM or 30 mM or 250 mM imidazole respectively were used in pull-down assays. Detergents were added as indicated. The Ni^{++}-NTA resin was first equilibrated with buffer N and excess buffer removed to optain a 50:50 (resin:buffer) slurry. To 50 µl of this slurry, 50 µl of 1 mg/ml Flag-BAK-HMK-ΔTM-His_6, cMCL-1, or a 1:1 mixture of Flag-BAK-HMK-ΔTM-His_6:cMCL-1 were applied in the presence of different concentrations of IGEPAL or 3-[(3-cholamidopropyl) dimethylammonio]-1-propanesulfonic acid (CHAPS) as indicated. After an incubation time of 30 minutes at room temperature, the slurry was spin down at 7,000 rpm for 30 seconds and the supernatant was removed. The resin in the pellet was washed three times with 500 µl of buffer W and eluted with 45 µl of buffer E. The elution was then mixed with 15 µl of 4× SDS buffer for SDS-PAGE analysis. For BID-

BH3 peptide competition assays, all the buffers contained 0.1% IGEPAL. The Flag-BAK-HMK-ΔTM-His_6:cMCL-1 complex was first immobilized on Ni^{++}-NTA resin, and then the resin slurry prepared similarly. A range of BID-BH3 peptide concentrations were applied to the resin slurry followed by incubation for 30 minutes at room temperature, centrifugation at 7,000 rpm for 30 seconds and removal of the supernatant. The resin was washed three times with buffer W and eluted with buffer E. The elution and supernatant were then mixed with 4× SDS buffer and analyzed by SDS-PAGE.

4.5.5 Isothermal titration calorimetry (ITC) measurements

ITC was carried out on a MicroCal VP-ITC titration calorimeter controlled by the VPViewer software (MicroCal Inc., Northampton, MA). Experiments were performed in 50 mM Na·HEPES (pH 7.0) at 23˚C and consisted of 37 injections of 8 μl of 0.1 mM BAK-BH3 or BAK-BH3-L78A peptide into 1.45 ml of 0.01 mM human MCL-1 (four different constructs) to obtain a final peptide/protein ratio of 2:1. The calorimetric data were analyzed by ORIGIN software to determine thermodynamic binding constants.

4.5.6 NMR titrations

NMR titrations were carried on ^{15}N-labeled cMCL-1 or ^{15}N-labeled cBAK. Aliquots of unlabeled binding partners such as cMCL-1, cBAK, cBAK-L78A, BID-BH3, BAK-BH3-L78A, IGEPAL, and CHAPS stock solutions were titrated in until the saturation was achieved. The ^{1}H-^{15}N HSQC spectra were recorded on a Bruker Avance DRX600 MHz spectrometer, processed by NMRPipe (Frank Delaglio, 1995) and visualized by NmrViewJ 8.0 (Johnson and Blevins, 1994). Changes in chemical shifts of amide signals (calculated as $((\Delta^{1}\text{H ppm})^2 + (0.2 \times \Delta^{15}\text{N ppm})^2)^{0.5}$) were plotted as a function of the residue number and mapped onto the 3D structures. The structure model for free human cMCL-1 was calculated by

Modeller 9v2 (Sali and Blundell, 1993) based on the free mmMCL-1 structure 1WSX (Day et al., 2005).

4.6 Acknowledgement

This work was supported by Canadian Institutes of Health Research grant MOP-81277. We would like to acknowledge GeminX for providing us the human Flag-BAK-HMK-ΔTM-His_6 and human MCL-1 expressing plasmids. We also thank Dr. Tudor Moldoveanu for generously sharing the calpain expression plasmid and cBAK backbone NMR assignments.

Chapter 5

Possible Regulatory Models for BAK's Activition

Q. Liu and K. Gehring (manuscript in preparation).

This following chapter serves as the thesis summary. It combines the results from chapter 2-4, speculates on the possible regulatory mechanisms for BAK-mediated MOMP, and describes future works to continue.

5.1 Prologue

Apoptosis, the process of programmed cell death in multicellular organisms, plays a vital role in cell turnover, homeostasis, and development (Opferman and Korsmeyer, 2003; Vaux and Korsmeyer, 1999). Defects in apoptosis are implicated in a variety of diseases, including cancer (Fesik, 2000). The BCL-2 family of proteins is central to the apoptotic regulation at mitochondria. They control the integrity of MOM (Chipuk et al., 2010); however, the detailed regulatory mechanisms remain unclear. In this thesis, using NMR spectroscopy, X-ray crystallography, isothermal titration calorimetry, gel-filtration chromatography, pull-down experiments, and mitochondrial activity assays, we developed some insights into the regulation. A summary of the findings and further discussion of possible regulatory models follow.

5.2 Summary of results

5.2.1 Successful screening for constructs and experimental conditions

Proper constructs are of great importance for the successes in protein expression, purification, and further structural studies. In this thesis, we developed constructs and purification protocols for three proteins BAK, MCL-1 and BID. The use of limited proteolysis by calpain helped remove the terminal unfolded portions from the expressed constructs. Calpain was also used to cleave the unfolded loop region in BID to activate this proapoptotic protein. The development of these protocols will definitely facilitate the research for these proteins.

Detergents have been widely used in the studies on membrane-targeted proteins to mimic the membrane environment (Fiedler et al., 2010), and also have been used for research on BAX (Hsu and Youle, 1997, 1998), BCL-X_L (Losonczi et al., 2000) and BCL-w (Denisov et al., 2006). Here, we described the detailed conditions for studies on BAK. In brief, the concentrations of the detergents

should be above their CMCs to provide micelles, for example 0.1% for IGEPAL and 2% for CHAPS. CHAPS is more suitable for studies on BAK, due to the small size of its micelle, little effects on BAK's α-helical conformation, and its success in promoting the interaction between BAK and MCL-1. The application of CHAPS will help to reveal more features of BAK.

5.2.2 Conformations of BAK

In this thesis, we identified five possible conformations for BAK: one monomer, two homo-dimers, one hetero-dimer, and one unfolded form.

Purified cBAK is a monomer as shown by size-exclusion chromatography. Although the two crystal structures are both homo-dimers, at the monomer level they are almost identical. BAK adopts a conserved α-helical fold as observed for other BCL-2 members. This allows its transmembrane region to be tail-anchored in MOM (Figure 5.1C). The monomer structure presents an hydrophobic groove, which is blocked by the side-chains of R88 and Y89, and prevent a direct interaction with BH3 peptides. Additionally, the novel site for BH3-binding, observed in BAX (Gavathiotis et al., 2008), is also unavailable in BAK. The extended side chains of E32, R36, P64 and R156 and the formation of helix α2 (which is an unfolded loop region in other BCL-2 homologs) form another obstruction for BAK to be a BH3-acceptor.

The two crystal structures revealed two distinct homo-dimerization sites. In the zinc-mediated dimer (Figure 5.1B), D160 and H164 coordinate a zinc ion in a tetrahedral geometry to form a symmetric dimerization interface running along the surfaces formed by BAK helices α4 and α6. In the disulfide-bond linked dimer (Figure 5.1A), dimerization is dependent on the oxidation between two cysteine residues (C166) from each monomer. These two adjacent dimerizing sites revealed an activity-sensor for the regulation of BAK. As shown by cyt c release assays, zinc inbibits BAK's activity and oxidation releases BAK from zinc inhibition.

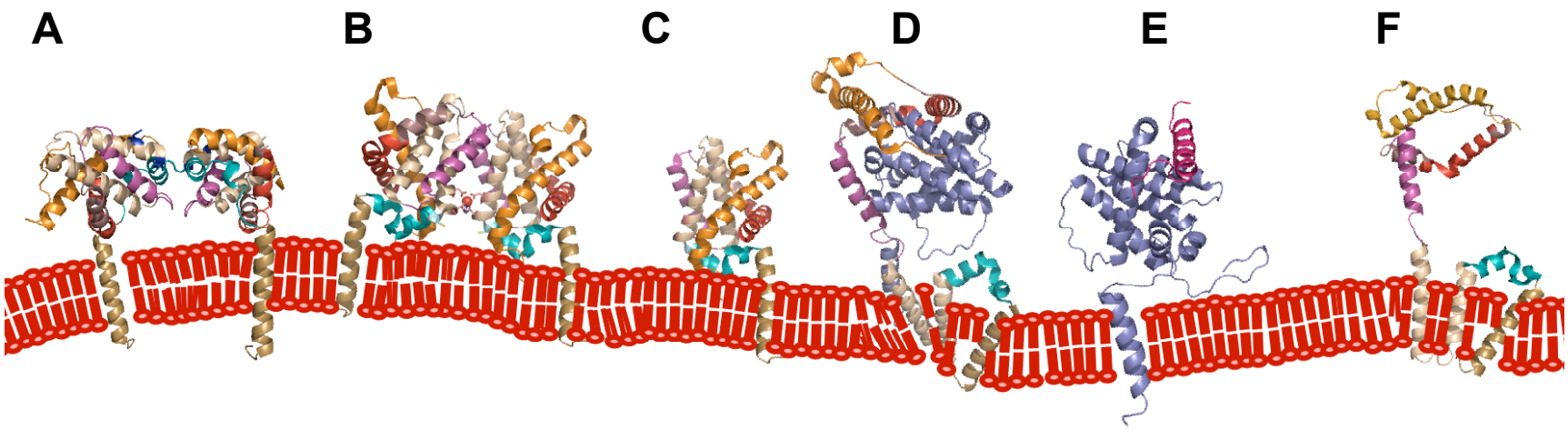

Figure 5.1: Possible conformations for BAK and MCL-1 with their TM regions. (A) Disulfide-bond linked BAK homo-dimer. (B) Zinc-mediated BAK homo-dimer. (C) MOM tail-anchored BAK monomer. (D) Complex of MCL-1:BAK. (E) Complex of MCL-1:BID-BH3. (F) Unfolded BAK released from complex with MCL-1 by BID-BH3. Among these conformations of BAK, (A) (C) and (F) are active, while (B) and (D) revealed inactive forms.

We also observed a conformation in which the BAK BH3 region is engaged in the hydrophobic groove of MCL-1 (Figure 5.1D). This hetero-dimer provides the most direct proof of the mechanism of BAK's inhibition by MCL-1. The BID-BH3 peptide, which has high affinity to MCL-1, can easily disrupt the complex of MCL-1:BAK through binding MCL-1 (Figure 5.1E). The released BAK from the complex exists in an unfolded conformation (Figure 5.1F), which may undergo oligomerization and permeablize MOM. The success of BID-BH3 peptide to compete with BAK for binding to MCL-1 gives hope that small-molecule BH3 mimetics can be used to initiate apoptosis in tumor cells.

5.2.3 Hetero-dimers of MCL-1

In addition to the hetero-dimerization with BAK in detergents, we determined the selectivity of MCL-1 in binding BH3 peptides derived from BH3-only proteins. By ITC and NMR titrations, we showed that MCL-1 has strong preference for binding BIM, Noxa, MULE and BID. We also detected the protein-protein interaction between MCL-1 and truncated BID *in vitro*, which is similar to the interaction between MCL-1 and BID-BH3 peptide. The structure of the complex of MCL-1 and BID-BH3 (2KBW) was further solved by NMR spectroscopy (Figure 5.1E). This structural information not only helped to understand the docking of BID-BH3 in the hydrophobic pocket of MCL-1, but also provided explanations for the failure of MCL-1 to bind ABT-737. The pocket formed by F228, M231 and F270 in MCL-1 blocks the chloral-biphenyl group, and the side-chain of V216 results in a spatial restriction to the engagement of the nitrophenyl and the thiophenyl groups of ABT-737. Thus our complex structure may facilitate the screening and designing for MCL-1 targeted small molecule inhibitors.

5.3 Discussion of possible regulatory mechanisms

5.3.1 Mini-system

The BCL-2 members share some conserved features across the whole family and others across smaller sub-groups; however, each member brings its specific character to perform its non-redundant biological functions. We are not aiming to develop a perfect regulatory model suitable for the whole diverse family. Even for one protein, there are multiple leves of regulation. Accordingly, we define a mini-system consisting of BAK, MCL-1, and BID in order to discuss possible regulatory mechanisms for BAK. At the same time, we believe that an understanding of the regulation of BAK will shed light on the mechanisms of regulation of other BCL-2 members.

5.3.2 N-terminus inhibition for BAK

The disordered N-terminal sequence of BAK plays a negative role in regulating its cyt c release activity (Griffiths et al., 1999; Ruffolo and Shore, 2003). Our results in protein purification and mitochondria assays showed strong consistency with previous studies. N-terminal capping by FLAG or MEAS sequence allowed BAK's high-level expression and also prevented BAK-mediated cyt c release from mitochondria. Deletion of the N-terminal by either subcloning or calpain digestion resulted, respectively, in lack of expression and greatly increased cyt c release activity. Although the N-terminal truncation cannot alone initiate the cyt c release, it appears to be an important element in regulating BAK's activity.

5.3.3 A redox sensory as an activity-switch for BAK

BAK monomer may normally be tail-anchored in MOM through its TM region, with its cytosolic N-terminal domain adopting an α-helical bundle conformation (2IMT) (Figure 5.1C). In response to local signals (either high local zinc

concentration or oxidation pressure), BAK may form homo-dimers. The zinc-mediated dimer is inactive in permeablizing MOM and releasing cyt c from mitochondria (Figure 2.6), while the oxidized dimer shows activity comparable to the monomer, but with more resistence to inhibition by zinc. These indicate that the zinc-binding site (D160 and H164) might play an important role in controling BAK's activity and that the active –SH (in C166) is vital in regulating zinc binding and oxidation. These residues may form a specific regulatory sensor. When zinc is bound, the activity is turned off; oxidation provides a natural way to escape from zinc inhibition.

Since the publication of cBAK crystal structure, the studies on BAK activation have been largely stimulated. Ruth M. Kluck and her colleagues proposed a new model, which involves homo-dimerization via BH3:groove interactions (Dewson et al., 2008) and oligomerization via the α6:α6 interactions (Dewson et al., 2009). They observed that the formation of the α6:α6 interface doesn't require the zinc-binding site, and only occurs during BAK pro-apoptotic oligomerization. This supports our claim that the zinc-mediated homo-dimer is only implicated in inactive forms. On the other hand, they argued against the physiological role for zinc in directly regulating BAK function with following evidence: the failure of zinc-site mutagenesis to alter BAK function in cells, and the supraphysiological zinc levels required for inhibition *in vitro*. We would note that we observed the zinc inhibition in BAK-mediated cyt *c* release not only for exogenous cBAK, but also for endogenous BAK from $BAX^{-/-}$ cells at 10-fold lower zinc level (0.5 μM). Cyt *c* release by zinc binding-site mutants, reported in Dewson et al. 2009, also displayed some increased zinc resistance (Figure 4D in Dewson et al. 2009). As for the physiological concentration of free zinc, we note that although typically in the pico- or nano-molar ranges, time- or location-dependent fluctuations may be used to control biological functions (Colvin et al., 2010). Altogether, while we still believe the distinct effects of zinc in BAK regulation, further studies are required. For example, studies in $BAK^{-/-}/BAX^{-/-}$ cells could examine transfected forms of BAK that adopt conformations similar to the zinc-dimer or disulphide-

dimer. Detecting the activities of these mutant forms would more clearly delineate the roles of the different BAK dimers in mediating cyt *c* release and cell death.

5.3.4 Inhibition from MCL-1 and activation by cBID or BID-BH3

Our results from mitochondria assays clearly showed BAK's cyt c release activity could be inhibited by MCL-1 and activated by cBID. These results are consistent with the literature (Dunkle et al., 2010). However, this functional information cannot help us to answer how BAK is activated. The argument between CAM and DAM continues due to the failure in detecting the vital protein-protein interactions and in determining the order in which they proceed. In this thesis, we reported a conditional interaction between MCL-1 and BAK protein, which is dependent on the exposure of the BH3 region of BAK. Meanwhile, we also observed the protein-protein interaction between MCL-1 and cBID and the displacement of BAK from the complex of MCL-1:BAK by a BID-BH3 peptide. These data provided strong support for CAM, but also reveal its failure to explain how conformational changes of BAK are initiated. Although our BAK structure doesn't allow for the direct binding of a BID-BH3 peptide, we cannot exclude the possibility of the direct activation by tBID on BAK in light of the growing evidence for that mechanism (Kim et al., 2009). Thus, we propose a hybrid activating model: BAK can be activated by either the BH3-only activators or other factors (e.g. membrane alignment) that cause conformational changes; MCL-1 interacts with both BH3-only proteins and BAK that has its BH3 region accessible (Figure 4.11). This model not only combines the two popular models but also introduces crosstalk between them.

5.4 Future works

The selectivity of MCL-1 in binding BH3-only proteins was studied in this thesis using a panel of BH3-peptides. It provided deep insights into MCL-1 regulation, but still needs to be validated in live cells for a complete understanding, which

should facilliate the screening for drugs that specifically target MCL-1 and inhibits its function. The regulatory model of BAK and MCL-1 raised in my thesis is based on the *in vitro* data using truncated proteins, and therefore needs to be further proved *in vivo* or in native membrane environment using full-length proteins. Meanwhile, the conformation of BAK in high-order oligomer would display vital clues for the BAK-mediated pore formation and MOMP. Small angle X-ray spectroscopy (SAXS) and fluorescent techniques should be useful to examine the conformation of large molecules and the conformational changes of BAK upon activation.

5.5 Epilogue

Overall, this thesis reports the solution structure of the complex of cMCL-1:BID-BH3 and two crystal structures of BAK. I have studied protein-protein interactions between MCL-1 and cBID and between MCL-1 and BAK. This has lead to the development of a hybrid model for BAK activation. These structural studies provide insights into the regulatory mechanisms for BCL-2 family, and should facilitate the development of novel BH3 mimetics as small-molecule inhibitors of apoptosis.

References

Alvi, A.J., Austen, B., Weston, V.J., Fegan, C., MacCallum, D., Gianella-Borradori, A., Lane, D.P., Hubank, M., Powell, J.E., Wei, W., et al. (2005). A novel CDK inhibitor, CYC202 (R-roscovitine), overcomes the defect in p53-dependent apoptosis in B-CLL by down-regulation of genes involved in transcription regulation and survival. Blood 105, 4484-4491.

Amundson, S.A., Myers, T.G., Scudiero, D., Kitada, S., Reed, J.C., and Fornace, A.J., Jr. (2000). An informatics approach identifying markers of chemosensitivity in human cancer cell lines. Cancer Res 60, 6101-6110.

Antonsson, B. (2001). Bax and other pro-apoptotic Bcl-2 family "killer-proteins" and their victim the mitochondrion. Cell Tissue Res 306, 347-361.

Antonsson, B., Montessuit, S., Lauper, S., Eskes, R., and Martinou, J.C. (2000). Bax oligomerization is required for channel-forming activity in liposomes and to trigger cytochrome c release from mitochondria. Biochem J 345 Pt 2, 271-278.

Antonsson, B., Montessuit, S., Sanchez, B., and Martinou, J.C. (2001). Bax is present as a high molecular weight oligomer/complex in the mitochondrial membrane of apoptotic cells. J Biol Chem 276, 11615-11623.

Apte, S.S., Mattei, M.G., and Olsen, B.R. (1995). Mapping of the human BAX gene to chromosome 19q13.3-q13.4 and isolation of a novel alternatively spliced transcript, BAX delta. Genomics 26, 592-594.

Ashkenazi, A. (2002). Targeting death and decoy receptors of the tumour-necrosis factor superfamily. Nat Rev Cancer 2, 420-430.

Bae, J., Leo, C.P., Hsu, S.Y., and Hsueh, A.J. (2000). MCL-1S, a splicing variant of the antiapoptotic BCL-2 family member MCL-1, encodes a proapoptotic protein possessing only the BH3 domain. J Biol Chem 275, 25255-25261.

Barry, M., Heibein, J.A., Pinkoski, M.J., Lee, S.F., Moyer, R.W., Green, D.R., and Bleackley, R.C. (2000). Granzyme B short-circuits the need for caspase 8 activity during granule-mediated cytotoxic T-lymphocyte killing by directly cleaving Bid. Mol Cell Biol 20, 3781-3794.

Batistatou, A., Merry, D.E., Korsmeyer, S.J., and Greene, L.A. (1993). Bcl-2 affects survival but not neuronal differentiation of PC12 cells. J Neurosci 13, 4422-4428.

Black, D.L. (2000). Protein diversity from alternative splicing: a challenge for bioinformatics and post-genome biology. Cell 103, 367-370.

Bleicken, S., Classen, M., Padmavathi, P.V., Ishikawa, T., Zeth, K., Steinhoff, H.J., and Bordignon, E. (2010). Molecular details of Bax activation, oligomerization, and membrane insertion. J Biol Chem 285, 6636-6647.

Boise, L.H., Gonzalez-Garcia, M., Postema, C.E., Ding, L., Lindsten, T., Turka, L.A., Mao, X., Nunez, G., and Thompson, C.B. (1993). bcl-x, a bcl-2-related gene that functions as a dominant regulator of apoptotic cell death. Cell 74, 597-608.

Bonzon, C., Bouchier-Hayes, L., Pagliari, L.J., Green, D.R., and Newmeyer, D.D. (2006). Caspase-2-induced apoptosis requires bid cleavage: a physiological role for bid in heat shock-induced death. Mol Biol Cell 17, 2150-2157.

Bouillet, P., Huang, D.C., O'Reilly, L.A., Puthalakath, H., O'Connor, L., Cory, S., Adams, J.M., and Strasser, A. (2000). The role of the pro-apoptotic Bcl-2 family member bim in physiological cell death. Ann N Y Acad Sci 926, 83-89.

Breckenridge, D.G., Germain, M., Mathai, J.P., Nguyen, M., and Shore, G.C. (2003). Regulation of apoptosis by endoplasmic reticulum pathways. Oncogene 22, 8608-8618.

Brunelle, J.K., Shroff, E.H., Perlman, H., Strasser, A., Moraes, C.T., Flavell, R.A., Danial, N.N., Keith, B., Thompson, C.B., and Chandel, N.S. (2007). Loss of Mcl-1 protein and inhibition of electron transport chain together induce anoxic cell death. Mol Cell Biol 27, 1222-1235.

Brunger, A.T., Adams, P.D., Clore, G.M., DeLano, W.L., Gros, P., Grosse-Kunstleve, R.W., Jiang, J.S., Kuszewski, J., Nilges, M., Pannu, N.S., et al. (1998). Crystallography & NMR system: A new software suite for macromolecular structure determination. Acta Crystallogr D Biol Crystallogr 54, 905-921.

Cartron, P.F., Gallenne, T., Bougras, G., Gautier, F., Manero, F., Vusio, P., Meflah, K., Vallette, F.M., and Juin, P. (2004). The first alpha helix of Bax plays a necessary role in its ligand-induced activation by the BH3-only proteins Bid and PUMA. Mol Cell 16, 807-818.

Cartron, P.F., Oliver, L., Martin, S., Moreau, C., LeCabellec, M.T., Jezequel, P., Meflah, K., and Vallette, F.M. (2002). The expression of a new variant of the pro-apoptotic molecule Bax, Baxpsi, is correlated with an increased survival of glioblastoma multiforme patients. Hum Mol Genet 11, 675-687.

Cavanagh, J. (1996). Protein NMR spectroscopy : principles and practice (San Diego: Academic Press).

Cavarretta, I.T., Neuwirt, H., Untergasser, G., Moser, P.L., Zaki, M.H., Steiner, H., Rumpold, H., Fuchs, D., Hobisch, A., Nemeth, J.A., and Culig, Z. (2007). The antiapoptotic effect of IL-6 autocrine loop in a cellular model of advanced prostate cancer is mediated by Mcl-1. Oncogene 26, 2822-2832.

Certo, M., Del Gaizo Moore, V., Nishino, M., Wei, G., Korsmeyer, S., Armstrong, S.A., and Letai, A. (2006). Mitochondria primed by death signals determine cellular addiction to antiapoptotic BCL-2 family members. Cancer Cell 9, 351-365.

Chang, B.S., Minn, A.J., Muchmore, S.W., Fesik, S.W., and Thompson, C.B. (1997). Identification of a novel regulatory domain in Bcl-X(L) and Bcl-2. EMBO J 16, 968-977.

Chauhan, D., Velankar, M., Brahmandam, M., Hideshima, T., Podar, K., Richardson, P., Schlossman, R., Ghobrial, I., Raje, N., Munshi, N., and Anderson, K.C. (2007). A novel Bcl-2/Bcl-X(L)/Bcl-w inhibitor ABT-737 as therapy in multiple myeloma. Oncogene 26, 2374-2380.

Chen, L., Willis, S.N., Wei, A., Smith, B.J., Fletcher, J.I., Hinds, M.G., Colman, P.M., Day, C.L., Adams, J.M., and Huang, D.C. (2005). Differential targeting of prosurvival Bcl-2 proteins by their BH3-only ligands allows complementary apoptotic function. Mol Cell 17, 393-403.

Chen, M., He, H., Zhan, S., Krajewski, S., Reed, J.C., and Gottlieb, R.A. (2001). Bid is cleaved by calpain to an active fragment in vitro and during myocardial ischemia/reperfusion. J Biol Chem 276, 30724-30728.

Chen, S., Dai, Y., Harada, H., Dent, P., and Grant, S. (2007). Mcl-1 down-regulation potentiates ABT-737 lethality by cooperatively inducing Bak activation and Bax translocation. Cancer Res 67, 782-791.

Chen-Levy, Z., Nourse, J., and Cleary, M.L. (1989). The bcl-2 candidate proto-oncogene product is a 24-kilodalton integral-membrane protein highly expressed in lymphoid cell lines and lymphomas carrying the t(14;18) translocation. Mol Cell Biol 9, 701-710.

Cheng, E.H., Kirsch, D.G., Clem, R.J., Ravi, R., Kastan, M.B., Bedi, A., Ueno, K., and Hardwick, J.M. (1997). Conversion of Bcl-2 to a Bax-like death effector by caspases. Science 278, 1966-1968.

Chipuk, J.E., Bouchier-Hayes, L., Kuwana, T., Newmeyer, D.D., and Green, D.R. (2005). PUMA couples the nuclear and cytoplasmic proapoptotic function of p53. Science 309, 1732-1735.

Chipuk, J.E., and Green, D.R. (2008). How do BCL-2 proteins induce mitochondrial outer membrane permeabilization? Trends Cell Biol 18, 157-164.

Chipuk, J.E., Moldoveanu, T., Llambi, F., Parsons, M.J., and Green, D.R. (2010). The BCL-2 family reunion. Mol Cell 37, 299-310.

Chittenden, T., Flemington, C., Houghton, A.B., Ebb, R.G., Gallo, G.J., Elangovan, B., Chinnadurai, G., and Lutz, R.J. (1995). A conserved domain in Bak, distinct from BH1 and BH2, mediates cell death and protein binding functions. EMBO J 14, 5589-5596.

Chou, J.J., Li, H., Salvesen, G.S., Yuan, J., and Wagner, G. (1999). Solution structure of BID, an intracellular amplifier of apoptotic signaling. Cell 96, 615-624.

Chuang, P.I., Morefield, S., Liu, C.Y., Chen, S., Harlan, J.M., and Willerford, D.M. (2002). Perturbation of B-cell development in mice overexpressing the Bcl-2 homolog A1. Blood 99, 3350-3359.

Cikala, M., Wilm, B., Hobmayer, E., Bottger, A., and David, C.N. (1999). Identification of caspases and apoptosis in the simple metazoan Hydra. Curr Biol 9, 959-962.

Clohessy, J.G., Zhuang, J., and Brady, H.J. (2004). Characterisation of Mcl-1 cleavage during apoptosis of haematopoietic cells. Br J Haematol 125, 655-665.

Clohessy, J.G., Zhuang, J., de Boer, J., Gil-Gomez, G., and Brady, H.J. (2006). Mcl-1 interacts with truncated Bid and inhibits its induction of cytochrome c release and its role in receptor-mediated apoptosis. J Biol Chem 281, 5750-5759.

Clore, G.M., and Gronenborn, A.M. (1994). Multidimensional heteronuclear nuclear magnetic resonance of proteins. Methods Enzymol 239, 349-363.

Collaborative Computational Project, N., 1994 (1994). The CCP4 suite: Progams for Protein Crystallography. Acta Cryst. D50, 760-763.

Colvin, R.A., Holmes, W.R., Fontaine, C.P., and Maret, W. (2010). Cytosolic zinc buffering and muffling: Their role in intracellular zinc homeostasis. Metallomics 2, 306-317.

Craig, R.W. (2002). MCL1 provides a window on the role of the BCL2 family in cell proliferation, differentiation and tumorigenesis. Leukemia 16, 444-454.

Czabotar, P.E., Lee, E.F., van Delft, M.F., Day, C.L., Smith, B.J., Huang, D.C., Fairlie, W.D., Hinds, M.G., and Colman, P.M. (2007). Structural insights into the degradation of Mcl-1 induced by BH3 domains. Proc Natl Acad Sci U S A 104, 6217-6222.

Dai, H., Meng, X.W., Lee, S.H., Schneider, P.A., and Kaufmann, S.H. (2009). Context-dependent Bcl-2/Bak interactions regulate lymphoid cell apoptosis. J Biol Chem 284, 18311-18322.

Datta, S.R., Dudek, H., Tao, X., Masters, S., Fu, H., Gotoh, Y., and Greenberg, M.E. (1997). Akt phosphorylation of BAD couples survival signals to the cell-intrinsic death machinery. Cell 91, 231-241.

Day, C.L., Chen, L., Richardson, S.J., Harrison, P.J., Huang, D.C., and Hinds, M.G. (2005). Solution structure of prosurvival Mcl-1 and characterization of its binding by proapoptotic BH3-only ligands. J Biol Chem 280, 4738-4744.

Day, C.L., Smits, C., Fan, F.C., Lee, E.F., Fairlie, W.D., and Hinds, M.G. (2008). Structure of the BH3 domains from the p53-inducible BH3-only proteins Noxa and Puma in complex with Mcl-1. J Mol Biol 380, 958-971.

Degli Esposti, M., Ferry, G., Masdehors, P., Boutin, J.A., Hickman, J.A., and Dive, C. (2003). Post-translational modification of Bid has differential effects on its susceptibility to cleavage by caspase 8 or caspase 3. J Biol Chem 278, 15749-15757.

Dejean, L.M., Martinez-Caballero, S., Guo, L., Hughes, C., Teijido, O., Ducret, T., Ichas, F., Korsmeyer, S.J., Antonsson, B., Jonas, E.A., and Kinnally, K.W. (2005). Oligomeric Bax is a component of the putative cytochrome c release channel MAC, mitochondrial apoptosis-induced channel. Mol Biol Cell 16, 2424-2432.

Delano, W.L. (2008). The PyMOL Molecular Graphics System.

Denault, J.B., and Salvesen, G.S. (2002). Caspases: keys in the ignition of cell death. Chem Rev 102, 4489-4500.

Deng, Y., Ren, X., Yang, L., Lin, Y., and Wu, X. (2003). A JNK-dependent pathway is required for TNFalpha-induced apoptosis. Cell 115, 61-70.

Denisov, A.Y., Chen, G., Sprules, T., Moldoveanu, T., Beauparlant, P., and Gehring, K. (2006). Structural model of the BCL-w-BID peptide complex and its interactions with phospholipid micelles. Biochemistry 45, 2250-2256.

Denisov, A.Y., Madiraju, M.S., Chen, G., Khadir, A., Beauparlant, P., Attardo, G., Shore, G.C., and Gehring, K. (2003). Solution structure of human

BCL-w: modulation of ligand binding by the C-terminal helix. J Biol Chem 278, 21124-21128.

Denisov, A.Y., Sprules, T., Fraser, J., Kozlov, G., and Gehring, K. (2007). Heat-induced dimerization of BCL-xL through alpha-helix swapping. Biochemistry 46, 734-740.

Derenne, S., Monia, B., Dean, N.M., Taylor, J.K., Rapp, M.J., Harousseau, J.L., Bataille, R., and Amiot, M. (2002). Antisense strategy shows that Mcl-1 rather than Bcl-2 or Bcl-x(L) is an essential survival protein of human myeloma cells. Blood 100, 194-199.

Desagher, S., Osen-Sand, A., Montessuit, S., Magnenat, E., Vilbois, F., Hochmann, A., Journot, L., Antonsson, B., and Martinou, J.C. (2001). Phosphorylation of bid by casein kinases I and II regulates its cleavage by caspase 8. Mol Cell 8, 601-611.

Dewson, G., Kratina, T., Czabotar, P., Day, C.L., Adams, J.M., and Kluck, R.M. (2009). Bak activation for apoptosis involves oligomerization of dimers via their alpha6 helices. Mol Cell 36, 696-703.

Dewson, G., Kratina, T., Sim, H.W., Puthalakath, H., Adams, J.M., Colman, P.M., and Kluck, R.M. (2008). To trigger apoptosis, Bak exposes its BH3 domain and homodimerizes via BH3:groove interactions. Mol Cell 30, 369-380.

Dijkers, P.F., Medema, R.H., Lammers, J.W., Koenderman, L., and Coffer, P.J. (2000). Expression of the pro-apoptotic Bcl-2 family member Bim is regulated by the forkhead transcription factor FKHR-L1. Curr Biol 10, 1201-1204.

Ding, Q., Huo, L., Yang, J.Y., Xia, W., Wei, Y., Liao, Y., Chang, C.J., Yang, Y., Lai, C.C., Lee, D.F., et al. (2008). Down-regulation of myeloid cell leukemia-1 through inhibiting Erk/Pin 1 pathway by sorafenib facilitates chemosensitization in breast cancer. Cancer Res 68, 6109-6117.

Dong, L., Wang, W., Wang, F., Stoner, M., Reed, J.C., Harigai, M., Samudio, I., Kladde, M.P., Vyhlidal, C., and Safe, S. (1999). Mechanisms of transcriptional activation of bcl-2 gene expression by 17beta-estradiol in breast cancer cells. J Biol Chem 274, 32099-32107.

Dunkle, A., Dzhagalov, I., and He, Y.W. (2010). Mcl-1 promotes survival of thymocytes by inhibition of Bak in a pathway separate from Bcl-2. Cell Death Differ.

Earnshaw, W.C., Martins, L.M., and Kaufmann, S.H. (1999). Mammalian caspases: structure, activation, substrates, and functions during apoptosis. Annu Rev Biochem 68, 383-424.

Eischen, C.M., Rehg, J.E., Korsmeyer, S.J., and Cleveland, J.L. (2002). Loss of Bax alters tumor spectrum and tumor numbers in ARF-deficient mice. Cancer Res 62, 2184-2191.

Ekoff, M., Kaufmann, T., Engstrom, M., Motoyama, N., Villunger, A., Jonsson, J.I., Strasser, A., and Nilsson, G. (2007). The BH3-only protein Puma plays an essential role in cytokine deprivation induced apoptosis of mast cells. Blood 110, 3209-3217.

Eskes, R., Antonsson, B., Osen-Sand, A., Montessuit, S., Richter, C., Sadoul, R., Mazzei, G., Nichols, A., and Martinou, J.C. (1998). Bax-induced cytochrome C release from mitochondria is independent of the permeability transition pore but highly dependent on Mg2+ ions. J Cell Biol 143, 217-224.

Esposti, M.D., Erler, J.T., Hickman, J.A., and Dive, C. (2001). Bid, a widely expressed proapoptotic protein of the Bcl-2 family, displays lipid transfer activity. Mol Cell Biol 21, 7268-7276.

Feng, Y., Lin, Z., Shen, X., Chen, K., Jiang, H., and Liu, D. (2008). Bcl-xL forms two distinct homodimers at non-ionic detergents: implications in the dimerization of Bcl-2 family proteins. J Biochem 143, 243-252.

Fesik, S.W. (2000). Insights into programmed cell death through structural biology. Cell 103, 273-282.

Fesik, S.W. (2005). Promoting apoptosis as a strategy for cancer drug discovery. Nat Rev Cancer 5, 876-885.

Fiedler, S., Broecker, J., and Keller, S. (2010). Protein folding in membranes. Cell Mol Life Sci Epub ahead of print.

Fire, E., Gulla, S.V., Grant, R.A., and Keating, A.E. (2010). Mcl-1-Bim complexes accommodate surprising point mutations via minor structural changes. Protein Sci 19, 507-519.

Frank Delaglio, S.G., Geerten W. Vuister, Guang Zhu, John Pfeifer and Ad Bax (1995). NMRPipe: A multidimensional spectral processing system based on UNIX pipes. Journal of Biomolecular NMR 6, 277-293.

Frohlich, K.U., and Madeo, F. (2000). Apoptosis in yeast--a monocellular organism exhibits altruistic behaviour. FEBS Lett 473, 6-9.

Fulda, S., and Debatin, K.M. (2004). Apoptosis signaling in tumor therapy. Ann N Y Acad Sci 1028, 150-156.

Gabriel Cornilescu, F.D.a.A.B. (1999). Protein backbone angle restraints from searching a database for chemical shift and sequence homology. Journal of Biomolecular NMR 13, 289-302.

Gardai, S.J., Hildeman, D.A., Frankel, S.K., Whitlock, B.B., Frasch, S.C., Borregaard, N., Marrack, P., Bratton, D.L., and Henson, P.M. (2004). Phosphorylation of Bax Ser184 by Akt regulates its activity and apoptosis in neutrophils. J Biol Chem 279, 21085-21095.

Gavathiotis, E., Suzuki, M., Davis, M.L., Pitter, K., Bird, G.H., Katz, S.G., Tu, H.C., Kim, H., Cheng, E.H., Tjandra, N., and Walensky, L.D. (2008). BAX activation is initiated at a novel interaction site. Nature 455, 1076-1081.

George, N.M., Evans, J.J., and Luo, X. (2007). A three-helix homo-oligomerization domain containing BH3 and BH1 is responsible for the apoptotic activity of Bax. Genes Dev 21, 1937-1948.

Germain, M., and Duronio, V. (2007). The N terminus of the anti-apoptotic BCL-2 homologue MCL-1 regulates its localization and function. J Biol Chem 282, 32233-32242.

Gillissen, B., Wendt, J., Richter, A., Muer, A., Overkamp, T., Gebhardt, N., Preissner, R., Belka, C., Dorken, B., and Daniel, P.T. (2010). Endogenous Bak inhibitors Mcl-1 and Bcl-xL: differential impact on TRAIL resistance in Bax-deficient carcinoma. J Cell Biol 188, 851-862.

Goping, I.S., Gross, A., Lavoie, J.N., Nguyen, M., Jemmerson, R., Roth, K., Korsmeyer, S.J., and Shore, G.C. (1998). Regulated targeting of BAX to mitochondria. J Cell Biol 143, 207-215.

Green, D.R., and Kroemer, G. (2004). The pathophysiology of mitochondrial cell death. Science 305, 626-629.

Green, D.R., and Reed, J.C. (1998). Mitochondria and apoptosis. Science 281, 1309-1312.

Griffiths, G.J., Dubrez, L., Morgan, C.P., Jones, N.A., Whitehouse, J., Corfe, B.M., Dive, C., and Hickman, J.A. (1999). Cell damage-induced conformational changes of the pro-apoptotic protein Bak in vivo precede the onset of apoptosis. J Cell Biol 144, 903-914.

Grinberg, M., Sarig, R., Zaltsman, Y., Frumkin, D., Grammatikakis, N., Reuveny, E., and Gross, A. (2002). tBID Homooligomerizes in the mitochondrial membrane to induce apoptosis. J Biol Chem 277, 12237-12245.

Gross, A., Yin, X.M., Wang, K., Wei, M.C., Jockel, J., Milliman, C., Erdjument-Bromage, H., Tempst, P., and Korsmeyer, S.J. (1999). Caspase cleaved

BID targets mitochondria and is required for cytochrome c release, while BCL-XL prevents this release but not tumor necrosis factor-R1/Fas death. J Biol Chem 274, 1156-1163.

Guntert, P. (2004). Automated NMR structure calculation with CYANA. Methods Mol Biol 278, 353-378.

Hacker, G. (2000). The morphology of apoptosis. Cell Tissue Res 301, 5-17.

Hacker, G., and Weber, A. (2007). BH3-only proteins trigger cytochrome c release, but how? Arch Biochem Biophys 462, 150-155.

Hamasaki, A., Sendo, F., Nakayama, K., Ishida, N., Negishi, I., and Hatakeyama, S. (1998). Accelerated neutrophil apoptosis in mice lacking A1-a, a subtype of the bcl-2-related A1 gene. J Exp Med 188, 1985-1992.

Han, J., Goldstein, L.A., Gastman, B.R., Rabinovitz, A., and Rabinowich, H. (2005). Disruption of Mcl-1.Bim complex in granzyme B-mediated mitochondrial apoptosis. J Biol Chem 280, 16383-16392.

Hengartner, M.O., Ellis, R.E., and Horvitz, H.R. (1992). Caenorhabditis elegans gene ced-9 protects cells from programmed cell death. Nature 356, 494-499.

Herrant, M., Jacquel, A., Marchetti, S., Belhacene, N., Colosetti, P., Luciano, F., and Auberger, P. (2004). Cleavage of Mcl-1 by caspases impaired its ability to counteract Bim-induced apoptosis. Oncogene 23, 7863-7873.

Hinds, M.G., Lackmann, M., Skea, G.L., Harrison, P.J., Huang, D.C., and Day, C.L. (2003). The structure of Bcl-w reveals a role for the C-terminal residues in modulating biological activity. EMBO J 22, 1497-1507.

Hochhauser, E., Kivity, S., Offen, D., Maulik, N., Otani, H., Barhum, Y., Pannet, H., Shneyvays, V., Shainberg, A., Goldshtaub, V., et al. (2003). Bax ablation protects against myocardial ischemia-reperfusion injury in transgenic mice. Am J Physiol Heart Circ Physiol 284, H2351-2359.

Hockenbery, D.M. (1992). The bcl-2 oncogene and apoptosis. Semin Immunol 4, 413-420.

Horie, C., Suzuki, H., Sakaguchi, M., and Mihara, K. (2002). Characterization of signal that directs C-tail-anchored proteins to mammalian mitochondrial outer membrane. Mol Biol Cell 13, 1615-1625.

Hsu, Y.T., and Youle, R.J. (1997). Nonionic detergents induce dimerization among members of the Bcl-2 family. J Biol Chem 272, 13829-13834.

Hsu, Y.T., and Youle, R.J. (1998). Bax in murine thymus is a soluble monomeric protein that displays differential detergent-induced conformations. J Biol Chem 273, 10777-10783.

Ito, T., Deng, X., Carr, B., and May, W.S. (1997). Bcl-2 phosphorylation required for anti-apoptosis function. J Biol Chem 272, 11671-11673.

Ivashyna, O., Garcia-Saez, A.J., Ries, J., Christenson, E.T., Schwille, P., and Schlesinger, P.H. (2009). Detergent activated BAX protein is a monomer. J Biol Chem 284, 23935-23946.

Jeffers, J.R., Parganas, E., Lee, Y., Yang, C., Wang, J., Brennan, J., MacLean, K.H., Han, J., Chittenden, T., Ihle, J.N., et al. (2003). Puma is an essential mediator of p53-dependent and -independent apoptotic pathways. Cancer Cell 4, 321-328.

Johnson, B.A., and Blevins, R.A. (1994). NMR View: A computer program for the visualization and analysis of NMR data. Journal of Biomolecular NMR 4, 603-614.

Jonas, E.A., Hickman, J.A., Chachar, M., Polster, B.M., Brandt, T.A., Fannjiang, Y., Ivanovska, I., Basanez, G., Kinnally, K.W., Zimmerberg, J., et al. (2004). Proapoptotic N-truncated BCL-xL protein activates endogenous mitochondrial channels in living synaptic terminals. Proc Natl Acad Sci U S A 101, 13590-13595.

Kaufmann, T., Schlipf, S., Sanz, J., Neubert, K., Stein, R., and Borner, C. (2003). Characterization of the signal that directs Bcl-x(L), but not Bcl-2, to the mitochondrial outer membrane. J Cell Biol 160, 53-64.

Kawasaki, T., Yokoi, S., Tsuda, H., Izumi, H., Kozaki, K., Aida, S., Ozeki, Y., Yoshizawa, Y., Imoto, I., and Inazawa, J. (2007). BCL2L2 is a probable target for novel 14q11.2 amplification detected in a non-small cell lung cancer cell line. Cancer Sci 98, 1070-1077.

Ke, N., Godzik, A., and Reed, J.C. (2001). Bcl-B, a novel Bcl-2 family member that differentially binds and regulates Bax and Bak. J Biol Chem 276, 12481-12484.

Kerr, J.F. (1965). A histochemical study of hypertrophy and ischaemic injury of rat liver with special reference to changes in lysosomes. J Pathol Bacteriol 90, 419-435.

Kerr, J.F. (1995). Neglected opportunities in apoptosis research. Trends Cell Biol 5, 55-57.

Kerr, J.F., Wyllie, A.H., and Currie, A.R. (1972). Apoptosis: a basic biological phenomenon with wide-ranging implications in tissue kinetics. Br J Cancer 26, 239-257.

Kim, H., Rafiuddin-Shah, M., Tu, H.C., Jeffers, J.R., Zambetti, G.P., Hsieh, J.J., and Cheng, E.H. (2006). Hierarchical regulation of mitochondrion-dependent apoptosis by BCL-2 subfamilies. Nat Cell Biol 8, 1348-1358.

Kim, H., Tu, H.C., Ren, D., Takeuchi, O., Jeffers, J.R., Zambetti, G.P., Hsieh, J.J., and Cheng, E.H. (2009). Stepwise activation of BAX and BAK by tBID, BIM, and PUMA initiates mitochondrial apoptosis. Mol Cell 36, 487-499.

Kiryu-Seo, S., Hirayama, T., Kato, R., and Kiyama, H. (2005). Noxa is a critical mediator of p53-dependent motor neuron death after nerve injury in adult mouse. J Neurosci 25, 1442-1447.

Kluck, R.M., Bossy-Wetzel, E., Green, D.R., and Newmeyer, D.D. (1997). The release of cytochrome c from mitochondria: a primary site for Bcl-2 regulation of apoptosis. Science 275, 1132-1136.

Knudson, C.M., Johnson, G.M., Lin, Y., and Korsmeyer, S.J. (2001). Bax accelerates tumorigenesis in p53-deficient mice. Cancer Res 61, 659-665.

Knudson, C.M., Tung, K.S., Tourtellotte, W.G., Brown, G.A., and Korsmeyer, S.J. (1995). Bax-deficient mice with lymphoid hyperplasia and male germ cell death. Science 270, 96-99.

Kobayashi, S., Lee, S.H., Meng, X.W., Mott, J.L., Bronk, S.F., Werneburg, N.W., Craig, R.W., Kaufmann, S.H., and Gores, G.J. (2007). Serine 64 phosphorylation enhances the antiapoptotic function of Mcl-1. J Biol Chem 282, 18407-18417.

Konopleva, M., Contractor, R., Tsao, T., Samudio, I., Ruvolo, P.P., Kitada, S., Deng, X., Zhai, D., Shi, Y.X., Sneed, T., et al. (2006). Mechanisms of apoptosis sensitivity and resistance to the BH3 mimetic ABT-737 in acute myeloid leukemia. Cancer Cell 10, 375-388.

Konopleva, M., Watt, J., Contractor, R., Tsao, T., Harris, D., Estrov, Z., Bornmann, W., Kantarjian, H., Viallet, J., Samudio, I., and Andreeff, M. (2008). Mechanisms of antileukemic activity of the novel Bcl-2 homology domain-3 mimetic GX15-070 (obatoclax). Cancer Res 68, 3413-3420.

Korsmeyer, S.J., Wei, M.C., Saito, M., Weiler, S., Oh, K.J., and Schlesinger, P.H. (2000). Pro-apoptotic cascade activates BID, which oligomerizes BAK or BAX into pores that result in the release of cytochrome c. Cell Death Differ 7, 1166-1173.

Kutzki, O., Park, H.S., Ernst, J.T., Orner, B.P., Yin, H., and Hamilton, A.D. (2002). Development of a potent Bcl-x(L) antagonist based on alpha-helix mimicry. J Am Chem Soc 124, 11838-11839.

Kuwana, T., Bouchier-Hayes, L., Chipuk, J.E., Bonzon, C., Sullivan, B.A., Green, D.R., and Newmeyer, D.D. (2005). BH3 domains of BH3-only proteins differentially regulate Bax-mediated mitochondrial membrane permeabilization both directly and indirectly. Mol Cell 17, 525-535.

Kuwana, T., Mackey, M.R., Perkins, G., Ellisman, M.H., Latterich, M., Schneiter, R., Green, D.R., and Newmeyer, D.D. (2002). Bid, Bax, and lipids cooperate to form supramolecular openings in the outer mitochondrial membrane. Cell 111, 331-342.

Labi, V., Erlacher, M., Kiessling, S., Manzl, C., Frenzel, A., O'Reilly, L., Strasser, A., and Villunger, A. (2008). Loss of the BH3-only protein Bmf impairs B cell homeostasis and accelerates gamma irradiation-induced thymic lymphoma development. J Exp Med 205, 641-655.

Lamzin, V.S., and Perrakis, A. (2000). Current state of automated crystallographic data analysis. Nat Struct Biol 7 Suppl, 978-981.

Lang, G., Gombert, W.M., and Gould, H.J. (2005). A transcriptional regulatory element in the coding sequence of the human Bcl-2 gene. Immunology 114, 25-36.

Laskowski, R.A., Rullmannn, J.A., MacArthur, M.W., Kaptein, R., and Thornton, J.M. (1996). AQUA and PROCHECK-NMR: programs for checking the quality of protein structures solved by NMR. J Biomol NMR 8, 477-486.

Lauria, F., Raspadori, D., Rondelli, D., Ventura, M.A., Fiacchini, M., Visani, G., Forconi, F., and Tura, S. (1997). High bcl-2 expression in acute myeloid leukemia cells correlates with CD34 positivity and complete remission rate. Leukemia 11, 2075-2078.

Lessene, G., Czabotar, P.E., and Colman, P.M. (2008). BCL-2 family antagonists for cancer therapy. Nat Rev Drug Discov 7, 989-1000.

Letai, A., Bassik, M.C., Walensky, L.D., Sorcinelli, M.D., Weiler, S., and Korsmeyer, S.J. (2002). Distinct BH3 domains either sensitize or activate mitochondrial apoptosis, serving as prototype cancer therapeutics. Cancer Cell 2, 183-192.

Leu, J.I., Dumont, P., Hafey, M., Murphy, M.E., and George, D.L. (2004). Mitochondrial p53 activates Bak and causes disruption of a Bak-Mcl1 complex. Nat Cell Biol 6, 443-450.

Li, H., Zhu, H., Xu, C.J., and Yuan, J. (1998). Cleavage of BID by caspase 8 mediates the mitochondrial damage in the Fas pathway of apoptosis. Cell 94, 491-501.

Li, J., Viallet, J., and Haura, E.B. (2008). A small molecule pan-Bcl-2 family inhibitor, GX15-070, induces apoptosis and enhances cisplatin-induced apoptosis in non-small cell lung cancer cells. Cancer Chemother Pharmacol 61, 525-534.

Lindsten, T., Ross, A.J., King, A., Zong, W.X., Rathmell, J.C., Shiels, H.A., Ulrich, E., Waymire, K.G., Mahar, P., Frauwirth, K., et al. (2000). The combined functions of proapoptotic Bcl-2 family members bak and bax are essential for normal development of multiple tissues. Mol Cell 6, 1389-1399.

Lithgow, T., van Driel, R., Bertram, J.F., and Strasser, A. (1994). The protein product of the oncogene bcl-2 is a component of the nuclear envelope, the endoplasmic reticulum, and the outer mitochondrial membrane. Cell Growth Differ 5, 411-417.

Liu, J., Durrant, D., Yang, H.S., He, Y., Whitby, F.G., Myszka, D.G., and Lee, R.M. (2005). The interaction between tBid and cardiolipin or monolysocardiolipin. Biochem Biophys Res Commun 330, 865-870.

Liu, Q., Moldoveanu, T., Sprules, T., Matta-Camacho, E., Mansur-Azzam, N., and Gehring, K. (2010). Apoptotic regulation by MCL-1 through heterodimerization. J Biol Chem 285, 19615-19624.

Liu, Q.A., and Hengartner, M.O. (1999). The molecular mechanism of programmed cell death in C. elegans. Ann N Y Acad Sci 887, 92-104.

Liu, X., Dai, S., Zhu, Y., Marrack, P., and Kappler, J.W. (2003). The structure of a Bcl-xL/Bim fragment complex: implications for Bim function. Immunity 19, 341-352.

Losonczi, J.A., Olejniczak, E.T., Betz, S.F., Harlan, J.E., Mack, J., and Fesik, S.W. (2000). NMR studies of the anti-apoptotic protein Bcl-xL in micelles. Biochemistry 39, 11024-11033.

Lovell, J.F., Billen, L.P., Bindner, S., Shamas-Din, A., Fradin, C., Leber, B., and Andrews, D.W. (2008). Membrane binding by tBid initiates an ordered series of events culminating in membrane permeabilization by Bax. Cell 135, 1074-1084.

Luo, X., Budihardjo, I., Zou, H., Slaughter, C., and Wang, X. (1998). Bid, a Bcl2 interacting protein, mediates cytochrome c release from mitochondria in response to activation of cell surface death receptors. Cell 94, 481-490.

Mandic, A., Viktorsson, K., Molin, M., Akusjarvi, G., Eguchi, H., Hayashi, S.I., Toi, M., Hansson, J., Linder, S., and Shoshan, M.C. (2001). Cisplatin induces the proapoptotic conformation of Bak in a deltaMEKK1-dependent manner. Mol Cell Biol 21, 3684-3691.

Mandic, A., Viktorsson, K., Strandberg, L., Heiden, T., Hansson, J., Linder, S., and Shoshan, M.C. (2002). Calpain-mediated Bid cleavage and calpain-independent Bak modulation: two separate pathways in cisplatin-induced apoptosis. Mol Cell Biol 22, 3003-3013.

Martin, S.S., and Vuori, K. (2004). Regulation of Bcl-2 proteins during anoikis and amorphosis. Biochim Biophys Acta 1692, 145-157.

Mathai, J.P., Germain, M., Marcellus, R.C., and Shore, G.C. (2002). Induction and endoplasmic reticulum location of BIK/NBK in response to apoptotic signaling by E1A and p53. Oncogene 21, 2534-2544.

McDonnell, J.M., Fushman, D., Milliman, C.L., Korsmeyer, S.J., and Cowburn, D. (1999). Solution structure of the proapoptotic molecule BID: a structural basis for apoptotic agonists and antagonists. Cell 96, 625-634.

McRee, D. (1992). A visual protein crystallographic software system for X11/XView. J.Mol.Graph. 10, 44-46.

Meiler, J., Prompers, J.J., Peti, W., Griesinger, C., and Bruschweiler, R. (2001). Model-free approach to the dynamic interpretation of residual dipolar couplings in globular proteins. J Am Chem Soc 123, 6098-6107.

Michels, J., O'Neill, J.W., Dallman, C.L., Mouzakiti, A., Habens, F., Brimmell, M., Zhang, K.Y., Craig, R.W., Marcusson, E.G., Johnson, P.W., and Packham, G. (2004). Mcl-1 is required for Akata6 B-lymphoma cell survival and is converted to a cell death molecule by efficient caspase-mediated cleavage. Oncogene 23, 4818-4827.

Miyashita, T., Harigai, M., Hanada, M., and Reed, J.C. (1994). Identification of a p53-dependent negative response element in the bcl-2 gene. Cancer Res 54, 3131-3135.

Miyashita, T., and Reed, J.C. (1995). Tumor suppressor p53 is a direct transcriptional activator of the human bax gene. Cell 80, 293-299.

Modrek, B., Resch, A., Grasso, C., and Lee, C. (2001). Genome-wide detection of alternative splicing in expressed sequences of human genes. Nucleic Acids Res 29, 2850-2859.

Moldoveanu, T., Hosfield, C.M., Lim, D., Elce, J.S., Jia, Z., and Davies, P.L. (2002). A Ca(2+) switch aligns the active site of calpain. Cell 108, 649-660.

Moldoveanu, T., Liu, Q., Tocilj, A., Watson, M., Shore, G., and Gehring, K. (2006). The X-ray structure of a BAK homodimer reveals an inhibitory zinc binding site. Mol Cell 24, 677-688.

Montessuit, S., Mazzei, G., Magnenat, E., and Antonsson, B. (1999). Expression and purification of full-length human Bax alpha. Protein Expr Purif 15, 202-206.

Motoyama, N., Wang, F., Roth, K.A., Sawa, H., Nakayama, K., Negishi, I., Senju, S., Zhang, Q., Fujii, S., and et al. (1995). Massive cell death of immature hematopoietic cells and neurons in Bcl-x-deficient mice. Science 267, 1506-1510.

Muchmore, S.W., Sattler, M., Liang, H., Meadows, R.P., Harlan, J.E., Yoon, H.S., Nettesheim, D., Chang, B.S., Thompson, C.B., Wong, S.L., et al. (1996). X-ray and NMR structure of human Bcl-xL, an inhibitor of programmed cell death. Nature 381, 335-341.

Murshudov, G.N., Vagin, A.A., and Dodson, E.J. (1997). Refinement of macromolecular structures by the maximum-likelihood method. Acta Crystallogr D Biol Crystallogr 53, 240-255.

Nakano, K., and Vousden, K.H. (2001). PUMA, a novel proapoptotic gene, is induced by p53. Mol Cell 7, 683-694.

Neilan, J.G., Lu, Z., Afonso, C.L., Kutish, G.F., Sussman, M.D., and Rock, D.L. (1993). An African swine fever virus gene with similarity to the proto-oncogene bcl-2 and the Epstein-Barr virus gene BHRF1. J Virol 67, 4391-4394.

Nguyen, M., Marcellus, R.C., Roulston, A., Watson, M., Serfass, L., Murthy Madiraju, S.R., Goulet, D., Viallet, J., Belec, L., Billot, X., et al. (2007). Small molecule obatoclax (GX15-070) antagonizes MCL-1 and overcomes MCL-1-mediated resistance to apoptosis. Proc Natl Acad Sci U S A 104, 19512-19517.

Nguyen, M., Millar, D.G., Yong, V.W., Korsmeyer, S.J., and Shore, G.C. (1993). Targeting of Bcl-2 to the mitochondrial outer membrane by a COOH-terminal signal anchor sequence. J Biol Chem 268, 25265-25268.

Nie, C., Tian, C., Zhao, L., Petit, P.X., Mehrpour, M., and Chen, Q. (2008). Cysteine 62 of Bax is critical for its conformational activation and its proapoptotic activity in response to H2O2-induced apoptosis. J Biol Chem 283, 15359-15369.

Norbury, C.J., and Hickson, I.D. (2001). Cellular responses to DNA damage. Annu Rev Pharmacol Toxicol 41, 367-401.

Nunez, G., London, L., Hockenbery, D., Alexander, M., McKearn, J.P., and Korsmeyer, S.J. (1990). Deregulated Bcl-2 gene expression selectively prolongs survival of growth factor-deprived hemopoietic cell lines. J Immunol 144, 3602-3610.

O'Connor, L., Strasser, A., O'Reilly, L.A., Hausmann, G., Adams, J.M., Cory, S., and Huang, D.C. (1998). Bim: a novel member of the Bcl-2 family that promotes apoptosis. EMBO J 17, 384-395.

O'Connor, R., Fennelly, C., and Krause, D. (2000). Regulation of survival signals from the insulin-like growth factor-I receptor. Biochem Soc Trans 28, 47-51.

O'Neill, J.W., Manion, M.K., Maguire, B., and Hockenbery, D.M. (2006). BCL-XL dimerization by three-dimensional domain swapping. J Mol Biol 356, 367-381.

Oda, E., Ohki, R., Murasawa, H., Nemoto, J., Shibue, T., Yamashita, T., Tokino, T., Taniguchi, T., and Tanaka, N. (2000). Noxa, a BH3-only member of the Bcl-2 family and candidate mediator of p53-induced apoptosis. Science 288, 1053-1058.

Oliver, P.M., Vass, T., Kappler, J., and Marrack, P. (2006). Loss of the proapoptotic protein, Bim, breaks B cell anergy. J Exp Med 203, 731-741.

Oltersdorf, T., Elmore, S.W., Shoemaker, A.R., Armstrong, R.C., Augeri, D.J., Belli, B.A., Bruncko, M., Deckwerth, T.L., Dinges, J., Hajduk, P.J., et al. (2005). An inhibitor of Bcl-2 family proteins induces regression of solid tumours. Nature 435, 677-681.

Oltvai, Z.N., Milliman, C.L., and Korsmeyer, S.J. (1993). Bcl-2 heterodimerizes in vivo with a conserved homolog, Bax, that accelerates programmed cell death. Cell 74, 609-619.

Opferman, J.T., Iwasaki, H., Ong, C.C., Suh, H., Mizuno, S., Akashi, K., and Korsmeyer, S.J. (2005). Obligate role of anti-apoptotic MCL-1 in the survival of hematopoietic stem cells. Science 307, 1101-1104.

Opferman, J.T., and Korsmeyer, S.J. (2003). Apoptosis in the development and maintenance of the immune system. Nat Immunol 4, 410-415.

Opferman, J.T., Letai, A., Beard, C., Sorcinelli, M.D., Ong, C.C., and Korsmeyer, S.J. (2003). Development and maintenance of B and T lymphocytes requires antiapoptotic MCL-1. Nature 426, 671-676.

Ottiger, M., Delaglio, F., and Bax, A. (1998). Measurement of J and dipolar couplings from simplified two-dimensional NMR spectra. J Magn Reson 131, 373-378.

Pagliari, L.J., Kuwana, T., Bonzon, C., Newmeyer, D.D., Tu, S., Beere, H.M., and Green, D.R. (2005). The multidomain proapoptotic molecules Bax and Bak are directly activated by heat. Proc Natl Acad Sci U S A 102, 17975-17980.

Pearson, G.R., Luka, J., Petti, L., Sample, J., Birkenbach, M., Braun, D., and Kieff, E. (1987). Identification of an Epstein-Barr virus early gene encoding a second component of the restricted early antigen complex. Virology 160, 151-161.

Peng, J.W., and Wagner, G. (1994). Investigation of protein motions via relaxation measurements. Methods Enzymol 239, 563-596.

Perez-Galan, P., Roue, G., Villamor, N., Campo, E., and Colomer, D. (2007). The BH3-mimetic GX15-070 synergizes with bortezomib in mantle cell lymphoma by enhancing Noxa-mediated activation of Bak. Blood 109, 4441-4449.

Petros, A.M., Medek, A., Nettesheim, D.G., Kim, D.H., Yoon, H.S., Swift, K., Matayoshi, E.D., Oltersdorf, T., and Fesik, S.W. (2001). Solution structure of the antiapoptotic protein bcl-2. Proc Natl Acad Sci U S A 98, 3012-3017.

Pietsch, E.C., Perchiniak, E., Canutescu, A.A., Wang, G., Dunbrack, R.L., and Murphy, M.E. (2008). Oligomerization of BAK by p53 utilizes conserved residues of the p53 DNA binding domain. J Biol Chem 283, 21294-21304.

Plesnila, N., Zinkel, S., Amin-Hanjani, S., Qiu, J., Korsmeyer, S.J., and Moskowitz, M.A. (2002). Function of BID -- a molecule of the bcl-2 family -- in ischemic cell death in the brain. Eur Surg Res 34, 37-41.

Print, C.G., Loveland, K.L., Gibson, L., Meehan, T., Stylianou, A., Wreford, N., de Kretser, D., Metcalf, D., Kontgen, F., Adams, J.M., and Cory, S. (1998). Apoptosis regulator bcl-w is essential for spermatogenesis but appears otherwise redundant. Proc Natl Acad Sci U S A 95, 12424-12431.

Puthalakath, H., Huang, D.C., O'Reilly, L.A., King, S.M., and Strasser, A. (1999). The proapoptotic activity of the Bcl-2 family member Bim is regulated by interaction with the dynein motor complex. Mol Cell 3, 287-296.

Puthalakath, H., Villunger, A., O'Reilly, L.A., Beaumont, J.G., Coultas, L., Cheney, R.E., Huang, D.C., and Strasser, A. (2001). Bmf: a proapoptotic BH3-only protein regulated by interaction with the myosin V actin motor complex, activated by anoikis. Science 293, 1829-1832.

Qian Liu, T.M., Tara Sprules, Edna Matta-Camacho, Nura Mansur-Azzam, and Kalle Gehring (2010). Apoptotic regulation by MCL-1 through hetero-dimerization. The Journal of Biological Chemistry.

Real, P.J., Benito, A., Cuevas, J., Berciano, M.T., de Juan, A., Coffer, P., Gomez-Roman, J., Lafarga, M., Lopez-Vega, J.M., and Fernandez-Luna, J.L. (2005). Blockade of epidermal growth factor receptors chemosensitizes breast cancer cells through up-regulation of Bnip3L. Cancer Res 65, 8151-8157.

Reed, J.C. (1999). Fenretinide: the death of a tumor cell. J Natl Cancer Inst 91, 1099-1100.

Reed, J.C. (2000). Mechanisms of apoptosis. Am J Pathol 157, 1415-1430.

Reed, J.C. (2006). Proapoptotic multidomain Bcl-2/Bax-family proteins: mechanisms, physiological roles, and therapeutic opportunities. Cell Death Differ 13, 1378-1386.

Reiners, J.J., Jr., Caruso, J.A., Mathieu, P., Chelladurai, B., Yin, X.M., and Kessel, D. (2002). Release of cytochrome c and activation of pro-caspase-9 following lysosomal photodamage involves Bid cleavage. Cell Death Differ 9, 934-944.

Renshaw, S.A., Dempsey, C.E., Barnes, F.A., Bagstaff, S.M., Dower, S.K., Bingle, C.D., and Whyte, M.K. (2004). Three novel Bid proteins generated by alternative splicing of the human Bid gene. J Biol Chem 279, 2846-2855.

Richardson, H., and Kumar, S. (2002). Death to flies: Drosophila as a model system to study programmed cell death. J Immunol Methods 265, 21-38.

Rinkenberger, J.L., Horning, S., Klocke, B., Roth, K., and Korsmeyer, S.J. (2000). Mcl-1 deficiency results in peri-implantation embryonic lethality. Genes Dev 14, 23-27.

Ruffolo, S.C., and Shore, G.C. (2003). BCL-2 selectively interacts with the BID-induced open conformer of BAK, inhibiting BAK auto-oligomerization. J Biol Chem 278, 25039-25045.

Sadowsky, J.D., Fairlie, W.D., Hadley, E.B., Lee, H.S., Umezawa, N., Nikolovska-Coleska, Z., Wang, S., Huang, D.C., Tomita, Y., and Gellman, S.H. (2007). (alpha/beta+alpha)-peptide antagonists of BH3 domain/Bcl-x(L) recognition: toward general strategies for foldamer-based inhibition of protein-protein interactions. J Am Chem Soc 129, 139-154.

Sali, A., and Blundell, T.L. (1993). Comparative protein modelling by satisfaction of spatial restraints. J Mol Biol 234, 779-815.

Salvesen, G.S., and Renatus, M. (2002). Apoptosome: the seven-spoked death machine. Dev Cell 2, 256-257.

Saraogi, I., and Hamilton, A.D. (2008). alpha-Helix mimetics as inhibitors of protein-protein interactions. Biochem Soc Trans 36, 1414-1417.

Sartorius, U., Schmitz, I., and Krammer, P.H. (2001). Molecular mechanisms of death-receptor-mediated apoptosis. Chembiochem 2, 20-29.

Savill, J., Mooney, A., and Hughes, J. (1996). What role does apoptosis play in progression of renal disease? Curr Opin Nephrol Hypertens 5, 369-374.

Sawai, H., and Domae, N. (2009). Differential roles for Bak in Triton X-100- and deoxycholate-induced apoptosis. Biochem Biophys Res Commun 378, 529-533.

Scatena, C.D., Stewart, Z.A., Mays, D., Tang, L.J., Keefer, C.J., Leach, S.D., and Pietenpol, J.A. (1998). Mitotic phosphorylation of Bcl-2 during normal cell cycle progression and Taxol-induced growth arrest. J Biol Chem 273, 30777-30784.

Schiavone, N., Rosini, P., Quattrone, A., Donnini, M., Lapucci, A., Citti, L., Bevilacqua, A., Nicolin, A., and Capaccioli, S. (2000). A conserved AU-rich element in the 3' untranslated region of bcl-2 mRNA is endowed with a destabilizing function that is involved in bcl-2 down-regulation during apoptosis. FASEB J 14, 174-184.

Schinzel, A., Kaufmann, T., and Borner, C. (2004). Bcl-2 family members: integrators of survival and death signals in physiology and pathology [corrected]. Biochim Biophys Acta 1644, 95-105.

Schuler, M., and Green, D.R. (2001). Mechanisms of p53-dependent apoptosis. Biochem Soc Trans 29, 684-688.

Sedlak, T.W., Oltvai, Z.N., Yang, E., Wang, K., Boise, L.H., Thompson, C.B., and Korsmeyer, S.J. (1995). Multiple Bcl-2 family members demonstrate selective dimerizations with Bax. Proc Natl Acad Sci U S A 92, 7834-7838.

Seto, M., Jaeger, U., Hockett, R.D., Graninger, W., Bennett, S., Goldman, P., and Korsmeyer, S.J. (1988). Alternative promoters and exons, somatic mutation and deregulation of the Bcl-2-Ig fusion gene in lymphoma. EMBO J 7, 123-131.

Sevilla, L., Zaldumbide, A., Pognonec, P., and Boulukos, K.E. (2001). Transcriptional regulation of the bcl-x gene encoding the anti-apoptotic Bcl-xL protein by Ets, Rel/NFkappaB, STAT and AP1 transcription factor families. Histol Histopathol 16, 595-601.

She, Q.B., Solit, D.B., Ye, Q., O'Reilly, K.E., Lobo, J., and Rosen, N. (2005). The BAD protein integrates survival signaling by EGFR/MAPK and PI3K/Akt kinase pathways in PTEN-deficient tumor cells. Cancer Cell 8, 287-297.

Shi, B., Triebe, D., Kajiji, S., Iwata, K.K., Bruskin, A., and Mahajna, J. (1999). Identification and characterization of baxepsilon, a novel bax variant missing the BH2 and the transmembrane domains. Biochem Biophys Res Commun 254, 779-785.

Shibata, M.A., Liu, M.L., Knudson, M.C., Shibata, E., Yoshidome, K., Bandey, T., Korsmeyer, S.J., and Green, J.E. (1999). Haploid loss of bax leads to accelerated mammary tumor development in C3(1)/SV40-TAg transgenic mice: reduction in protective apoptotic response at the preneoplastic stage. EMBO J 18, 2692-2701.

Shibue, T., Takeda, K., Oda, E., Tanaka, H., Murasawa, H., Takaoka, A., Morishita, Y., Akira, S., Taniguchi, T., and Tanaka, N. (2003). Integral role of Noxa in p53-mediated apoptotic response. Genes Dev 17, 2233-2238.

Shuker, S.B., Hajduk, P.J., Meadows, R.P., and Fesik, S.W. (1996). Discovering high-affinity ligands for proteins: SAR by NMR. Science 274, 1531-1534.

Sieghart, W., Losert, D., Strommer, S., Cejka, D., Schmid, K., Rasoul-Rockenschaub, S., Bodingbauer, M., Crevenna, R., Monia, B.P., Peck-Radosavljevic, M., and Wacheck, V. (2006). Mcl-1 overexpression in hepatocellular carcinoma: a potential target for antisense therapy. J Hepatol 44, 151-157.

Skulachev, V.P. (2002). Programmed death in yeast as adaptation? FEBS Lett 528, 23-26.

Solomon, M., Belenghi, B., Delledonne, M., Menachem, E., and Levine, A. (1999). The involvement of cysteine proteases and protease inhibitor genes in the regulation of programmed cell death in plants. Plant Cell 11, 431-444.

Stoka, V., Turk, B., Schendel, S.L., Kim, T.H., Cirman, T., Snipas, S.J., Ellerby, L.M., Bredesen, D., Freeze, H., Abrahamson, M., et al. (2001). Lysosomal protease pathways to apoptosis. Cleavage of bid, not pro-caspases, is the most likely route. J Biol Chem 276, 3149-3157.

Strasser, A., Puthalakath, H., Bouillet, P., Huang, D.C., O'Connor, L., O'Reilly, L.A., Cullen, L., Cory, S., and Adams, J.M. (2000). The role of bim, a proapoptotic BH3-only member of the Bcl-2 family in cell-death control. Ann N Y Acad Sci 917, 541-548.

Sun, Y.F., Yu, L.Y., Saarma, M., Timmusk, T., and Arumae, U. (2001). Neuron-specific Bcl-2 homology 3 domain-only splice variant of Bak is anti-apoptotic in neurons, but pro-apoptotic in non-neuronal cells. J Biol Chem 276, 16240-16247.

Sutton, V.R., Davis, J.E., Cancilla, M., Johnstone, R.W., Ruefli, A.A., Sedelies, K., Browne, K.A., and Trapani, J.A. (2000). Initiation of apoptosis by granzyme B requires direct cleavage of bid, but not direct granzyme B-mediated caspase activation. J Exp Med 192, 1403-1414.

Suzuki, M., Youle, R.J., and Tjandra, N. (2000). Structure of Bax: coregulation of dimer formation and intracellular localization. Cell 103, 645-654.

Tait, S.W., de Vries, E., Maas, C., Keller, A.M., D'Santos, C.S., and Borst, J. (2007). Apoptosis induction by Bid requires unconventional ubiquitination and degradation of its N-terminal fragment. J Cell Biol 179, 1453-1466.

Tittel, J.N., and Steller, H. (2000). A comparison of programmed cell death between species. Genome Biol 1, REVIEWS0003.

Trudel, S., Stewart, A.K., Li, Z., Shu, Y., Liang, S.B., Trieu, Y., Reece, D., Paterson, J., Wang, D., and Wen, X.Y. (2007). The Bcl-2 family protein inhibitor, ABT-737, has substantial antimyeloma activity and shows synergistic effect with dexamethasone and melphalan. Clin Cancer Res 13, 621-629.

Tsujimoto, Y., and Croce, C.M. (1986). Analysis of the structure, transcripts, and protein products of bcl-2, the gene involved in human follicular lymphoma. Proc Natl Acad Sci U S A 83, 5214-5218.

Uhlmann, E.J., D'Sa-Eipper, C., Subramanian, T., Wagner, A.J., Hay, N., and Chinnadurai, G. (1996). Deletion of a nonconserved region of Bcl-2 confers a novel gain of function: suppression of apoptosis with concomitant cell proliferation. Cancer Res 56, 2506-2509.

Upreti, M., Galitovskaya, E.N., Chu, R., Tackett, A.J., Terrano, D.T., Granell, S., and Chambers, T.C. (2008). Identification of the major phosphorylation site in Bcl-xL induced by microtubule inhibitors and analysis of its functional significance. J Biol Chem 283, 35517-35525.

Vagin, A., and Teplyakov, A. (2000). An approach to multi-copy search in molecular replacement. Acta Crystallogr D Biol Crystallogr 56, 1622-1624.

Valentijn, A.J., Upton, J.P., and Gilmore, A.P. (2008). Analysis of endogenous Bax complexes during apoptosis using blue native PAGE: implications for Bax activation and oligomerization. Biochem J 412, 347-357.

van Delft, M.F., Wei, A.H., Mason, K.D., Vandenberg, C.J., Chen, L., Czabotar, P.E., Willis, S.N., Scott, C.L., Day, C.L., Cory, S., et al. (2006). The BH3 mimetic ABT-737 targets selective Bcl-2 proteins and efficiently induces apoptosis via Bak/Bax if Mcl-1 is neutralized. Cancer Cell 10, 389-399.

Vaux, D.L., Cory, S., and Adams, J.M. (1988). Bcl-2 gene promotes haemopoietic cell survival and cooperates with c-myc to immortalize pre-B cells. Nature 335, 440-442.

Vaux, D.L., and Korsmeyer, S.J. (1999). Cell death in development. Cell 96, 245-254.

Veis, D.J., Sorenson, C.M., Shutter, J.R., and Korsmeyer, S.J. (1993). Bcl-2-deficient mice demonstrate fulminant lymphoid apoptosis, polycystic kidneys, and hypopigmented hair. Cell 75, 229-240.

Walensky, L.D., Kung, A.L., Escher, I., Malia, T.J., Barbuto, S., Wright, R.D., Wagner, G., Verdine, G.L., and Korsmeyer, S.J. (2004). Activation of apoptosis in vivo by a hydrocarbon-stapled BH3 helix. Science 305, 1466-1470.

Walensky, L.D., Pitter, K., Morash, J., Oh, K.J., Barbuto, S., Fisher, J., Smith, E., Verdine, G.L., and Korsmeyer, S.J. (2006). A stapled BID BH3 helix directly binds and activates BAX. Mol Cell 24, 199-210.

Wang, G.Q., Wieckowski, E., Goldstein, L.A., Gastman, B.R., Rabinovitz, A., Gambotto, A., Li, S., Fang, B., Yin, X.M., and Rabinowich, H. (2001). Resistance to granzyme B-mediated cytochrome c release in Bak-deficient cells. J Exp Med 194, 1325-1337.

Warr, M.R., Acoca, S., Liu, Z., Germain, M., Watson, M., Blanchette, M., Wing, S.S., and Shore, G.C. (2005). BH3-ligand regulates access of MCL-1 to its E3 ligase. FEBS Lett 579, 5603-5608.

Wattenberg, B., and Lithgow, T. (2001). Targeting of C-terminal (tail)-anchored proteins: understanding how cytoplasmic activities are anchored to intracellular membranes. Traffic 2, 66-71.

Wei, M.C., Lindsten, T., Mootha, V.K., Weiler, S., Gross, A., Ashiya, M., Thompson, C.B., and Korsmeyer, S.J. (2000). tBID, a membrane-targeted death ligand, oligomerizes BAK to release cytochrome c. Genes Dev 14, 2060-2071.

Wei, M.C., Zong, W.X., Cheng, E.H., Lindsten, T., Panoutsakopoulou, V., Ross, A.J., Roth, K.A., MacGregor, G.R., Thompson, C.B., and Korsmeyer, S.J. (2001). Proapoptotic BAX and BAK: a requisite gateway to mitochondrial dysfunction and death. Science 292, 727-730.

Weng, C., Li, Y., Xu, D., Shi, Y., and Tang, H. (2005). Specific cleavage of Mcl-1 by caspase-3 in tumor necrosis factor-related apoptosis-inducing ligand (TRAIL)-induced apoptosis in Jurkat leukemia T cells. J Biol Chem 280, 10491-10500.

Werner, A.B., Tait, S.W., de Vries, E., Eldering, E., and Borst, J. (2004). Requirement for aspartate-cleaved bid in apoptosis signaling by DNA-damaging anti-cancer regimens. J Biol Chem 279, 28771-28780.

White, F.A., Keller-Peck, C.R., Knudson, C.M., Korsmeyer, S.J., and Snider, W.D. (1998). Widespread elimination of naturally occurring neuronal death in Bax-deficient mice. J Neurosci 18, 1428-1439.

Willis, S.N., Chen, L., Dewson, G., Wei, A., Naik, E., Fletcher, J.I., Adams, J.M., and Huang, D.C. (2005). Proapoptotic Bak is sequestered by Mcl-1 and Bcl-xL, but not Bcl-2, until displaced by BH3-only proteins. Genes Dev 19, 1294-1305.

Willis, S.N., Fletcher, J.I., Kaufmann, T., van Delft, M.F., Chen, L., Czabotar, P.E., Ierino, H., Lee, E.F., Fairlie, W.D., Bouillet, P., et al. (2007). Apoptosis initiated when BH3 ligands engage multiple Bcl-2 homologs, not Bax or Bak. Science 315, 856-859.

Wilson, B.E., Mochon, E., and Boxer, L.M. (1996). Induction of bcl-2 expression by phosphorylated CREB proteins during B-cell activation and rescue from apoptosis. Mol Cell Biol 16, 5546-5556.

Wolter, K.G., Hsu, Y.T., Smith, C.L., Nechushtan, A., Xi, X.G., and Youle, R.J. (1997). Movement of Bax from the cytosol to mitochondria during apoptosis. J Cell Biol 139, 1281-1292.

Wyttenbach, A., and Tolkovsky, A.M. (2006). The BH3-only protein Puma is both necessary and sufficient for neuronal apoptosis induced by DNA damage in sympathetic neurons. J Neurochem 96, 1213-1226.

Yang, E., Zha, J., Jockel, J., Boise, L.H., Thompson, C.B., and Korsmeyer, S.J. (1995). Bad, a heterodimeric partner for Bcl-XL and Bcl-2, displaces Bax and promotes cell death. Cell 80, 285-291.

Yao, Y., Bobkov, A.A., Plesniak, L.A., and Marassi, F.M. (2009). Mapping the interaction of pro-apoptotic tBID with pro-survival BCL-XL. Biochemistry 48, 8704-8711.

Yin, X.M., Oltvai, Z.N., and Korsmeyer, S.J. (1994). BH1 and BH2 domains of Bcl-2 are required for inhibition of apoptosis and heterodimerization with Bax. Nature 369, 321-323.

Young, R.L., and Korsmeyer, S.J. (1993). A negative regulatory element in the bcl-2 5'-untranslated region inhibits expression from an upstream promoter. Mol Cell Biol 13, 3686-3697.

Zeitlin, B.D., Zeitlin, I.J., and Nor, J.E. (2008). Expanding circle of inhibition: small-molecule inhibitors of Bcl-2 as anticancer cell and antiangiogenic agents. J Clin Oncol 26, 4180-4188.

Zha, J., Weiler, S., Oh, K.J., Wei, M.C., and Korsmeyer, S.J. (2000). Posttranslational N-myristoylation of BID as a molecular switch for targeting mitochondria and apoptosis. Science 290, 1761-1765.

Zhai, D., Jin, C., Satterthwait, A.C., and Reed, J.C. (2006). Comparison of chemical inhibitors of antiapoptotic Bcl-2-family proteins. Cell Death Differ 13, 1419-1421.

Zhan, Q., Bieszczad, C.K., Bae, I., Fornace, A.J., Jr., and Craig, R.W. (1997). Induction of BCL2 family member MCL1 as an early response to DNA damage. Oncogene 14, 1031-1039.

Zhang, L., Shimizu, S., Sakamaki, K., Yonehara, S., and Tsujimoto, Y. (2004). A caspase-8-independent signaling pathway activated by Fas ligation leads to exposure of the Bak N terminus. J Biol Chem 279, 33865-33874.

Zhong, Q., Gao, W., Du, F., and Wang, X. (2005). Mule/ARF-BP1, a BH3-only E3 ubiquitin ligase, catalyzes the polyubiquitination of Mcl-1 and regulates apoptosis. Cell 121, 1085-1095.

Zhou, H., Hou, Q., Hansen, J.L., and Hsu, Y.T. (2007). Complete activation of Bax by a single site mutation. Oncogene 26, 7092-7102.

Zhou, M., Demo, S.D., McClure, T.N., Crea, R., and Bitler, C.M. (1998). A novel splice variant of the cell death-promoting protein BAX. J Biol Chem 273, 11930-11936.

Zhu, X., Wang, Y., Ogawa, O., Lee, H.G., Raina, A.K., Siedlak, S.L., Harris, P.L., Fujioka, H., Shimohama, S., Tabaton, M., et al. (2004). Neuroprotective properties of Bcl-w in Alzheimer disease. J Neurochem 89, 1233-1240.

Ziegler, U., and Groscurth, P. (2004). Morphological features of cell death. News Physiol Sci 19, 124-128.

Zinkel, S.S., Ong, C.C., Ferguson, D.O., Iwasaki, H., Akashi, K., Bronson, R.T., Kutok, J.L., Alt, F.W., and Korsmeyer, S.J. (2003). Proapoptotic BID is required for myeloid homeostasis and tumor suppression. Genes Dev 17, 229-239.